THE STUDY ON THE INTERPLAY OF LOCAL AND ITINERANT ELECTRONS IN IRON BASED SUPERCONDUCTING MATERIALS USING HUBBARD MODEL HOPPING WITH INTRA AND INTER COULOMB INTERACTION

A DISSERTATION SUBMITTED TO THE SCHOOL OF GRADUATE STUDIES OF ADDIS ABABA UNIVERSITY
IN PARTIAL FULFILLMENT OF THE REQUIREMENTS FOR THE DEGREE OF DOCTOR OF PHILOSOPHY IN PHYSICS

BY
Tadesse Desta Gidey
(tad4aau@gmail.com)

ADDIS ABABA UNIVERSITY
ADDIS ABABA, ETHIOPIA
NOVEMBER 2017

ADDIS ABABA UNIVERSITY
SCHOOL OF GRADUATE STUDIES

The undersigned hereby certify that they have read and recommend to the Faculty of School of Graduate Studies for acceptance a thesis entitled "**The Study on the interplay of local and itinerant electrons in iron based superconducting materials using Hubbard Model Hopping with intra and inter Coulomb interaction**" by **Tadesse Desta Gidey** in partial fulfillment of the requirements for the degree of **Doctor of Philosophy**.

Dated: November 2017

External Examiner: _____
Professor Biplap Sanyal

Internal Examiner: _____
Dr. Chernet Amente

Research Supervisor: _____
Professor Pooran Singh

Chairman: _____
Dr. Teshome Senbeta

ADDIS ABABA UNIVERSITY

Date: **November 2017**

Author: **Tadesse Desta Gidey**

Title: **The Study on the interplay of local and itinerant electrons in iron based superconducting materials using Hubbard Model Hopping with intra and inter Coulomb interaction**

Department: **Physics**

Degree: **Ph.D.** Convocation: **November** Year: **2017**

Permission is herewith granted to Addis Ababa University to circulate and to have copied for non-commercial purposes, at its discretion, the above title upon the request of individuals or institutions.

Signature of Author

It is dedicated to my wife Nigsti G/meskel and my father Desta Gidey for their unwavering support and encouragement.

Table of Contents

List of Tables

List of Figures

Abstract

In this dissertation the interplay of localized and itinerant electrons in iron based superconducting systems using the Hubbard model is theoretically studied. By developing a model Hamiltonian for the system and by using quantum field theory Green's function formalism, we have obtained mathematical expressions for superconducting transition temperature(T_C), spin density wave transition temperature(T_{sdw}), superconductivity order parameter(Δ_{Sc}) and spin density wave order parameter(Δ_{sdw}). By employing the experimental and theoretical values of the parameters in the obtained expressions, phase diagrams of superconducting transition temperature(T_C) versus superconducting order parameter(Δ_{Sc}) and spin density wave transition temperature (T_{sdw}) versus spin density wave order parameter(Δ_{sdw}) have been plotted. By combining the two phase diagrams, the possible coexistence of superconductivity and spin density wave (SDW) in Ferropnictide $Ba_{1-x}K_xFe_2As_2$ is demonstrated. Thus, in both the SDW and SC phases, the coexistence of the itinerant electrons and the local moments are crucial to the underlying mechanisms. Starting with a model Hamiltonian consisting of a pairing interaction, magnetic interactions of Heisenberg type by local electrons and an interaction of itinerant electrons with localized electrons and using Greens function technique, the expressions for superconducting order parameter ($\Delta(T)$) and the superconducting transition temperature, T_C are determined. The expressions indicate that magnetization suppresses superconductivity, and there might be a coexistence below critical temperature. The result also suggest the importance of the concept of localized and itinerant electron system in theoretical work. Moreover, the exchange field dependence of the Hubbard model with a attractive, effective,

pairwise, nearest neighbour interaction via the Hartree-Fock-Gorkov approximation is explore. Based on the spin-generalised Bogoliubov-de-Gennes (BdG) equations, we obtained expressions of gap equations (superconducting order parameters), specific heat capacity, Magnetization and magnetic susceptibility for singlet and triplet superconductors in the presence and absence of exchange field is obtained. By developing the model Hamiltonian for the system and using the double time temperature-dependent Greens function formalism, the expressions for superconducting transition temperature (Tc) as a function of electron coupling constant (λ_{elc}), equation of motion for parallel and anti parallel spin pairing and temperature dependent of magnetization for both itinerant and localized electrons hoping with intra and inter Coulomb interactions is obtained. Based on the general features of multi-bands and intermediate coupling strengths, a phenomenological theory of coexistence of itinerant and localized electrons have been proposed to describe the low-energy physics in iron-based superconductors. By using the experimental and theoretical values of the parameters in the obtained expressions, the plots of superconducting transition temperature versus electron coupling constant (λ_{elc}), superconducting transition temperature (Tc) versus superconducting order parameter (Δ) and magnetization vesus superconducting transition temperature are plotted and demonstrated the possibility of the interplay of itinerant and localized electrons in iron based superconductors.

Acknowledgements

I would like to express my sincere thanks to my advisor Prof. Pooran Singh for his unlimited and constructive guidance, advice, suggestions, comments his scientific excitement, integral view on research and overly enthusiasm, has made a deep impression on me. I would like to thank professor Biplap Sanyal, for his permission and support to visit, use VASP and other facilities in Uppsala University, Sweden. I would further thank Dr. Gebregziabher Kahsay (Bahir Dar University, Ethiopia) who gave me comments and suggestions on my dissertation. I acknowledge the financial support of Addis Ababa University Graduate office, SIDA, and Jigjiga University.

I am grateful to Dr. Teshome Senbeta, chairman of the Department, w/r Tsilat Adinew, secretary of the Department of physics and Dr. Belayne Mesfin, the former chairman of the Department of Physics, AAU, for their help through out my contact with the Department.

I would like to thank to my wonderful family, especially my father Desta Gidey, my wife Nigsti G/meskel and my mother in law Lemlem G/kidan, Without their love and support, throughout my life, and particularly in the last three year, none of this would have been possible.

I am grateful to all my friends for providing encouragement and support during my work and for being with me for all the time. Finally, I would like to express my thanks from the bottom of my heart to all my family members for their love and support. Lastly, I thank the Almighty God for everything.

Tadesse Desta Gidey
November, 2017

Chapter 1

Introduction

One of the most fascinating phenomena in condensed matter physics is superconductivity, discovered by H. Kamerlingh Onnes in 1911 [1]. He discovered that, when cooling mercury below T_c =4.2K, the resistivity of mercury abruptly dropped to a value close to zero and it became superconducting. Superconductivity is the ability of a material to lose its electrical resistivity below a critical temperature T_c, and expel any external magnetic field from the bulk, thus leading to ideal diamagnetism. The latter effect is the so called Meissner-Ochsenfeld effect, discovered by Meissner and Ochsenfeld in 1933 [2]. It opened the way towards a deeper understanding of superconductivity.

More than 25 years after its first discovery by Bednorz and Muller [3], the phenomenon of high-temperature superconductivity has not lost any of its original fascination. However, despite the tremendous efforts made by scientists over the years, the phenomenon of high T_c superconductivity has not lost any of its mysteries. As conventional superconductivity and its corresponding effects are very well understood

and described by the BCS theory [4], high T_c superconductivity still lacks a conclusive theoretical description which can be confirmed by experimental results. In the BCS theory, the formation of pairs of electrons with opposite momenta and spins [$\mathbf{k}$,$\uparrow$], [$\mathbf{k}$,$\downarrow$] resulting in pairs with zero total net momentum $\mathbf{k} = 0$ and zero total net spin $\mathbf{S} = 0$, known as Cooper pairs and the resulting creation of a condensate state of the Cooper pairs is capable of explaining the characteristic effects such as the zero electric resistivity and the Meissner effect.

As the operating coupling mechanism is responsible for the formation of Cooper pairs, the BCS theory considers electron phonon coupling effects as the main driving mechanism, with an exchange of virtual phonons providing the pairing of the electrons. In high T_c materials, however, the electron phonon coupling alone does not supply coupling strengths which is sufficient to explain the high critical temperatures observed in these materials. So, in order to maintain the concept of Cooper pairs for unconventional or low T_c superconductivity, the main task is to find a pairing mechanism which is capable of handling the high critical temperatures. The proximity of magnetically ordered states and superconductivity in the phase diagram of high T_c materials is the main motivation for the consideration of possible relations between the pairing mechanism of Cooper pairs and magnetic degrees of freedom, where an exchange of spin fluctuations is discussed as possible contribution to the coupling of electrons to Cooper pairs. Magnetic degrees of freedom, in this case magnons or paramagnons, however, are much more difficult to investigate than phonons, as in the case of the BCS superconductors.

Since the discovery of unconventional superconductivity in Iron-based superconductors in 2008 [5], great efforts have been made to investigate the properties of these materials theoretically as well as experimentally by applying a variety of techniques. With its direct access to magnetic properties in general and especially dynamical magnetic excitations, neutron scattering plays a major role in the investigations of magnetism in the iron based superconductors.

This dissertation is organized in seven chapters.

• Chapter one deals with the general introduction

• Chapter two gives a brief introduction to the main characteristics of Iron-based superconducting materials. The intention of this chapter is not to provide a detailed overview of this particular field but to introduce some of the main characteristics of Iron-based superconductors.

• Chapter three deals with the basic properties and experimental details of the sample of iron based superconductor $Ba_{1-x}K_xFe_2As_2$ superconductor and a general theoretical description of the interplay between SC and SDW.

• Chapter four provides the theoretical study of the interplay of localized and itinerant electron in iron based superconductors by considering model Hamiltonian of Heisenberg type.

• Chapter five discusses the mathematical Techniques for the Hubbard model and

includes the basic formulae of the Hubbard model.

• Chapter six focuses on the formulation of the problem for the exchange field dependence of the Hubbard model using Hartree-Fock-Gorkov approximation and spin-generalised Bogoliubov-de-Gennes (BdG) equations, we obtained expressions of gap equations (superconducting order parameters) for singlet and triplet superconductors. By developing the Model Hamiltonian, we will calculate the Superconducting order parameter, Magnetization, specific heat capacity and Transition Temperature (T_{sc})for both singlet and triplet superconductors and using equation of Motion, we obtain superconducting Order parameter and magnetic order parameter in both pure localized and itinerant regions.

• Finally, Chapter Seven provides a brief summary of the obtained results discussed in detail in the previous chapters and makes the conclusion of the research work.

Chapter 2

Iron-based Superconductors

2.1 General Overview

Superconducting materials are characterized by the presence of mainly two characteristic effects, the effect of zero electric resistivity and the Meissner-Ochsenfeld effect, a complete exclusion of any interior magnetic field from the sample, for temperatures below a critical temperature T_c [1, 2]. The discovery of the phenomenon of zero electric resistivity in mercury was soon followed by the observation of the effect in other materials, such as tin, lead and metallic alloys. A microscopic understanding of the phenomenon was, however, not given until 1957 when Bardeen, Cooper and Schrieffer provided a theoretical approach suitable to describe the observed effects [4] by developing the so-called the BCS theory.

The main point of the BCS theory is the formation of Cooper pairs. Below the critical temperature, two electrons with opposite momenta and spins[$\mathbf{k}$,$\uparrow$], [-$\mathbf{k}$,$\downarrow$] form a paired state with zero total net momentum $\mathbf{k=0}$, zero total net spin $\mathbf{S=0}$ and a consequential S-wave symmetry of the Cooper pair wave function. The bosonic character of these Cooper pairs leads to the formation of a large Bose Einstein condensate,

which is capable of explaining many of the observed phenomena. In the BCS theory, the formation of the Cooper pairs is caused by an attractive potential between the two electrons due to the interaction via exchange bosons, in this case virtual phonons. In a descriptive picture; an electron that travels via the positively charged lattice of atomic nuclei interacts with the positive charges and leaves behind a small deformation of the lattice. A second electron with opposite spin and momentum feels the attractive potential of the enhancement of positive charges caused by the lattice deformation and thus indirectly interacts with the first electron and both electrons form the Cooper pairs.

For low temperatures, when many of these electron pairs are formed, the quantum mechanical wave functions of the Cooper pairs align and form a collective state, the Bose-Einstein condensate of the superconducting state. Once the condensate is formed, the Cooper pairs don't feel potentials not sufficient to break up the Cooper pair state which prevents them from scattering processes with either the lattice or other particles. This results in the onset of superconductivity with zero electric resistivity and in lowering of the superconducting ground state energy and consequently in a gap in the single particle excitation spectrum as excitations are only possible for energies that break up the Cooper pairs. This energy gap has its greatest value for low temperature and gradually decreases to zero when approaching the critical temperature T_c,

$$\Delta(T) = 3.52 k_B T_c \sqrt{1 - \frac{T}{T_c}} \tag{2.1.1}$$

T_c itself is proportional to the coupling strength of the Cooper pairs which is related to the interaction potential V,

$$k_B T_c = 1.14 E_D e^{-1/N(E_F)V} \tag{2.1.2}$$

where

k_B is Boltzmann's constant

E_D is the Debye cut off energy

$N(E_F)$ is the density of states at the Fermi level and

V is the interaction potential responsible for pair formation of the Cooper pairs, which in the BCS theory is provided by the electron phonon interactions.

The weakness of electron-phonon coupling in combination with the low Debye energy for the BCS superconducting materials leads to typical critical temperatures not higher than 30K.

2.2 Discovery of High-Tc superconductivity in Iron-based superconductors

For years the effect of high T_c superconductivity has been studied mainly in cuprate materials which almost lead to the conclusion that, substantial copper content might be an obligatory condition for materials to exhibit high-temperature superconductivity.

In 2008 this misconception was clearly disproved as **Kamihara et al**. discovered high-temperature superconductivity in a copper free material, $\mathbf{LaFeAsO_{1-x}F_x}$ with

T_c =26K [5]. This finding, which immediately was followed by the discovery of superconductivity for a great number of other Iron-based superconducting materials, caused a lot of excitement in the community and propelled the field of high Tc superconductivity, which at that time had slowed down a bit compared to the beginnings of 1986, back to be one of the most exciting fields in condensed matter physics. With the discovery by Kamihara et al. a real rush for new compositions with even higher critical temperatures was started and within a short span of time numerous discoveries were made. It was found that, by replacing lanthanum in $LaFeAsO_{1-x}F_x$ by magnetic rare earths such as **Ce, Sm, Nd or Pr** the critical temperature could easily by increased up to 56K [6, 7], which achieved much higher T_c values. Materials with this type of composition crystallize in the tetragonal ZrCuSiAs-type structure and are labeled as the 1111-family of the Iron-based superconductors.

Simultaneously another class of Fe-based superconductors was discovered by Rotter et al. and observed superconductivity with T_c = 38K in (Ba;K)Fe_2As_2 [8]. Subsquently, other superconductors with this type of composition were found, which all crystalize in the body centered tetragonal $ThCr_2Si_2$-type structure and are labeled as the 122-class of Fe-based superconducting materials. In addition to the 1111- and 122-family of superconductors, two additional classes were found, the 111-family represented by LiFeAs with T_c = 18K [9,10] and the binary 11-family of αFeSe materials first observed by Hsu et al. with T_c = 8K [11].

2.3 Basic properties of Iron based Superconductors

2.3.1 Family of Iron based Superconductors

There are several different structural families of iron based superconductors [12, 13]. The four most frequently studied structural families are the so called '1111', '122', '111' and '11' families. They are frequently named according to the stoichiometries of their parent compounds.

1111 Family

Following the discovery of high-T_c superconductivity in $LaFeAsO_{1-x}F_x$, T_c is rapidly increased by exchanging lanthanum with rare earth ions of smaller atomic radii in LnFeAsO and appropriate carrier doping or creating oxygen deficiencies, until it reached a maximum value of $\sim$ 56K until now in $Gd_{1-x}Th_xFeAsO$. This family LnFeAsO came to be known as 1111 family. LaFePO was discovered by Kamihara et al. in 2006 and was the first 1111 compound to show superconductivity, but with very low Tc ($\sim$5-7K). In addition to $LaFeAsO_{1-x}F_x$, the most remarkable 1111 compounds that show high-Tc superconductivity discovered until now are: $SmFeAsO_{1-x}F_x$ (Tc $\approx$ 43K), $CeFeAsO_{1-x}F_x$ (Tc $\approx$ 41K) and $NdFeAsO_{1-x}F_x$ (Tc $\approx$51K) [14, 15] .

111 family

X. C. Wang et al. reported the discovery of another new superconducting iron arsenide system LiFeAs (111 family). Superconductivity with T_c up to 18K was found in these compounds [16, 17].

11 family

F.C. Hsu et al. reported the observation of superconductivity with zero resistance transition temperature at 8K in the PbO-type α- FeSe compound known as 11 family. Although FeSe has been studied quite extensively, a key observation is that the clean superconducting phase exists only in those samples prepared with intentional Se deficiency [16, 18].

122 Family

M. Rotter et al. proposed $BaFe_2As_2$ as a potential new parent compound based on the similarities between $BaFe_2As_2$ and LaFeAsO. In fact, both compounds contain identical (FeAs) layers, and have the same charge in accordance with: $Ba^{2+}[(FeAs)^{-}]_2$ versus$(LaO)^{+}(FeAs)^{-}$. Partial replacement of Barium with Potassium (hole doping) induced superconductivity at 38K in $Ba_{0.6}K_{0.4}Fe_2As_2$, the first member of a new family of superconducting iron arsenides known as the 122 family. This discovery was followed by reports of similar compounds with: strontium (Tc $\approx$37K), calcium (Tc $\approx$20K), and europium (Tc $\approx$32K) [19, 20].

2.3.2 Structural Properties for Iron-based superconductors

Similar to cuprate materials, Iron-based superconductors crystallize in layered crystal structures. As illustrated in figure 2.1 for the four main classes of Iron-based materials, these layered crystal structures are organized in an alternate stacking of Fe_2As_2-layers and layers containing the other elements of the composition. The only exception are the 11 family materials. Here, the Fe_2As_2 -layers are substituted by $Fe_2(Se/Te)_2$-layers, in the absence of additional buffer layers.

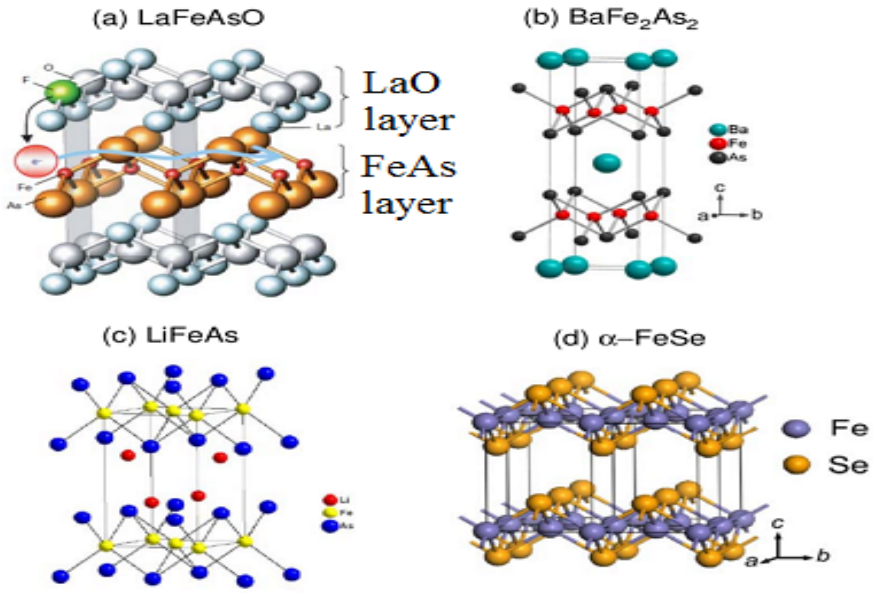

Figure 2.1: Crystal structure of the four main classes of Fe-based materials [21].

From band structure calculations it is known that, the density of states at the Fermi energy $N(E_F)$ is dominated by the Fe 3d states and thus it is believed that, the Fe_2As_2-layers ($Fe_2(Se/Te)_2$-layers) are the conduction layers and are responsible for the superconductivity in the system. These Fe_2As_2-layers are organized in a way where each Fe-atom is surrounded by a tetrahedron of four As-atoms. The shape of these tetrahedra surrounding the Fe-atoms in fact might impact the formation of the superconducting phase as it has been suggested that less distorted tetrahedra lead to higher critical temperatures. As a result, it was even proposed that, the structural effects caused by doping might even be more important for the creation of superconductivity than the additional charge carriers provided by the introduction of foreign atoms to the system.

At room temperature, all structures exhibit a tetragonal symmetry which with decreasing temperature will make a transition into a phase with lower orthorhombic symmetry. With the introduction of foreign atoms to the structure, this tetragonal-orthorhombic phase transition is gradually suppressed in temperature which is accompanied by a reduction of the orthorhombic distortion. This suppression of orthorhombic distortion might in fact be beneficial to the formation of superconductivity in the system [21].

In 1995 Zimmer et al. [22] studied the series of LnFePO (Ln= La - Nd, Sm, Gd) which crystallizes in the ZrCuSiAs type structure. These '1111' compounds exhibit the highest transition temperature (Tc) amongst all iron based superconductors (FeSCs) with $T_c = 56K$ for $Sr_{1-x}Sm_xFFeAs$ [23]. The '122' compounds crystallize in the $ThCr_2Si_2$ structure and are the best investigated FeSCs due to the availability of relatively large high quality single crystals. The highest Tc is observed in the '122' families in $Ba_{1-x}K_xFe_2As_2$ with $T_c^{max} = 38K$ [8]. The '111' families crystallize in the tetragonal Cu_2Sb structure. A representative is $Li_{1-\delta}FeAs$ which turns superconducting at $T_c^{max} = 18K$ [24]. A member of the '11' families is $FeSe_{0.5}Te_{0.5}$, which crystallizes in the $\alpha - PbO$ structure. Here, thin films with $T_c^{max} = 17K$ were grown [25].

2.3.3 Phase Diagrams for Iron based Superconductors

The phase diagrams of the main classes of Iron-based superconducting materials show a great amount of similarities not just between the different classes of Iron-based materials but also to the phase diagrams of cuprate materials. Similar to the cuprates, all undoped Iron-based materials exhibit long range antiferromagnetic order, as in this case the Fe^{2+} moments form a magnetic sublattice. The magnetic order sets in after the crystal structure has made a transition from tetragonal to orthorhombic symmetry. In the 11-materials both phase transitions, magnetic and structural, occur simultaneously at the same temperature whereas for the 122-class the two transitions start to separate for higher doping concentrations. For 1111-class even the undoped materials exhibit a temperature difference of up to 20K between the structural and magnetic transition.

Orbital ordering and nematic ordering have been proposed [26] to explain this large temperature difference, but a conclusive explanation of this effect is not found to this date. Doping the system with foreign atoms is one method to suppress the magnetic order and eventually induce superconductivity to the system. The doping can be conducted in several different ways, as basically all elements of the material can be replaced by foreign atoms. Depending on the introduction of these foreign atoms, they absorb or emit electrons from or to the system. Thus, the doping is referred to as either hole- or electron-doping. Increased doping concentration leads to a continuous suppression of the magnetic and nuclear transition temperatures which is accompanied by a continuous reduction of the ordered magnetic moment and orthorhombic distortion of the crystal structure. As soon as the long range order is suppressed, the

system becomes superconducting and aside for a small phase present in 122-families the superconducting phase is related to a tetragonal crystal structure. For some 122-families [27] and 1111-materials [28, 29] superconductivity even sets in before the magnetic order is completely suppressed, which leads to a coexistence of static magnetic order and superconductivity and which clearly illustrates the compatibility of magnetism and superconductivity in these materials.

The superconducting phase forms a dome-like shape in the phase diagram where the highest Tc is reached for a certain doping level (optimally doped), whereas both lower doping (under doped) and higher doping concentrations (over doped) lead to lower T_c and an eventual complete suppression of superconductivity. In contrast to the 1111- and 122-families, in the 11-families the suppression of the long range magnetic order does not imply an immediate onset of superconductivity and instead both phases are separated by a phase with short range spin glass like magnetic order and filamentary superconductivity. Bulk superconductivity does not occur in these materials unless the short range spin glass order is completely suppressed [30].

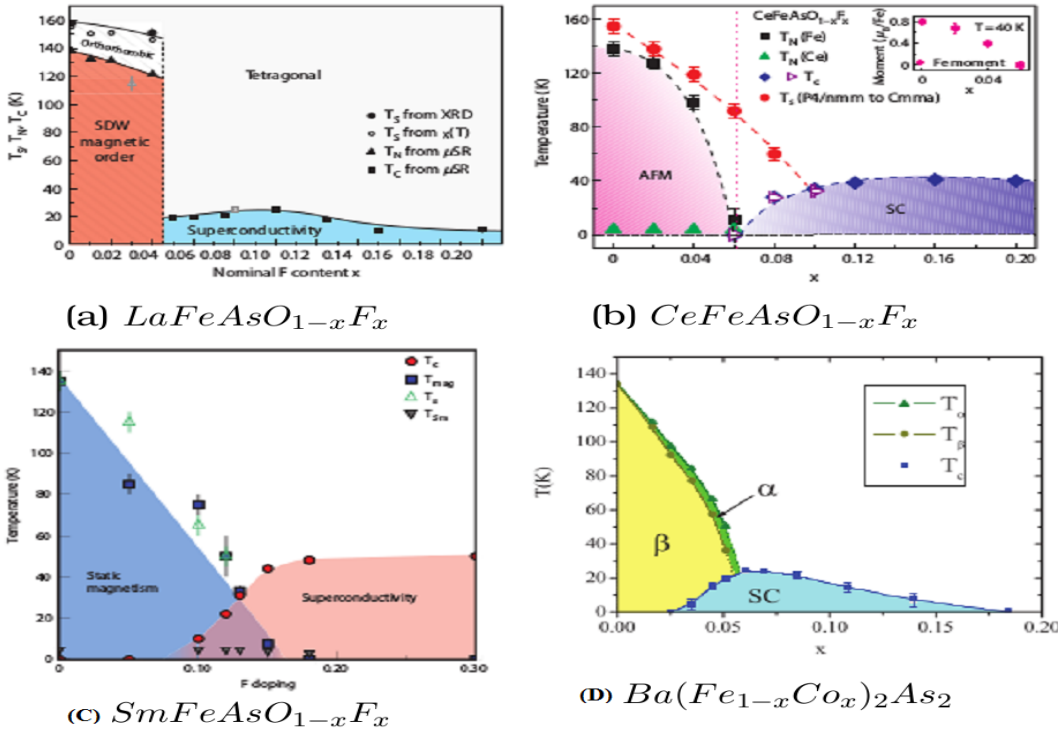

(a) $LaFeAsO_{1-x}F_x$ (b) $CeFeAsO_{1-x}F_x$

(c) $SmFeAsO_{1-x}F_x$ (d) $Ba(Fe_{1-x}Co_x)_2As_2$

Figure 2.2: Phase diagrams determined based on experimental data for (a) $LaFeAsO_{1-x}F_x$ [31], (b) $CeFeAsO_{1-x}F_x$ [32], (c) $SmFeAsO_{1-x}F_x$ [33] and (d) $Ba(Fe_{1-x}Co_x)_2$ As_2 [34].

2.3.4 Band structure, Fermi surfaces, and DOS of Iron based superconductors

Electronic band structure calculation has been popular after the discovery of DFT in 1960. It is one of the important parameter to study various properties of materials, such as electrical and structural. Experimentally electronic band structure and Fermi surfaces can be determined by different techniques including Angle Resolved Photo Emission Spectroscopy(ARPES) and de Haas-Van Alphen(dHvA) effect.

First principal calculation also leads to obtain electronic band structure and Fermi surfaces. Figure 2.3 shows the band structure of undoped 1111(LaFeAsO) and undoped 122 ($BaFe_2As_2$), reproduced by the concept of non spin polarized calculation [35]. The lattice parameters were based on the experimental result. The result of the calculation shows that Fe 3d orbital bands are present near the Fermi energy. The figure also shows 5 bands are crossing the Fermi level, that depicts the multi band nature of the iron based compounds.

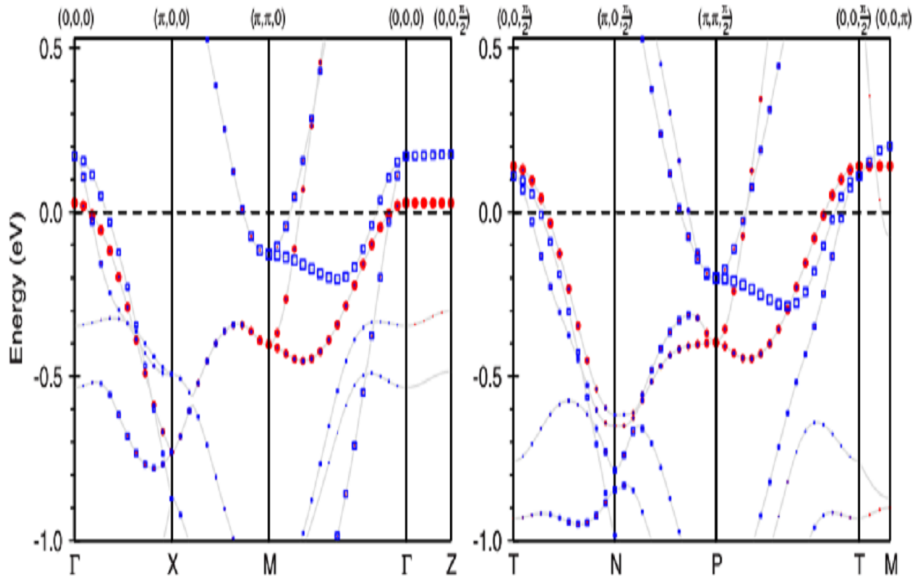

Figure 2.3: Band structure of LaFeAsO(left) and $BaFe_2As_2$(right) [35].

The Fermi surface (FS) in most pnictides includes electron-like cylinders in the corners of the Brillouin zone and the hole-like cylinders along the $\Gamma - Z$ line (Fig 2.4). But there is still a difference among the different families of iron based superconductors. For instance, the 1111-family undoped shows 2-dimensionality and the 122-family undoped one is 3-dimensional in character. Fig 2.4 shows the Fermi surfaces of non

magnetic LaFeAsO and $BaFe_2As_2$ [36]. Density of State (DOS) in superconductiv-

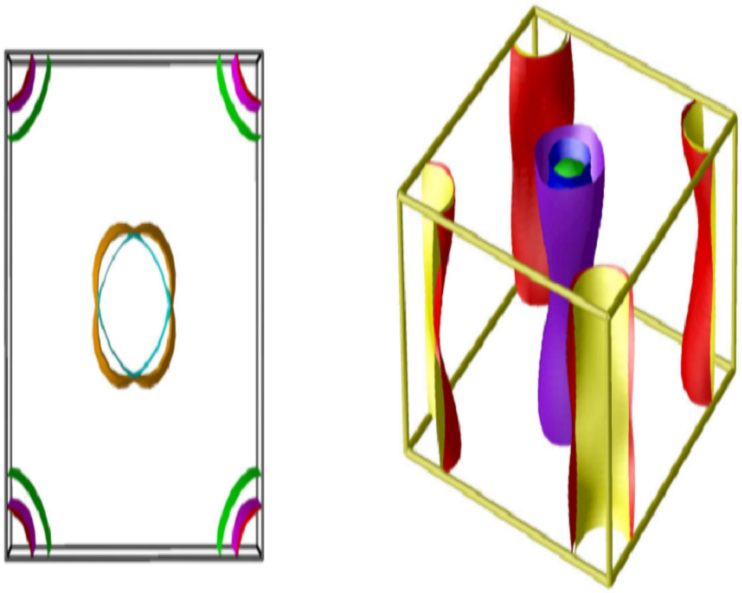

Figure 2.4: Fermi surfaces of LaFeAsO(left) and $BaFe_2As_2$(right) [36].

ity is an important parameter to understand several properties. If the number of DOS near the Fermi level is changing, for instance by doping, then the properties of the material may change dramatically. Applying Density Functional theory (DFT) as implemented in Quantum Espresso(QE) code one can calculate the DOS of compounds up on substitution. Fig 2.5 is a typical example for DOS of LaOFeAs and $Ba_{1-x}K_xFe_2As_2$.

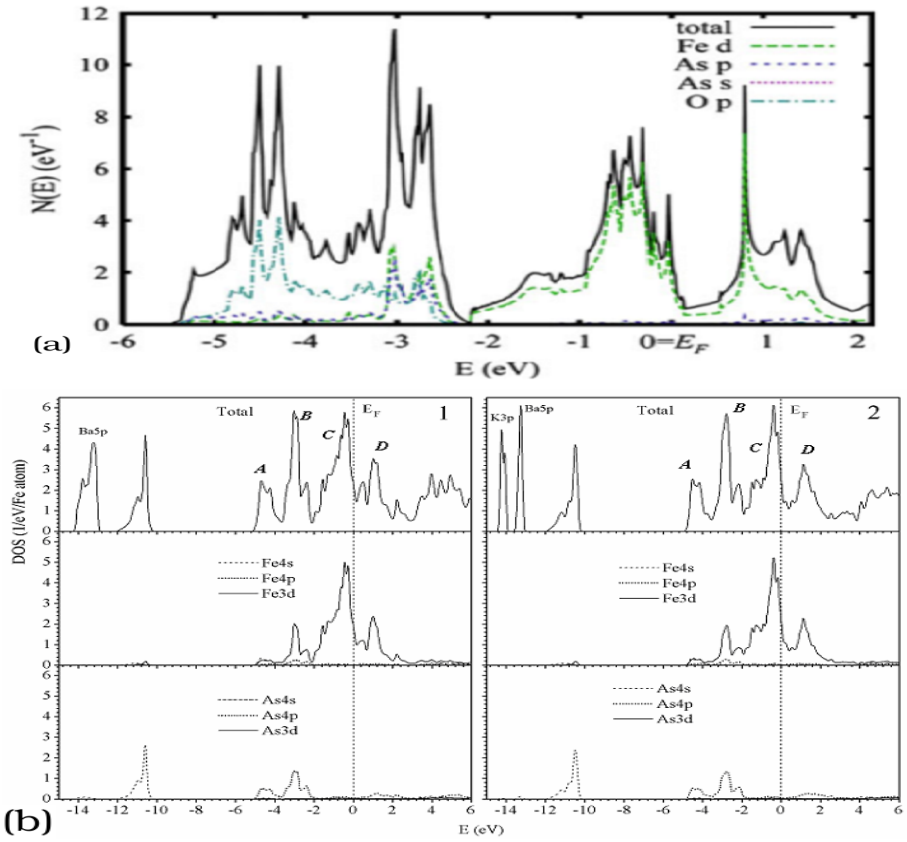

Figure 2.5: (a) Calculated density of states in LaOFeAs (solid line) and partial contributions to it from the orbitals of Fe, As and O (dashed lines) (b) Total and partial densities of states for $BaFe_2As_2$ (1) and $Ba_{0.5}K_{0.5}Fe_2As_2$ (2) [37].

2.4 The Interplay of Superconductivity and Magnetism in iron Based Superconductors

The interplay of magnetism and superconductivity is a fundamental problem in condensed matter physics. These two phenomena were thought mutually antagonistic. In conventional superconductors, the BCS theory of superconductivity, local magnetic

moments break up the spin-singlet Cooper pairs and hence strongly suppress superconductivity, an effect known as pair-breaking. Typically, magnetic fields destroy superconductivity because the energy they generate perturbs the close interaction between pairs of electrons that is a prerequisite for superconductivity. The most common way that a magnetic field destroys superconductivity is by disturbing the orbital effect, by acquiring more and more energy from the magnetic field. Once this energy becomes greater than that which unites the two electrons, the electron pairs break apart and superconductivity is suppressed. The other way magnetic fields can destroy superconductivity is when two electrons have what is called opposite spins, this is when in addition to the two electrons orbiting to one another, they also are spinning like tops but in opposite directions, called s-wave spin. When the magnetic field is turned on, one electron gains energy while the other loses. "If the difference is bigger than the amount of energy holding the electrons together, then they fly apart and superconductivity has gone," explained Naughton [38].

However, in a limited class of inter-metallic systems, superconductivity occurs even though magnetic ions with a local moment occupy all of one specific crystallographic site, which is well isolated and de-coupled from the conduction path. The possible coexistence of superconductivity with various types of magnetism carried by localized magnetic moments and itinerant electrons is critically discussed in connection with several existing materials such as rare earth ternary compounds [$(RE)Mo_6S_8$, (RE=Gd,Tb,Dy and Er) $(RE)Mo_6S_8$ and $(RE)Rh_4B_4$], (RE=Nd, Sm and Tm magnetic system [39], and has been recently revitalized by the discovery of the RNi_2B_2C (R=Y,Tm,Ho) system. In all the three systems, both SC and anti-ferromagnetic

(AFM) ordered states coexist.

The coexistence of superconductivity and ferromagnetism in the same compound has been put forward theoretically by V. Ginzburg in 1957 [40]. In his theoretical explanation, the coexistence of magnetism and superconductivity occurs when ferromagnetic field is smaller than the thermodynamic critical field of superconductor. The coexistence of superconductivity and antiferromagnetism is quite peaceful and very weakly influences each other, because the antiferromagnetic molecular field is effectively averaged out within the scale of the superconducting coherence length.

Superconductivity coexisting with ferromagnetic order was observed in UGe_2 and $URhGe$. This superconducting phase is found within the ferromagnetic phase and disappears in the paramagnetic region. The coexisting superconductivity with ferromagnetic is strongly suggesting that the pairing mechanism is magnetic in origin [41].

The interplay of superconductivity and magnetism has been studied in iron based superconductors theoretically and experimentally [42, 43]. Superconductivity could be obtained by applying either external pressure or doping. In most iron based superconductors, both electron and hole doping on parent compounds cause superconductivity. Upon doping, for example, potassium do magnetism gradually disappears with a lowering of the spin density wave transition temperature [44]. Generally, substitution of element in the 122 parent compounds may lead to suppression of spin density wave and eventual appearance of superconductivity [45].

2.5 Spin, charge and orbital orderings in iron-based superconductors

Many compounds of iron-based superconductors have been found and new materials are still being discovered. Basically, they can be divided into two categories, pnictides and chalcogenides. On the other hand, they can also be divided as 1111 compounds (e.g., LaFeAsO), 122 compounds (e.g., $SrFe_2As_2$), 111 compounds (e.g., LiFeAs), 11 compounds (e.g., FeTe/Se), 245 compounds (e.g., $K_2Fe_4Se_5$), and so on. All these materials share a common layered structure based on a planar layer of iron atoms joined by pnictogen or chalcogen anions. It is widely believed that, their superconductivity is based on the common iron layers, similar to the cuprate superconductors. The modern experimental probes, such as angle-resolved photoemission spectroscopy (ARPES), scanning tunneling microscopy (STM), neutron scattering, inelastic X-ray scattering (IXS) and X-ray diffraction (XRD) can provide important information for these materials.

Most parent compounds of iron-based superconductors are bad metals (245 compounds are semiconductors), which is an important difference between iron-based and cuprate superconductors. Band structure calculations have shown a finite density of states near the Fermi level [46]. Fermi pockets and finite resistances are observed in ARPES experiments and transport experiments, respectively [47, 48]. These results support the importance of itinerant electrons. On the other hand, local density approximation (LDA) band structure calculations indicate that the Fe 3d orbitals are strongly hybridized, and play a key role in the density of states near the Fermi level,

especially at d_{xz} and d_{yz} [49, 50]. This character suggests that iron-based superconductors have a multi-orbital nature, which is different from cuprates.

Although the pairing symmetry is still under debate, it is apparently not the conventional s wave. Actually, an $s^{\pm}$ wave pairing symmetry is more favored [49], and short range spin fluctuations are believed to be a medium for Cooper pairing. Before doping, the parent compounds of most iron-based superconductors show long range antiferromagnetic orders. The corresponding spin wave calculations can give consistent magnetic excitations with neutron scattering experiments [51]. The magnetism can also be understood by the itinerant electron picture because the parent compounds are bad metals. Within this picture, the long range magnetic order arises from the Fermi surface nesting. It is worth mentioning that, iron-based superconductors may share a common mechanism with cuprates, though they have different pairing symmetries.

The metallic nature of iron-based superconductors tells us that, the correlations are relatively weaker compared to cuprates whose parent compounds are Mott insulators. More in-depth studies suggest that, most iron-based superconductors are in the intermediately-correlated regime [52, 53]. Since in most iron-based superconductors, the on-site Coulomb repulsion, U, is found in an intermediate range between the strong correlation side (cuprate superconductors) and the non-interacting side (BCS superconductors) based on the fact that most parent compounds of the iron-based superconductors are antiferromagnetic (AFM) bad metals with poor conductivity [54].

Numerical calculations indicate that, U, for Fe in iron-based superconductors is approximately half of that for Cu in cuprates [55]. Actually, it is not completely right to fit iron-based superconductors in one correlated regime. Theoretical investigations using multi-orbital models have shown that, the values of U distribute in a wide regime [56]. As a result, both the weak-coupling and the strong-coupling models are used in studying iron-based superconductors. So far, the theoretical models can be divided into three kinds: weak-coupling theories, strong-coupling theories and hybrid theories which are also called local-itinerant theories. The weak-coupling theories, called itinerant theories deals with the itinerant electrons and regard iron-based superconductors as BCS-like superconductors, with the electron pairing arising from the spin fluctuation exchange. The strong-coupling theories are centered on the local magnetic moments and consider that, the superconductivity originates from doping the proximate Mott insulator, which are based on the resonating valence bond (RVB) theories. The hybrid theories combine the above two. They assume that, both the itinerant electrons and the local magnetic moments survive and contribute to superconductivity. The itinerant electrons contribute to the Fermi surface and the local magnetic moments provide the pairing glue.

2.6 Multiband effect on Iron pnictides superconductors

2.6.1 Brief Introduction to Multiband Effect

Main peculiarity of new iron based superconductors is their multiple-band nature. As there are multiple bands at the Fermi surface, there is the possibility for multi-band

Superconductivity. Electronic structure in a narrow enough energy interval around the Fermi level is formed practically only from d-states of Fe. Fermi surface consists of several hole -like and electron-like cylinders and on each its "own" energy gap can be formed. Phonon interaction alone seems too weak to explain the high Tc. In several theoretical papers [49] the multiband superconductivity is discussed as a possible explanation for the high Tc. Indeed, it has been long known that multiband effects can strongly enhance superconductivity. This is particularly relevant in the case of iron pnictides, which appear to be moderately correlated electron systems, with large number of Fe d bands at and near the Fermi level. Another advantage of this mechanism is that the interband pair interaction (pairing between the bands) can enhance superconductivity irrespective of whether it is attractive or repulsive provided that the gaps in different bands have the same or opposite signs, respectively. The former is the familiar s-wave while the latter is the extended s-wave superconductivity or $S_{\pm}$. This $S_{\pm}$ state, with the superconducting gap having the opposite sign on hole and electron sections of the Fermi surface (FS), emerges as a natural explanation for the superconductivity in Fe based compounds given the proximity of these materials to various nesting-driven spin-density-wave (SDW) and related instabilities and absence of obvious strong attractive interaction.

Note that the main role of different band parameters arises through their different densities of states, DOSs, (The states in the bands and their dependence on energy are described by DOSs), the parameter which is independent of doping for two-dimensional (2D) parabolic bands. Naturally, the real hole and electron bands in Fe pnictides are neither ideal parabolas nor identical to each other (nor entirely

2D for that matter). Naturally, the band with the larger coupling exhibits the larger gap, if the corresponding couplings support the actual pairing state which, however, has not been specified in our approach.

The new class of Iron-based compounds as the cuprates and the heavy fermions have all some similar characteristics. For example the high values of rate $2\Delta/T_c$ or the presence of the pseudogap [57]. For all three class of material it is proposed that, the superconductivity is mediated by antiferromagnetic spin fluctuations. The most obvious difference is that almost all the iron compounds present a multiband behavior while in HTSC and in heavy fermions this behavior was detected only in some particular cases.

The multiband nature of Iron-based superconductors may give rise to a multi-gap scenario that is indeed emerging from many different experimental data with evidence for rather high gap ratios. In this regard neither a three-band BCS model [49, 58] is adequate (it can only account for the gap ratio and Tc but not for the exact experimental gap values) nor a four-band Eliashberg model [59] with small values of the coupling constants and large boson energies because the calculated critical temperature has turned out to be larger than the experimental one.

The high experimental value of the larger gap suggests that high values of the coupling constants might be necessary to explain the experimental data within a three-band model [60,61]. One has therefore to employ the Eliashberg theory for strong coupling superconductors [60, 61]. A three-band Eliashberg model allows reproducing various

experimental data, indicating that these compounds can represent a case of dominant negative interband-channel superconductivity ($s_{\pm}$ wave symmetry) with small typical boson energies ($\sim$10meV) but too high values of the electron-boson coupling constants ($1.2 \leq \lambda_{tot} \leq 5.8$). The way to solve this problem is suggested by experimental measurement of Inosov and coworkers [62]. They found that the temperature evolution of the spin resonance energy follows the superconducting energy gap and this fact should indicate a feedback effect of the condensate on the spin fluctuations.

2.6.2 The Multiband Effect on Superconducting transition Temprature (T_c)

Recently, Lee et.al. had suggested that the magnitude of structural and magnetic distortion of $FeAs_4$ tetrahedron is a good measure of Tc and he proposed that parent compounds with highly symmetric FeAs tetrahedron have the potential of high Tc when suitable amount carriers are doped. On the other hand he found that experimentally short-range correlated disorder created large scale spin and charge of textures particularly in homogeneous at low doping and correlation in the disorder tend to increase Tc because of presence of the large clusters of strong coupling and decrease the spin stiffness. In iron pnictides, the degree of nesting between the various Fermi sheets and the magnitude and anisotropy of the Fermi velocities is believed to be important for the paring mechanism [63].

Conventional band structure calculations only include many-body effects at the mean field level in strongly interacting systems, there can be substantial renormalization of the effective masses or Fermi velocities due to electron-phonon or electron-electron

interactions and this enhancement can be determined from quantum oscillations. Furthermore, quantum oscillations can provide unique access to the details of a Fermi surface which suffers reconstruction by breaking up a large Fermi surface into many small pockets due to structural or magnetic instabilities (such as charge density waves(CDWs) and spin density waves(SDWs)). Thus, One of the key ingredients to understanding high-temperature superconductivity in pnictides and in cuprates could be linked to understanding the evolution of the Fermi surface topology from a reconstructed Fermi surface in the AFM (under doped) phase to a large Fermi surface (over doped phase). By varying an external parameter (pressure, doping or a magnetic field), a second-order quantum phase transition, or a quantum critical point under the SC dome, may separate a PM Fermi liquid regime from the magnetically ordered state.

Quantum oscillation measurements are ideally suited to access a quantum critical point as a function of a tuning parameter as they provide the effective mass of the elementary fermionic excitations that can be traced across the quantum critical point. In pnictides, a possible way to access such a critical point under the SC dome is through an isovalent substitution of phosphorus at the arsenic site in $BaFe_2As_2$ and quantum oscillations indeed suggest an increase in the effective masses and nesting between the electron and hole pockets upon approaching the maximum Tc.

To attain higher Tc on the basis of this phase diagram, it is desirable to have higher position of the pnictogen while keeping lattice constants not reduced. On the other hand, we have to keep in mind that such a variation in the lattice parameters also

enhances the tendency toward magnetism. In this sense, the superconductivity will have to compete with the magnetism/ structural phase transition in a more severe manner as the height and/or the lattice constants are increased. Namely, too much increase in the height and/or the lattice constants can be unfavorable for superconductivity in that the magnetism/structural phase transition, which may take place at high temperatures, can dominate over superconductivity. In such a case, applying pressure to reduce the lattice constants and/or doping carriers can be effective to suppress the magnetism or the structural phase transition, which may take place at high temperatures, can dominate over superconductivity.

Chapter 3

Samples and Experimental details

In this chapter, basic properties and experimental details of the sample of iron based superconductors (FeSCs) in the superconducting state will be reviewed. Special emphasize is placed on the superconductors $Ba_{1-x}K_xFe_2As_2$ compound and their properties relevant for the presented study.

3.1 Introduction

$(Ba_{1-x}K_x)Fe_2As_2$ belongs to the more general family of compounds called Iron Arsenic superconductors. Hence this family of compounds represents a second class of High Tc superconductors due to their high superconducting transition temperatures [5, 64]. Further more, $(Ba_{1-x}K_x)Fe_2As_2$ superconductors have the highest known Tc of the AFe_2As_2 compounds [5, 65] and also when compared with compounds with the same crystal structure where the highest Tc reached was 26K for the borocarbide YPd_2B_2C [66, 67].

After the discovery of $La(O/F)FeAs$ compounds, researchers shifted their focus to finding similar compounds. Rotter et al . [68] proposed that $BaFe_2As_2$ could be doped to become a superconductor due to the presence of iron arsenic layers as well as having the same charge and similar magnetic and electric properties as $La(O/F)FeAs$. When lanthanum was chosen as the first doping element, only the antiferromagnetic transition was suppressed but no superconductivity was observed [68, 69]. Instead potassium was used to create a hole-doped superconductor with a Tc of $38.1K$. A week later, Wang et al. and Ni et al. created single crystals of $(Ba_{1-x}K_x)Fe_2As_2$ using the flux methods [69, 70].

3.2 Crystal Structure and Phase Diagram of $(Ba_{1-x}K_x)Fe_2As_2$

The ternary parent compound, $BaFe_2As_2$, has a body centered tetragonal structure at $300K$ belonging to the $ThCr_2Si_2$ structure as shown in Figure 3.1.

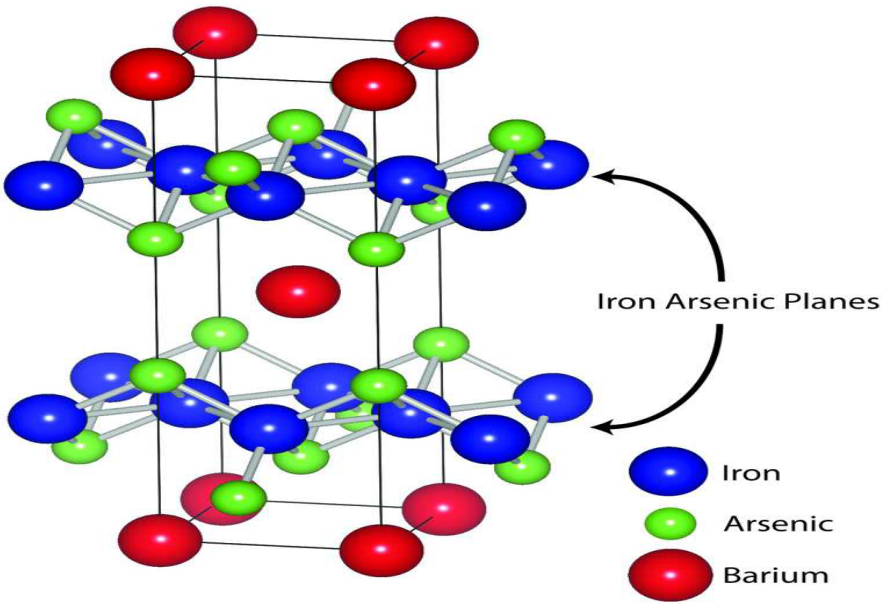

Figure 3.1: The tetragonal crystal structure of $BaFe_2As_2$ with barium sites in red, iron sites in blue and arsenic sites in green [69].

Barium sites are located on the four corners of the top and bottom and one at the body center while the iron and arsenic forms sheets located above and below the body center barium site [67]. The two iron arsenic sheets consist of edge-sharing $FeAs_4$ tetrahedra with a mirror plane located at the center barium site [71, 72]. The structural phase transition transforms the crystal structure from tetragonal to orthorhombic. For example in polycrystalline $BaFe_2As_2$, the **a** and **b** axes are expanded from equality with a value of $3.9625\mathring{A}$ at $300K$ to $5.6146\mathring{A}$ and $5.5742\mathring{A}$ respectively in the orthorhombic structure at $20K$. The **c** axis decreases from $13.01\mathring{A}$ in the tetragonal phase at $300K$ to $12.94\mathring{A}$ in the orthorhombic phase at $20K$ [67].

KFe_2As_2 also has tetragonal crystal structure albeit the lattice parameters change

to 3.8414$\mathring{A}$ and 13.839$\mathring{A}$ for **a** and **c** respectively. KFe_2As_2 has a large **c/a** ratio and exhibits no orthorhombic distortion transition [73]. With the addition of potassium to $BaFe_2As_2$, the lattice parameter **a** decreases to a minimum of 3.84$\mathring{A}$ for $x = 1.0$ while the parameter **c** increases to maximum of 13.84$\mathring{A}$ for $x = 1.0$. Furthermore, the Fe-Fe bond length and the bond angle ε of the As-Fe-As bond decreases monotonically as x increases. When $x = 0.2 - 0.3$, it was observed that the orthorhombic phase disappears and the crystal structure remains tetragonal, as seen in figure 3.2. The exact placement and overall order of the barium and the potassium sites in the crystal structure is however still unclear [72].

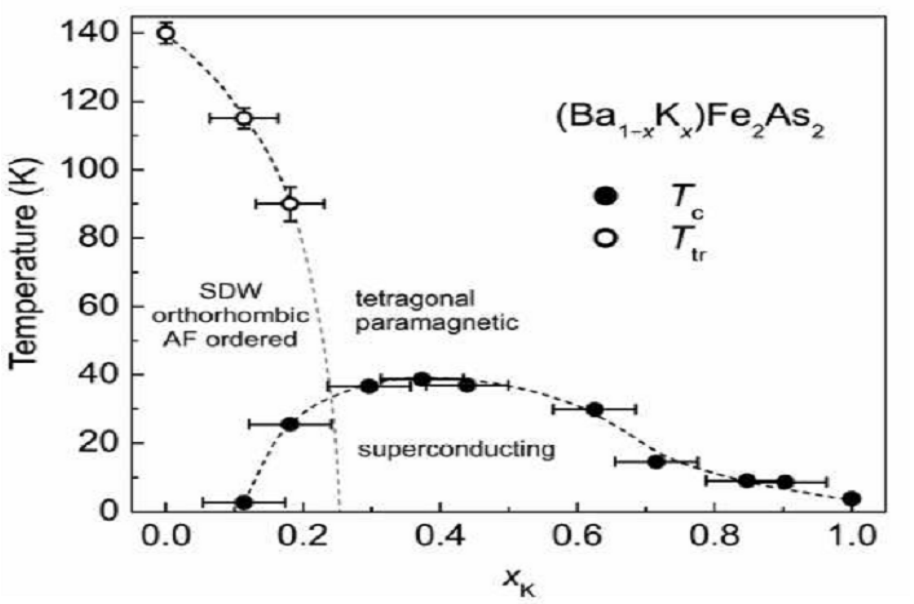

Figure 3.2: Phase diagram of $Ba_{1-x}K_xFe_2As_2$ (hole doped). T_c and T_{tr} indicate the superconducting and tetragonal to orthorhombic transition temperature, respectively with $x = 0 - 1$. [74]

Figs.3.2 show the phase diagram of hole doped $Ba_{1-x}K_xFe_2As_2$ and superconductivity and antiferromagnetic ordering coexists at least in the under-doped region of

$Ba_{1-x}K_xFe_2As_2$ ($x = 0.2$). The control parameter in the phase diagram of the IBSCs can be either doping or pressure. The neutral Ba atom has an electronic configuration of $[Xe]6s^2$ while the neutral K atom has an electronic configuration of $[Ar]4s^1$. Hence, one hole is added to the unit cell by this replacement (hole doping, $Ba_{1-x}K_xFe_2As_2$).

3.3 Magnetic Properties of $Ba_{1-x}K_xFe_2As_2$

The parent compound, $BaFe_2As_2$, is a paramagnetic metal with a coupled structural and magnetic transition. The coupled structural and magnetic transitions causes the crystal structure to become orthorhombic and a spin density wave (SDW) is observed [66, 68].

3.3.1 Paramagnetism

For $BaFe_2As_2$, the temperature dependent magnetic susceptibility varies depending on the method used to produce the sample. Rotter et al. observed that polycrystalline $BaFe_2As_2$ (see figure 3.3) is paramagnetic up to $140K$ followed by an abrupt drop in susceptibility [66].

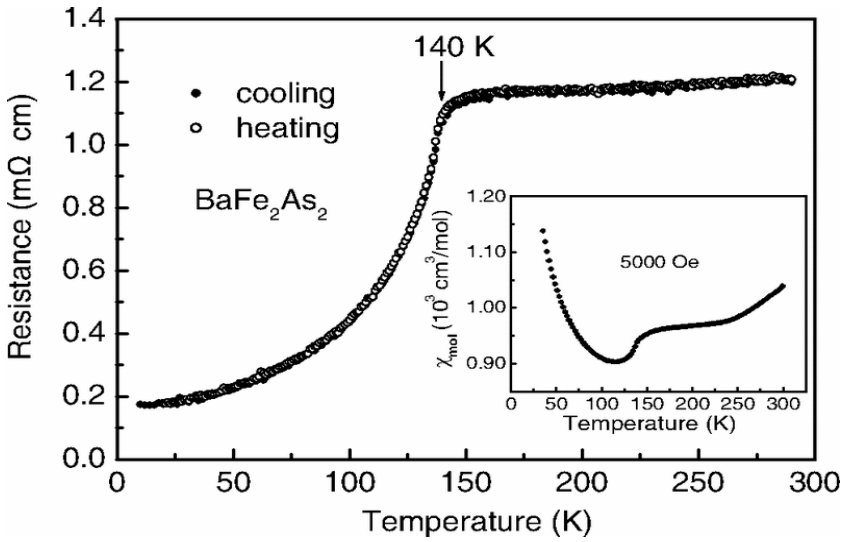

Figure 3.3: Dc electrical resistance of $BaFe_2As_2$ ($I = 100\mu A$). Inset: Magnetic susceptibility for poly-crystalline $BaFe_2As_2$ where $H = 5000G$ or 0.5T. The increase in the susceptibility below 100 K was attributed to ferromagnetic impurities [66].

3.3.2 Spin Density Wave and Antiferromagnetic Order

An interesting aspect in non-superconducting AFe_2As_2 compounds is the presence of a magnetic transition between $140K$ and $200K$ [66,73]. In a similar compound, Dong et al. [75] proposed that the magnetic transition in $La(O/F)FeAs$ is caused by a Spin Density Wave (SDW)[1] transition due to the strong nesting of the Fermi surface[2] with commensurate SDW vector [3] $\mathbf{Q} = (\pi, \pi, 0)$. Using neutron diffraction measurements, Huang et al. observed that, Nesting of the Fermi surface with $\mathbf{Q} = (\pi, \pi, 0)$ and a SDW was also present in $BaFe_2As_2$ [18].

[1]A Spin Density Wave (SDW) occurs when the spin of the electrons have a spatial oscillation with wavelength of $\lambda = \frac{2\pi}{\|\mathbf{Q}\|}$. The SDW state has a lower ground state energy than the Fermi sea resulting in the formation of an energy gap at the Fermi surface.

[2]Nesting of the Fermi surface occurs when the surfaces of two different energy bands are connected by a vector $\mathbf{Q}$ (SDW vector).

[3]Commensurate SDW vector occur when the SDW vector has the same periodicity as the crystal lattice.

The orthorhombic distortion of the crystal lattice causes the crystal structure to transform from tetragonal to orthorhombic while the SDW transition results in the formation of antiferromagnetic order causing the moment of the iron atoms to become parallel with the longer a axis in the orthorhombic phase [18,71]. The magnetic structure of the $BaFe_2As_2$ can be seen in figure 3.4.

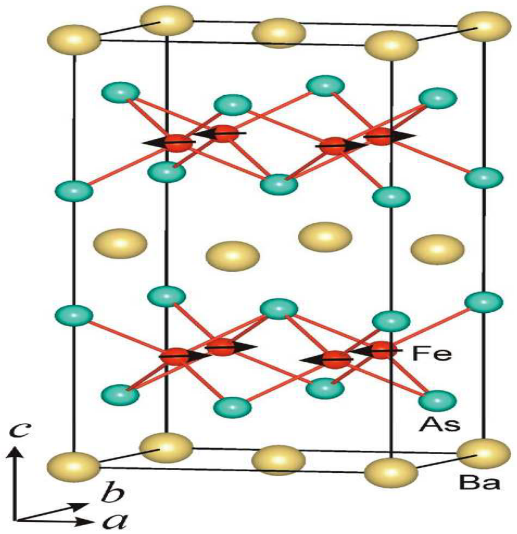

Figure 3.4: Magnetic structure of $BaFe_2As_2$ in the orthorhombic crystal structure showing the alignment of the iron atom moments [76].

3.4 Superconductivity in $Ba_{1-x}K_xFe_2As_2$

Superconductivity in $BaFe_2As_2$ compound can be induced by two methods: chemical doping [72,77] and/or the application of pressure [78]. The highest Tc superconductors containing barium, iron and arsenic can be seen in Table 3.1. The addition of a chemical dopant and/or the application of pressure on $BaFe_2As_2$ results in the

suppression of the SDW and hence the reduction of magnetic order. Superconductivity is observed when the magnetic order is sufficiently weak thus superconductivity and weak magnetic order can still coexist [72, 78, 79]. The exact mechanism for the emergence of superconductivity is however still unknown.

Table 3.1: The highest Tc's of superconductors containing the fundamental elements of barium, iron and arsenic belonging to the AFe_2As_2 compounds. The crystal structure of all compounds is tetragonal.

Compounds	**Condition for Superconductivity**	**Reference**
$BaFe_2As_2$	Pressure: 40 kbar with a Tc ≈29K	Alireza et al. [78]
$Ba_{1-x}K_xFe_2As_2$	Hole-doped with a Tc ≈ 38K for $x \approx 0.4$	Rotter et al. [72]
$Ba(Fe_{1-x}Co_x)_2As_2$	Electron-doped with a Tc ≈ 23K for $x \approx 0.074$	Tanatar et al. [81]
$BaFe_{2-x}Ni_xAs_2$	Electron-doped with a Tc ≈ 21K for $x \approx 0.10$	Liu et al. [80]
$BaFe_{2-x}Ru_xAs_2$	Isovalent doping with a Tc ≈ 21K for $x \approx 0.75$	Paulraj et al. [82]
$BaFe_2(As_{1-x}P_x)_2$	Isovalent doping with a Tc ≈ 30K for $x \approx 0.35$	Jiang et al. [77]
$Ba(Fe_{1-x}Rh_x)_2As_2$	Isovalent doping with a Tc ≈ 23K for $x \approx 0.057$	Ni et al. [70]
$Ba(Fe_{1-x}Pd_x)_2As_2$	Hole-doped with a Tc ≈ 17K for $x \approx 0.043$	Tanatar et al. [81]

3.4.1 Chemical Doping

Chemical doping in $BaFe_2As_2$ can be achieved by doping the barium, iron or arsenic sites in the crystal structure [72, 77, 80]. The crystal structure of all the compounds in Table 3.1 is tetragonal but the effect of doping on the lattice parameters **a** and **c** changes depending on the sites that are replaced through doping. When the FeAs layer is doped by Ni, Co, or P, the **a** and **c** lattice parameters are both observed to decrease [77] as the dopant concentration increases. When potassium is used to dope the barium sites, the **a** lattice parameter is observed to decrease while the **c** lattice parameter increases as the potassium concentration increases. However, the changes in the lattice parameters of $(Ba_{1-x}K_x)Fe_2As_2$ are quite small since the unit

cell volume does not change [4].

The most critical factor for the observation of superconductivity in $BaFe_2As_2$ is the suppression of the SDW and its resulting magnetic order. When $BaFe_2As_2$ is doped by nickel, cobalt, potassium or phosphorous, the temperature of the SDW transition is observed to decrease and the SDW eventually disappears completely as the amount of dopant is increased.

3.4.2 Application of Pressure

The possibility of enhancing the superconductivity in Iron Arsenic compounds by pressure was first realized by Takahashi et al. while studying La(O/F)FeAs. At ambient pressure, La(O/F)FeAs has a Tc of $26K$ and under applied pressure the Tc increases to $46K$ at $\sim 4GPa$ or $40kbar$ [83]. In the non-doped [5] AFe_2As_2 compounds, superconductivity under applied pressure (see Figure 3.5(c)) is observed for $CaFe_2As_2$ ($T_c \approx 12K$ at $0.2GPa$)[38], $EuFe_2As_2$ ($T_c \approx 29.5K$ at $2GPa$)[39], $BaFe_2As_2$ ($T_c \approx 29K$ at $4GPa$) and $SrFe_2As_2$ ($T_c \approx 27K$ at $3GPa$)[29]. The application of pressure on doped superconducting AFe_2As_2 compounds can either decrease or increase the maximum T_c depending on the amount of dopant present, see Figure 3.5(b). In other words, if the doped superconducting AFe_2As_2 compound has the optimal (i.e. the highest possible T_c) or under doped then the application of pressure will increase the T_c. But if the compound is overdoped, the T_c will decrease with pressure [84, 85].

[4] $BaFe_2As_2$ has a unit cell volume of $203.86\mathring{A}^3$ while KFe_2As_2 has a unit cell volume of $203.49\mathring{A}^3$

[5] These compounds are non-superconductors at ambient pressure.

The most important property when considering the superconductivity under pressure is observed in $BaFe_2As_2$ and similar compounds show the suppression of the SDW transition with applied pressure. Torikachvili et al. proposed that the complete suppression of the SDW transition should occur around $80kbar$ or $8GPa$ based on extrapolation of their data [85]. Fukazawa et al. measured the evolution of T_c and T_{SDW} for $BaFe_2As_2$ using resistivity measurements to find the transition temperatures, see Figure 3.5(a). In Figure 3.5(a), the SDW transition temperature reaches a minimum of $\sim 70K$ at 9.0 GPa while the maximum T_c of $30K$ occurs at $\sim 4Gpa$ with coexistence of the SDW. Furthermore, it was observed that the complete suppression of the SDW occurs around 9 to $13GPa$ yielding a superconducting T_c between $15K$ and $20K$ [79]. Alireza et al. measured the T_c as a function of temperature using magnetic susceptibility up to $6GPa$ or $60kbar$ and constructed a $T - P$ phase diagram for $BaFe_2As_2$ and other AFe_2As_2 compounds, see Figure 3.5(c). In Figure 3.5(c), it can be seen clearly that, the maximum T_c is be observed to $30K$ at $\sim 4GPa$ or $40kbar$ for $BaFe_2As_2$ [78].

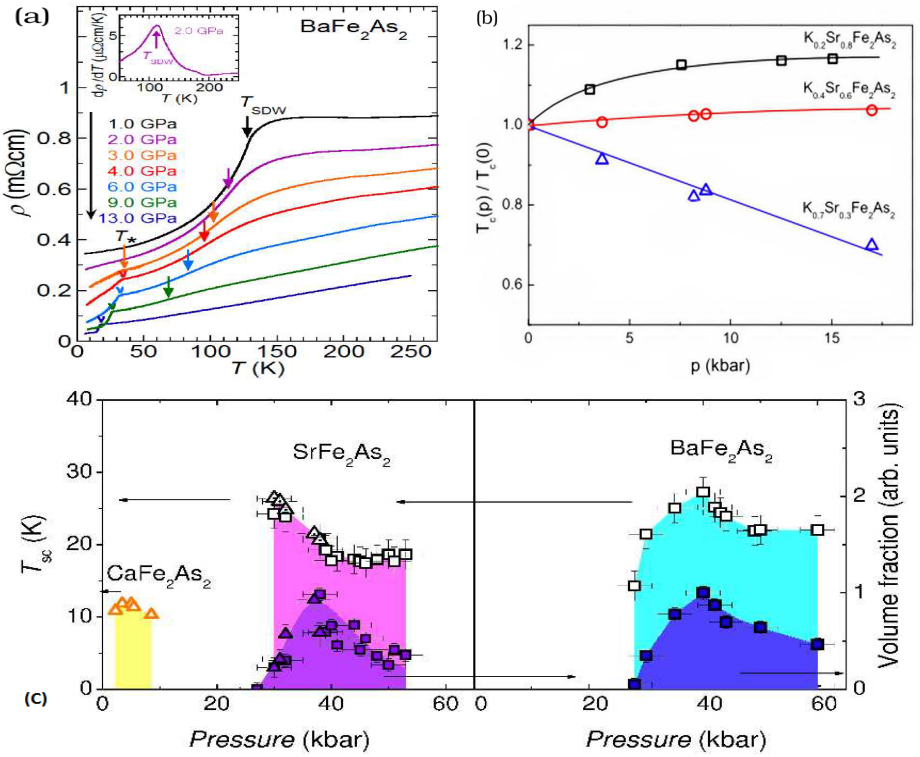

Figure 3.5: (a) The temperature dependence of the resistivity for $BaFe_2As_2$ under an applied pressure from $1.0GPa$ to $13GPa$. The SDW transition temperature is denoted by T_{SDW} while the superconducting transition temperature is denoted by T_* [79]. (b)The effect of pressure on the T_c of underdoped (Black or open squares), nearly optimal doped (Red or open circles) and overdoped (Blue or open triangles) samples of $K_{1-x}Sr_xFe_2As_2$, where $T_c(p)$ represents the T_c under pressure and $T_c(0)$ represents the T_c at ambient pressure [85]. (c) The pressure dependence of the Tc and volume fraction for AFe2As2 compounds which are superconducting under pressure [78]

3.5 Coexistence of Superconductivity and Spin density wave (SDW) in Ferropnictinde $Ba_{1-x}K_xFe_2As_2$

J Supercond Nov Magn (2016) 29:1433–1438
DOI 10.1007/s10948-015-3366-1

ORIGINAL PAPER

Coexistence of Superconductivity and Spin Density Wave (SDW) in Ferropnictide $Ba_{1-x}K_xFe_2As_2$

Tadesse Desta[1] · **Gebregziabher Kahsay**[2] · **Pooran Singh**[1]

Received: 12 August 2015 / Accepted: 31 December 2015 / Published online: 9 February 2016

Abstract This work focuses on the theoretical investigation of the coexistence of superconductivity and spin density wave (SDW) in ferropnictide $Ba_{1-x}K_xFe_2As_2$. By developing a model Hamiltonian for the system and by using quantum field theory Green's function formalism, we have obtained mathematical expressions for superconducting transition temperature (T_C), spin density wave transition temperature (T_{sdw}), superconductivity order parameter (Δ_{Sc}), and spin density wave order parameter (Δ_{sdw}). By employing the experimental and theoretical values of the parameters in the obtained expressions, phase diagrams of superconducting transition temperature (T_C) versus superconducting order parameter (Δ_{Sc}) and spin density wave transition temperature (T_{sdw}), versus spin density wave order parameter (Δ_{sdw}) have been plotted. By combining the two phase diagrams, we have demonstrated the possible coexistence of superconductivity and spin density wave (SDW) in ferropnictide $Ba_{1-x}K_xFe_2As_2$.

Keywords Superconductivity · Spin density wave (SDW) · Coexistence · Green function · Pnictides · $Ba_{1-x}K_xFe_2As_2$

✉ Tadesse Desta
tad4aau@gmail.com

Gebregziabher Kahsay
michige_90@yahoo.com

Pooran Singh
psinghgbpub@yahoo.com

[1] Department of Physics, Addis Ababa University, Addis Ababa, Ethiopia

[2] Department of Physics, College of Science, Bahir Dar University, Bahir Dar, Ethiopia

1 Introduction

Superconductivity was first observed by Kamerlingh Onnes in 1911 while he was investigating the electric resistivity of mercury at low temperatures [1]. He found that when mercury was cooled to a temperature below $T_C = 4.2$ K, he observed that the resistivity of mercury was dropped abruptly to a value close to zero and the material became superconducting. In 2008, high-temperature superconductor in a copper-free material $LaFeAsO_{1-x}F_x$ with $T_C = 26$ K was discovered by Kamihara et al. [2]. In recent times, high-temperature superconductors in iron based or ferropnictides having six different structures of the FeAs layers, such as 11, 111, 122, 1111, 32522, and 21311 (or 42622) families, have been found. By synthesis, $Ba_{1-x}K_xFe_2As_2$ superconductivity was observed with a critical temperature, $T_C = 38$ K [3]. This compound is known as a 122 family. A completely new class of high-temperature superconductors containing iron coordinated with pnictogen atoms (such as As or P), called iron pnictides, was discovered in 2008, and their pairing symmetry is still under investigation [4].

Superconductivity and magnetism are normally mutually exclusive states of electronic systems, and first-order transition between superconductivity and spin density wave orders has been reported in some pnictides. However, recent nuclear magnetic resonance (NMR) [5] and neutron scattering (NS) [6] experiments on $Ba(Fe_{1-x}Co_x)_2As_2$ indicated that spin density wave and superconducting phases coexist over some narrow range. Furthermore, K. Machida had demonstrated the coexistence of spin density wave and superconductivity in highly anisotropic materials [7]. Spin density wave is a kind of anti-ferromagnetic state with electron spin density forming a static wave. The density varies perpendicularly as a function of position with non-magnetization in the entire volume. The spin density wave

transition occurs when the spatial spin density modulation is due to delocalization or in itinerant electrons rather than localized ones. Usually, in the normal state, the density $\rho_{\uparrow}(r)$ of electron spins polarized upward with respect to any quantization axis is completely cancelled by $\rho_{\downarrow}(r)$ or downward polarized spins. In the spin density wave state, however, the difference $\sigma(r) = \rho_{\uparrow}(r) - \rho_{\downarrow}(r)$ is finite and modulates in space as a function of the position vector in the spin density wave state. Such tendency of forming SDW ground state takes place when it possesses nested pieces of Fermi-surface together with intermediate Coulomb correlation structure of alternating layers of Fe-As and Re-O layers where Fe-As layers are thought to be responsible for superconductivity. The parent compound or undoped compound of these systems is not superconducting itself and exhibits both a structural and magnetic phase transition. $BaFe_2As_2$ is a poor Pauli-paramagnetic metal that undergoes a structural and magnetic phase transition at 140 K, accompanied by strong anomalies in the specific heat, electrical resistance, and magnetic susceptibility [3].

2 Theoretical Model System Hamiltonian

In order to find the coexistence of spin density wave and superconductivity in $Ba_{1-x}K_xFe_2As_2$, let us consider the following model Hamiltonian:

$$\hat{H} = \hat{H}_1 + \hat{H}_2 + \hat{H}_3 \tag{1}$$

where

$$\hat{H}_1 = \sum\nolimits_{\kappa,\sigma} \epsilon_\kappa \hat{a}^{\dagger}_{\kappa,\sigma} \hat{a}_{\kappa,\sigma} \tag{2}$$

and is the Hamiltonian or energy of mobile (conduction) electrons,

$$\hat{H}_2 = \Delta_{SC} \sum\nolimits_{\kappa} \left(\hat{a}^{\dagger}_{\kappa\uparrow} \hat{a}^{\dagger}_{-\kappa\downarrow} + \hat{a}_{-k\downarrow} \hat{a}_{k\uparrow} \right) \tag{3}$$

and is the Hamiltonian of the interaction (electron-electron) BCS-type electron-electron pairing, through boson (phonon) exchange and

$$\hat{H}_3 = \Delta_{SDW} \sum\nolimits_{\kappa} \left(\hat{a}^{\dagger}_{\kappa+q\uparrow} \hat{a}^{\dagger}_{\kappa\downarrow} + \hat{a}_{k\downarrow} \hat{a}_{k+q\uparrow} \right) \tag{4}$$

and is the spin density wave Hamiltonian term.

Also, let $\Delta_{SC} = -V \sum_{\kappa} < \hat{a}^{\dagger}_{\kappa\uparrow} \hat{a}^{\dagger}_{-\kappa\downarrow} >= -V \sum_{k} < \hat{a}_{k\uparrow} \hat{a}_{-k\downarrow} >$ and is the superconducting order parameter and $\Delta_{SDW} = -U \sum_{\kappa} < \hat{a}^{\dagger}_{\kappa\uparrow} \hat{a}_{k-q\downarrow} >$ is the spin density wave order parameter, where V and U are the superconducting and spin density wave pairing interactions, respectively.

Here, the operators $\hat{a}^{\dagger}_{\kappa,\sigma}$ *and* $\hat{a}_{\kappa,\sigma}$ are the creation and annihilation operators for Fermionic operators, respectively.

2.1 Equation of Motion

Now, let us evaluate the following commutation relation for free electrons.

$$[\hat{a}_{\kappa\uparrow}, \hat{H}] = \left[\hat{a}_{\kappa\uparrow}, \hat{H}_1\right] + \left[\hat{a}_{\kappa\uparrow}, \hat{H}_2\right] + [\hat{a}_{\kappa\uparrow}, \hat{H}_3] \tag{5}$$

From which we obtain

$$[\hat{a}_{\kappa\uparrow}, \hat{H}_1] = [\hat{a}_{\kappa\uparrow}, \sum\nolimits_{p,\sigma} \epsilon_p \hat{a}^{\dagger}_{p,\sigma} \hat{a}_{p,\sigma} = \epsilon_\kappa \hat{a}_{\kappa,\uparrow} \tag{6}$$

Following a similar procedure as above, for the superconducting part, we get

$$\left[\hat{a}_{\kappa\uparrow}, \hat{H}_2\right] = \left[\hat{a}_{\kappa\uparrow}, \Delta_{SC} \sum\nolimits_{\kappa} \left(\hat{a}^{\dagger}_{\kappa\uparrow} \hat{a}^{\dagger}_{-\kappa\downarrow} + \hat{a}_{-k\downarrow} \hat{a}_{k\uparrow} \right)\right] = \Delta_{SC} \hat{a}^{\dagger}_{-\kappa\downarrow} \tag{7}$$

and

$$\begin{aligned} \left[\hat{a}_{\kappa\uparrow}, \hat{H}_3\right] &= \left[\hat{a}_{\kappa\uparrow}, \Delta_{SDW} \sum\nolimits_{\kappa} \left(\hat{a}^{\dagger}_{\kappa+q\uparrow} \hat{a}^{\dagger}_{\kappa\downarrow} + \hat{a}_{k\downarrow} \hat{a}_{k+q\uparrow} \right)\right] \\ &= \Delta_{SDW} \hat{a}_{k-q\downarrow} \end{aligned} \tag{8}$$

Substituting (6–8) into (1), we obtain

$$\omega \ll \hat{a}_{\kappa\uparrow}, \hat{a}^{\dagger}_{\kappa'\downarrow} \gg_{\omega} = \delta_{\kappa\kappa'} + \ll \left[\hat{a}_{\kappa\uparrow}, \hat{H}\right] \hat{a}^{\dagger}_{\kappa\uparrow} \gg_{\omega} \tag{9}$$

From which we get

$$\begin{aligned} \omega \ll \hat{a}_{\kappa\uparrow} \hat{a}^{\dagger}_{\kappa\uparrow} \gg &= 1 + \epsilon_\kappa \ll \hat{a}_{\kappa\uparrow}, \hat{a}^{\dagger}_{\kappa\uparrow} \gg \\ &\quad + \Delta_{SC} \ll \hat{a}^{\dagger}_{-\kappa\downarrow}, \hat{a}^{\dagger}_{\kappa\uparrow} \gg \\ &\quad + \Delta_{SDW} \ll \hat{a}_{k-q\downarrow}, \hat{a}^{\dagger}_{\kappa\uparrow} \gg \end{aligned}$$

$$\begin{aligned} (\omega - \epsilon_\kappa) \ll \hat{a}_{\kappa\uparrow}, \hat{a}^{\dagger}_{\kappa\uparrow} \gg &= 1 + \Delta_{SC} \ll \hat{a}^{\dagger}_{-\kappa\downarrow}, \hat{a}^{\dagger}_{\kappa\uparrow} \gg \\ &\quad + \Delta_{SDW} \ll \hat{a}_{k-q\downarrow}, \hat{a}^{\dagger}_{\kappa\uparrow} \gg \end{aligned}$$

Finally, we obtain

$$\begin{aligned} \ll \hat{a}_{\kappa\uparrow}, \hat{a}^{\dagger}_{\kappa\uparrow} \gg &= \frac{1}{(\omega - \epsilon_\kappa)} + \frac{\Delta_{SC}}{(\omega - \epsilon_\kappa)} \ll \hat{a}^{\dagger}_{-\kappa\downarrow}, \hat{a}^{\dagger}_{\kappa\uparrow} \gg \\ &\quad + \frac{\Delta_{SDW}}{(\omega - \epsilon_\kappa)} \ll \hat{a}_{k-q\downarrow}, \hat{a}^{\dagger}_{\kappa\uparrow} \gg \end{aligned} \tag{10}$$

Following a similar technique as above, one can also obtain the equation of motion for the expression $\ll \hat{a}^{\dagger}_{-\kappa\downarrow}, \hat{a}^{\dagger}_{\kappa\uparrow} \gg$,

$$\begin{aligned} (\omega + \epsilon_\kappa) \ll \hat{a}^{\dagger}_{-\kappa\downarrow}, \hat{a}^{\dagger}_{\kappa\uparrow} \gg &= \Delta_{SC} \ll \hat{a}_{k\uparrow}, \hat{a}^{\dagger}_{k\uparrow} \gg \\ &\quad - \Delta_{SDW} \ll \hat{a}^{\dagger}_{-\kappa+q\uparrow}, \hat{a}^{\dagger}_{\kappa\uparrow} \gg \end{aligned}$$

From which we obtain

$$\begin{aligned} \ll \hat{a}^{\dagger}_{-\kappa\downarrow}, \hat{a}^{\dagger}_{\kappa\uparrow} \gg &= \frac{\Delta_{SC}}{(\omega + \epsilon_\kappa)} \ll \hat{a}_{k\uparrow}, \hat{a}^{\dagger}_{k\uparrow} \gg - \frac{\Delta_{SDW}}{(\omega + \epsilon_\kappa)} \\ &\quad \ll \hat{a}^{\dagger}_{-\kappa+q\uparrow}, \hat{a}^{\dagger}_{\kappa\uparrow} \gg \end{aligned} \tag{11}$$

Similarly, the equation of motion for the expression $\ll \hat{a}_{k-q\downarrow}, \hat{a}^{\dagger}_{\kappa\uparrow} \gg$ is obtained to be

$$\begin{aligned} (\omega - \epsilon_{\kappa-q}) \ll \hat{a}_{k-q\downarrow}, \hat{a}^{\dagger}_{\kappa\uparrow} \gg &= -\Delta_{SC} \ll \hat{a}^{\dagger}_{-\kappa+q\uparrow}, \hat{a}^{\dagger}_{k\uparrow} \gg \\ &\quad + \Delta_{SDW} \ll \hat{a}_{k\uparrow}, \hat{a}^{\dagger}_{\kappa\uparrow} \gg \end{aligned}$$

which yields

$$\ll \hat{a}_{k-q\downarrow}, \hat{a}^{\dagger}_{\kappa\uparrow} \gg = -\frac{\Delta_{SC}}{(\omega - \epsilon_{\kappa-q})} \ll \hat{a}^{\dagger}_{-\kappa+q\uparrow}, \hat{a}^{\dagger}_{k\uparrow} \gg - \frac{\Delta_{SDW}}{(\omega - \epsilon_{\kappa-q})} \ll \hat{a}_{k\uparrow}, \hat{a}^{\dagger}_{\kappa\uparrow} \gg \quad (12)$$

Similarly, the equation of motion for the correlation, $\ll \hat{a}^{\dagger}_{-\kappa+q\uparrow}, \hat{a}^{\dagger}_{k\uparrow} \gg$, can be obtained following a similar technique. That is,

$$(\omega + \epsilon_{\kappa-q}) \ll \hat{a}^{\dagger}_{-\kappa+q\uparrow}, \hat{a}^{\dagger}_{\kappa\uparrow} \gg = -\Delta_{SC} \ll \hat{a}_{k-q\downarrow}, \hat{a}^{\dagger}_{k\uparrow} \gg - \Delta_{SDW} \ll \hat{a}^{\dagger}_{-\kappa\downarrow}, \hat{a}^{\dagger}_{\kappa\uparrow} \gg$$

Hence we get

$$\ll \hat{a}^{\dagger}_{-\kappa+q\uparrow}, \hat{a}^{\dagger}_{\kappa\uparrow} \gg = -\frac{\Delta_{SC}}{(\omega + \epsilon_{\kappa-q})} \ll \hat{a}_{k-q\downarrow}, \hat{a}^{\dagger}_{k\uparrow} \gg - \frac{\Delta_{SDW}}{(\omega + \epsilon_{\kappa-q})} \ll \hat{a}^{\dagger}_{-\kappa\downarrow}, \hat{a}^{\dagger}_{\kappa\uparrow} \gg \quad (13)$$

Substituting (10) and (13) into (11) and rearranging the expression, we obtain

$$\ll \hat{a}^{\dagger}_{-\kappa\downarrow}, \hat{a}^{\dagger}_{\kappa\uparrow} \gg = \frac{\Delta_{SC}(\omega + \epsilon_{\kappa-q})}{(\omega^2 - \epsilon_{\kappa}^2)(\omega + \epsilon_{\kappa-q}) - \left\{\Delta_{SC}^2(\omega + \epsilon_{\kappa-q}) + \Delta_{SDW}^2(\omega - \epsilon_{\kappa})\right\}} + \frac{\Delta_{SC}\Delta_{SDW}(\omega + \epsilon_{\kappa-q} + \omega + \epsilon_{\kappa})}{(\omega^2 - \epsilon_{\kappa}^2)(\omega + \epsilon_{\kappa-q}) - \left\{\Delta_{SC}^2(\omega + \epsilon_{\kappa-q}) + \Delta_{SDW}^2(\omega - \epsilon_{\kappa})\right\}} \ll \hat{a}_{k-q\downarrow}, \hat{a}^{\dagger}_{\kappa\uparrow} \gg \quad (14)$$

Similarly, by substituting (10) and (13) into (12) and by rearranging, we obtain

$$\ll \hat{a}_{k-q\downarrow}, \hat{a}^{\dagger}_{\kappa\uparrow} \gg = \frac{\Delta_{SC}(\omega + \epsilon_{\kappa-q})}{(\omega^2 - \epsilon_{\kappa-q}^2)(\omega - \epsilon_{\kappa}) - \left\{\Delta_{SC}^2(\omega - \epsilon_{\kappa}) + \Delta_{SDW}^2(\omega + \epsilon_{\kappa-q})\right\}} + \frac{\Delta_{SC}\Delta_{SDW}(\omega + \epsilon_{\kappa-q} + \omega + \epsilon_{\kappa})}{(\omega^2 - \epsilon_{\kappa}^2)(\omega + \epsilon_{\kappa-q}) - \left\{\Delta_{SC}^2(\omega + \epsilon_{\kappa-q}) + \Delta_{SDW}^2(\omega - \epsilon_{\kappa})\right\}} \ll \hat{a}_{-k\downarrow}, \hat{a}^{\dagger}_{\kappa\uparrow} \gg \quad (15)$$

Now, applying nesting condition such that $\epsilon_{\kappa} = -\epsilon_{\kappa\pm q}$, $\epsilon_{-\kappa} = -\epsilon_{\kappa\mp q}$, and the approximation $\epsilon_{\kappa} = \epsilon_{-\kappa}$, and after some rearrangements (14) and (15) can be written, respectively, as,

$$\ll \hat{a}^{\dagger}_{-\kappa\downarrow}, \hat{a}^{\dagger}_{\kappa\uparrow} \gg = \frac{1}{2}\left\{\frac{\Delta_{SC} + \Delta_{SDW}}{(\omega^2 - \epsilon_{\kappa}^2) - (\Delta_{SC} + \Delta_{SDW})^2} + \frac{\Delta_{SC} - \Delta_{SDW}}{(\omega^2 - \epsilon_{\kappa}^2) - (\Delta_{SC} - \Delta_{SDW})^2}\right\} \quad (16)$$

and

$$\ll \hat{a}_{k-q\downarrow}, \hat{a}^{\dagger}_{\kappa\uparrow} \gg = \frac{1}{2}\left\{\frac{\Delta_{SC} + \Delta_{SDW}}{(\omega^2 - \epsilon_{\kappa}^2) - (\Delta_{SC} + \Delta_{SDW})^2} + \frac{\Delta_{SDW} - \Delta_{SC}}{(\omega^2 - \epsilon_{\kappa}^2) - (\Delta_{SC} - \Delta_{SDW})^2}\right\} \quad (17)$$

Now, let us consider the following cases:

Case 1 The superconducting order parameters can be related to Green's function as

$$\Delta_{SC} = -\frac{V}{\beta}\sum\nolimits_{k} \ll \hat{a}^{\dagger}_{-\kappa\downarrow}, \hat{a}^{\dagger}_{\kappa\uparrow} \gg = -\frac{V}{2\beta}\sum\nolimits_{k,n}\left\{\frac{\Delta_{SC} + \Delta_{SDW}}{(\omega^2 - \epsilon_{\kappa}^2) - (\Delta_{SC} + \Delta_{SDW})^2} + \frac{\Delta_{SC} - \Delta_{SDW}}{(\omega^2 - \epsilon_{\kappa}^2) - (\Delta_{SC} - \Delta_{SDW})^2}\right\} \quad (18)$$

Using the expression $\omega \to i\omega_n$ and Matsubara's frequency [8], we get

$$\omega_n = (2n+1)\frac{\pi}{\beta} \quad (19)$$

Now, by changing the summation into integration and by introducing the density of states at the Fermi level, $N(0)$, we get

$$\Delta_{SC} = \beta N(0) V \int_0^{\hbar\omega_F} \left\{ (\Delta_{SC} + \Delta_{SDW}) \frac{1}{2\beta\epsilon} \tanh(\beta\epsilon/2) + (\Delta_{SC} - \Delta_{SDW}) \frac{1}{2\beta\epsilon'} \tanh\left(\beta\epsilon'/2\right) \right\} d\epsilon \quad (20)$$

where $\epsilon^2 = \epsilon_\kappa^2 + (\Delta_{SC} + \Delta_{SDW})^2$ and $\epsilon'^2 = \epsilon_\kappa^2 + (\Delta_{SC} - \Delta_{SDW})^2$

$$\frac{\tanh(\beta\epsilon/2)}{2\beta\epsilon} = \sum\nolimits_n \frac{1}{(2n+1)^2\pi^2 + (\beta\epsilon)^2}$$

$$\frac{\tanh\left(\beta\epsilon'/2\right)}{2\beta\epsilon'} = \sum\nolimits_n \frac{1}{(2n+1)^2\pi^2 + (\beta\epsilon')^2}$$

As $T \to 0K$, $\beta \to \infty$, so that $\tanh(\beta E/2) \to 1$

Thus, (20) becomes

$$\frac{1}{\lambda} = \ln\left(1.14\frac{\hbar\omega_F}{k_B T_c}\right) - \frac{7\Delta_{SDW}\beta^2\xi(3)}{8\pi^2} + \frac{\beta\Delta_{SDW}}{4} \ln\left\{\frac{\hbar\omega_F + \Delta_{SDW}}{\hbar\omega_F - \Delta_{SDW}}\right\}$$

From which we obtain

$$T_C = \frac{1.14}{k_B}\hbar\omega_F \exp\left(\frac{-1}{\lambda} - b\Delta_{SDW}\right) \quad (21)$$

where $\lambda = N(0)V$, $\beta = \frac{1}{k_B T_c}$, and $b = \frac{\beta}{4}\ln\left\{\frac{\hbar\omega_F + \Delta_{SDW}}{\hbar\omega_F - \Delta_{SDW}}\right\}$

Case 2 The spin density wave order parameter can be related with Green's function as

$$\Delta_{SDW} = -\frac{U}{\beta}\sum\nolimits_k \ll \hat{a}_{k-q\downarrow}, \hat{a}^\dagger_{\kappa\uparrow} \gg = -\frac{U}{2\beta}\sum\nolimits_k \left\{ \frac{\Delta_{SC} + \Delta_{SDW}}{\left(\omega^2 - \epsilon_\kappa^2\right) - (\Delta_{SC} + \Delta_{SDW})^2} + \frac{\Delta_{SDW} - \Delta_{SC}}{\left(\omega^2 - \epsilon_\kappa^2\right) - (\Delta_{SC} - \Delta_{SDW})^2} \right\} \quad (22)$$

Using the same procedure that we have used to calculate the transition temperature in Case 1, we can also determine the spin density wave transition temperature as follows:

$$\Delta_{SDW} = \beta\lambda' \int_0^{\hbar\omega_F} \left\{ (\Delta_{SC} + \Delta_{SDW}) \frac{1}{2\beta\epsilon} \tanh(\beta\epsilon/2) + (\Delta_{SDW} - \Delta_{SC}) \frac{1}{2\beta\epsilon'} \tanh\left(\beta\epsilon'/2\right) \right\} d\epsilon \quad (23)$$

At a low temperature, we get

$$\frac{1}{\lambda'} = \ln\left(1.14\frac{\hbar\omega_F}{k_B T_c}\right) - \frac{7\Delta_{SC}\beta^2\xi(3)}{8\pi^2} + \frac{\beta\Delta_{SC}}{4} \ln\left\{\frac{\hbar\omega_F + \Delta_{SC}}{\hbar\omega_F - \Delta_{SC}}\right\}$$

By neglecting the higher order terms, we obtain the spin density wave transition temperature to be

$$T_{SDW} = \frac{1.14}{k_B}\hbar\omega_F \exp\left(\frac{-1}{\lambda} + b\Delta_{SC}\right) \quad (24)$$

where $\lambda' = N(0)U$ and $b = \frac{\beta}{4}\ln\left\{\frac{\hbar\omega_F + \Delta_{SC}}{\hbar\omega_F - \Delta_{SC}}\right\}$

2.2 Superconducting Order Parameter in Pure Superconducting Region

In pure superconducting region, the superconducting order parameter of the spin density wave will become zero, i.e., $\Delta_{SDW} \to 0$

$$\frac{1}{\lambda} = \int_0^{\hbar\omega_F} \frac{\tanh\frac{\beta\sqrt{\epsilon_k^2 + \Delta_{SC}^2}}{2}}{\sqrt{\epsilon_k^2 + \Delta_{SC}^2}} d\epsilon \quad (25)$$

By using the technique of Laplace transform and by using integration by parts, (25) can be expressed as

$$\frac{1}{\lambda} = \ln\left(1.14\frac{\hbar\omega_F}{k_B T}\right) - \frac{7\Delta_{SC}\beta^2\xi(3)}{8\pi^2} \quad (26)$$

In pure superconducting region, (21) can be reduced to the well-known BCS model.

That is,

$$T_c = \frac{1.14\hbar\omega_F}{k_B} e^{\frac{-1}{\lambda}} \quad (27)$$

From this we can get

$$\frac{1}{\lambda} = \ln\left(1.14\frac{\hbar\omega_F}{k_B T_c}\right) \quad (28)$$

From (26) and (28), we get

$$\ln\left(1.14\frac{\hbar\omega_F}{k_B T_c}\right) = \ln\left(1.14\frac{\hbar\omega_F}{k_B T}\right) - \frac{7\Delta_{SC}\beta^2\xi(3)}{8\pi^2} \quad (29)$$

Rearranging (29), we have

$$\ln\frac{T}{T_C} = -\frac{7\Delta_{SC}\beta^2\xi(3)}{8\pi^2} \quad (30)$$

Using the relation in $(1-x) = -x - x^2/2 + \ldots$, we get

$$-(1 - T/T_c) \approx \ln(T/T_c) = -\Delta_{SC}^2 \left(\frac{1}{\pi k_B T_c}\right)^2 1.05 + \ldots$$

From which we can get

$$\Delta_{SC}(T) = 306 k_B T_c (1 - T/T_c)^{1/2} \quad (31)$$

Equation (31) shows how the superconducting order parameter, $\Delta_{Sc}(T)$, varies with temperature and it is similar to the Bardeen, Cooper and Schriffer (BCS) model.

From the BCS theory, $\Delta(0) \approx 2k_B T_c$. Now, using $T_C = 38$ K from the experimental value of $Ba_{1-x}K_xFe_2As_2$ [9], the superconducting order parameter, $\Delta(0)$, at zero temperature is given by $\Delta(0) = 9.42$ meV.

2.3 Spin Density Wave Order Parameter in Pure Spin Density Wave Region

In pure spin density wave region, the superconducting order parameter will become zero, that is, $\Delta_{Sc} \rightarrow 0$. Thus, we get

$$\frac{1}{\lambda'} = \int_0^{\hbar\omega_F} \frac{tanh\frac{\beta\sqrt{\epsilon^2{}_k+\Delta^2_{SDW}}}{2}}{\sqrt{\epsilon^2{}_k+\Delta^2_{SDW}}} d\epsilon \tag{32}$$

Equation (32) can be expressed as

$$\frac{1}{\lambda'} = \ln\left(1.14\frac{\hbar\omega_F}{k_B T}\right) - \frac{7\Delta_{SDW}\beta^2\xi(3)}{8\pi^2} \tag{33}$$

In pure SDW region, that is, for $\Delta_{Sc} = 0$, (24) becomes

$$T_{SDW} = \frac{1.14}{k_B}\hbar\omega_F e^{\frac{-1}{\lambda'}} \tag{34}$$

From which we can get

$$\frac{1}{\lambda'} = \ln\left(1.14\frac{\hbar\omega_F}{k_B T_{SDW}}\right) \tag{35}$$

Equating (33) and (35), we get

$$\ln\left(1.14\frac{\hbar\omega_F}{k_B T_{SDW}}\right) = \ln\left(1.14\frac{\hbar\omega_F}{k_B T}\right) - \frac{7\Delta_{SDW}\beta^2\xi(3)}{8\pi^2} \tag{36}$$

Rearranging (36), we obtain

$$\Delta_{SDW}(T) = 3.06 k_B T_{SDW}(1 - T/T_{SDW})^{1/2} \tag{37}$$

3 Results and Discussion

In this section, we describe the results which are obtained using the model Hamiltonian developed. We obtained the expressions for the superconducting ordering parameter (Δ_{Sc}) and SDW order parameter (Δ_{SDW}) with respect to superconducting transition temperature (T_C) and SDW transition temperature (T_{SDW}), respectively. In our analysis, we obtained the expression for pure superconducting region which can be reduced to the BCS model for $\Delta_{SDW} \rightarrow 0$. From (21), we observed that the spin density wave order parameter suppresses the transition temperature of superconductivity.

By employing (31) and the experimental value, T_C = 38 K, for $Ba_{1-x}K_xFe_2As_2$, and by using MATLAB script, we plotted the superconducting transition temperature (T_C) versus superconducting order parameter (Δ_{SC}) as shown in Fig. 1.

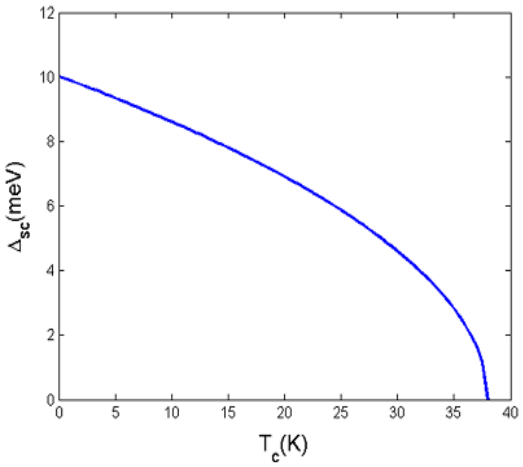

Fig. 1 Transition temperature (T_C) versus superconducting order parameter (Δ) for $Ba_{1-x}K_xFe_2As_2$ superconductor

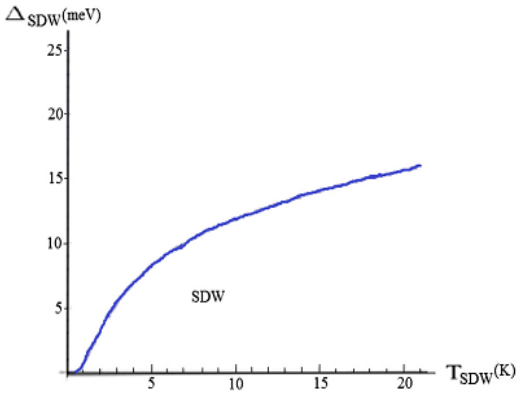

Fig. 2 SDW transition temperature (T_{SDW}) versus SDW order parameter (Δ_{SDW}) for $Ba_{1-x}K_xFe_2As_2$ superconductor

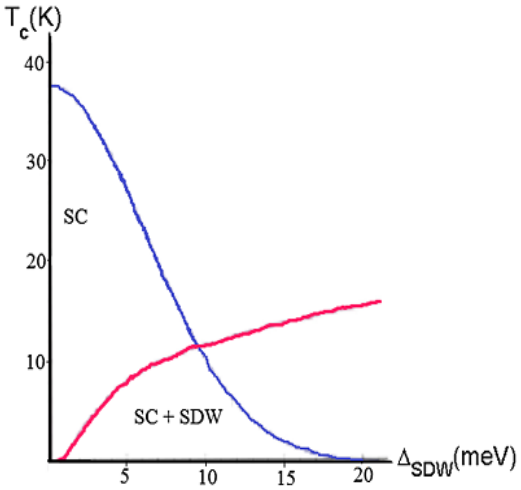

Fig. 3 Coexistence of superconductivity and spin density wave (SDW) in ferropnictide $Ba_{1-x}K_xFe_2As_2$

As can be observed from Fig. 1, as the temperature increases, the superconducting order parameter decreases and vanishes at the superconducting transition temperature (T_C). Furthermore, by employing (37) and (24), we plotted the SDW transition temperature (T_{SDW}) versus SDW order parameter (Δ_{SDW}) as demonstrated in Fig. 2.

It can be observed from Fig. 2 that the SDW transition temperature increases as the SDW order parameter increases.

Now, by combining Figs. 1 and 2, we obtained a region where both superconductivity and spin density wave coexist in ferropnictide $Ba_{1-x}K_xFe_2As_2$ as shown in Fig. 3.

4 Conclusion

In the present work, the coexistence of superconductivity and spin density wave (SDW) has been discussed using the model Hamiltonian. We have used the Green's function formalism to find the equation of motion that enables us to determine the superconducting and spin density wave order parameters. By plotting phase diagrams for $Ba_{1-x}K_xFe_2As_2$, we have demonstrated the possible coexistence of superconductivity and spin density wave in $Ba_{1-x}K_xFe_2As_2$. The result obtained is in good agreement with experimental observations [10].

References

1. Onnes, H.K.: Akad. Wet. (Amsterdam) **14**, 113 (1911)
2. Kamihara, Y., Watanabe, T., Hirano, M., Hosono, H.: Iron-based layered superconductor $LaO_{1-x}F_xFeAs$(x = 0.05-0.12) with T_C = 26 K. J. Am. Chem. Soc. **130**, 3296 (2008)
3. Rotter, M., Tegel, M., Johrendt, D.: Superconductivity at 38K in the iron arsenide. Phys. Rev. Lett. **101**, 107006 (2008)
4. Rotter, M., Tegel. M., Jorendt, D.: Superconductivity at 38K in the iron arsenide ($Ba_{1-x}K_x)Fe_2As_2$). Condmat. Supr. Con. **2**, 4630 (2008)
5. Manousakis, E., Ren, J., Meng, S., Kaxiras, E.: Is the nature of magnetic order in copper-oxides and in iron-pnictides different? Solid State Commun. **150**, 62 (2010)
6. Chu, J.H., Analytis, J.G., Kucharczyk, C., Fisher, I.R.: Determination of the phase diagram of the electron-doped superconductor $Ba(Fe_{1-x}Cox)_2As_2$. Phys. Rev. B **79**, 014506 (2009)
7. Machida, K.: Spin density wave and superconductivity in highly anisotropic materials. J. Phys. Soc. Jpn. **50**, 2195 (1981)
8. Zubarev, D.N.: Double-time green functions in statistical physics. Sov. Phys. Uspekhi **3**, 320 (1960)
9. Ding, H., Richard, P., Nakayama, K., Sugawara, T., Arakane, T., Sekiba, Y., Takayama, A., Souma, S., Sato, T., Takahashi, T., Wang, Z., Dai, X., Fang, Z., Chen1, G.F., Luo1, J.L., Wang, N.L.: Observation of Fermi-surface-dependent nodeless superconducting gaps in $Ba_{0.6}K_{0.4}Fe_2As_2$. Europhys. Lett. **83**, 47001 (2008)
10. Julien, M.H., Mayaffre, H., Horvatic, M., Berthier, C., Zhang, X.D., Wu, W., Chen, G.F., Wang, N.L., Luo, J.L.: Homogeneous versus inhomogeneous coexistence of magnetic order and superconductivity probed by NMR in Co and K-doped iron pnictides. EuroPhys. Lett. **87**, 37001 (2009)

Chapter 4

Theoretical Study of the Interplay of itinerant and localized electrons in iron based superconductors

4.1 Introduction

One key issue under early debate is about whether the iron $3d$ electrons should be treated as itinerant electrons or local moments. Underlying this dispute, there are two different schools of thought about the mechanism for superconductivity. these are

- the Bardeen-Cooper-Schieffer (BCS) theory in a weakly interacting metal [4,86] and
- the resonating valence bound (RVB) type of theory for a strongly correlated system like the cuprate [87, 88].

The BCS theory is based on a weakly correlated Fermi liquid state of itinerant electrons. At low temperatures, a Fermi liquid state will become unstable against any weak attractive interaction, which drives the electrons near Fermi surface to form Cooper pairs and condense, giving rise to superconductivity. The effective attraction

can be either mediated by phonons, plasomons, magnons etc, or originated from the bare electron interaction via the fluctuation-exchange (FLEX) or the renormalization group (RG) approaches. To make the attraction dominant at low-energy, the Coulomb repulsion must be effectively screened, which in turn requires the electrons be itinerant, such that the BCS theory usually works for a system of metallic normal state [89–91].

On the other hand, in a strongly correlated system like the cuprate, the electrons can be localized, due to the strong Coulomb interaction, to form a Mott insulator at half-filling. Here, its charge degree of freedom is gapped, while the remaining spin degree of freedom forms a lattice of fluctuating local moments. Superconductivity arises upon charge doping into the Mott insulator. The failure of a conventional BCS theory lies in that, the Coulomb repulsion becomes a dominant effect in shaping the electronic state instead of simply getting screened in the BCS theory. In such a single-band strongly correlated system, electron fractionalization is a natural consequence in which doped charges and localized spins behave distinctly as separated degrees of freedom. The underlying mechanism for superconductivity is generally known as an RVB theory because the singlet pairing of the local moments becomes partially charged upon doping, resembling the Cooper pairing, to give rise high-Tc superconductivity [87, 88].

While the BCS theory and the RVB theory lie in the opposite extremes of the electron correlations, most studies seem to agree on that, the iron-based compounds are intermediate correlated electron systems [52, 92]. In particular, the multi-band iron

3d electrons are involved in the low-energy sector in contrast to the single-band 3d electrons in the cuprates. A new possibility may arise in the low energy regime of the iron-based superconductors, in which the multi-band 3d electrons effectively behave as if some of them still remain itinerant near the Fermi energy and some of them become more localized like in a Mott insulator. Such a fractionalization into two more *conventional* subsystems of itinerant and localized electrons in a multi-band case is in sharp and interesting contrast with a novel fractionalization of electrons in a single band doped Mott insulator. Here, without doping into the Mott insulator, the itinerant electrons remain effectively separated from the local moments as independent degrees of freedom and two subsystems mutually interact with an intermediate coupling strength which can be tractable perturbatively.

4.2 Theories of itinerant and localized electrons for Iron-Based Superconductors

In general, there are three schools of theories: itinerant theory [49, 93] , localized theory [94, 95] and the hybrid theory of coexistent itinerant and localized electrons [96] as shown in table 4.1.

Table 4.1: Comparison of main-stream theories for iron-based superconductor.

Description	**Itinerant electron**	**Local moment**	**Hybrid**
Degrees of freedom	Itinerant electrons	Local moments	Coexistence of both
Electron correlation	Weak	Strong	Intermediate
Starting point	Fermi liquid	Mott insulator	Orbital-selective Mott
SC mechanism	BCS pairing	Spin RVB pairing	BCS pairing
Pairing glue	Electron collective fluctuation	Superexchange	Local moment fluctuation

The itinerant theory is built on the picture of pure itinerant electrons, which views the iron-based superconductor as a simple BCS superconductor with the electron pairing mediated by spin-fluctuations generated by the interaction amongst itinerant electrons. The local theory takes a strong correlation point of view and considers the iron-based superconductor as a multi-band version of doped Mott insulators similar to the cuprates. The co-existence theory emphasizes that, itinerant electrons and local moments should both exist in the iron-based materia, as independent degrees of freedom at least in the low-energy sector [97].

4.3 Minimal model

Our model Hamiltonian is composed of three terms

$$\hat{H} = \hat{H}_{it} + \hat{H}_{lo} + \hat{H}_{int} \tag{4.3.1}$$

where the first term is given by,

$$\begin{aligned} \hat{H}_{it} &= -\sum_{k\sigma} t_{ij} \hat{C}^{+}_{k\sigma} \hat{C}_{k\sigma} + h.c \\ &= -\sum_{k\sigma} t_{ij} \hat{C}^{+}_{k\sigma} \hat{C}_{k\sigma} - \sum_{kk'} V_{kk'} \hat{C}^{+}_{k\uparrow} \hat{C}^{+}_{-k\downarrow} \hat{C}_{-k'\downarrow} \hat{C}_{k'\uparrow} \end{aligned} \tag{4.3.2}$$

the term $\sum_{k\sigma} t_{ij} \hat{C}^{+}_{k\sigma} \hat{C}_{k\sigma}$ describes the Hamiltonian of total energy of the itinerant electrons in one electron band approximation [98]. Here the operator $\hat{C}^{+}_{k\sigma}(\hat{C}_{k\sigma})$ creates (annihilates) an electron with the wave vector k and the spin projection on z-axis $\sigma = \uparrow$ or $\downarrow$; $V_{kk'}$ is the pairing potential.

The second term is given by,

$$\hat{H}_{loc} = \sum_{i,j} J S_i . S_j \tag{4.3.3}$$

and describes the predominant interaction between the local moment by Heisenberg like model, and we considered only the nearest neighbor interaction. Here J is the nearest neighbor exchange that bridge by the As ions and it could be anti ferromagnetic in nature.

The third term which is given by,

$$\hat{H}_{int} = -g \sum_i \sigma_i . S_i \tag{4.3.4}$$

describes the interaction between the spin σ_i of the itinerant electrons and the five $3d$ spin S_i local moment located at site i, where g is the corresponding exchange constant.

To get an effective interaction we change the momentum term in to boson operator. Diagonalizing the Hamiltonian($\hat{H}_{loc}$) using Bogoliubov transformation,

$$\hat{C}_k = u_k \hat{b}_k + v_k \hat{b}^\dagger_{-k}$$

for boson,

$$|u_k|^2 - |v_k|^2 = 1$$

This can be parameterized by hyperbolic angle $u_k = \cosh\theta_k$, $v_k = \sinh\theta_k$, which is real and even under $k \longrightarrow -k$. The canonical form of the Hamiltonian in terms of spin waves,

$$\therefore \hat{H}_{loc} = E_0 + \sum_k \omega_k \hat{b}^\dagger_k \hat{b}_k \tag{4.3.5}$$

We obtained the itinerant electrons and localized electrons moment using relations in spin operators like,

$$S^\sigma_i = \hat{C}^\dagger_{i\sigma} \hat{C}_{i-\sigma}, \frac{1}{\hbar}\sigma^\dagger_i = \hat{C}^\dagger_{i\downarrow} \hat{C}_{i\uparrow}, \frac{1}{\hbar}\sigma^z_i = \frac{1}{2}\sum_\sigma z_\sigma n_{i\sigma}; (z_{\uparrow=+1}; z_\downarrow = -1)$$

The electrons in the valence band which are interacting with an anti ferromagnetically ordered, localized spin system can be described by,

$$\hat{H}_{int} = -\frac{1}{2} g\hbar \langle S^z \rangle \sum_{k\sigma} \hat{C}^{\dagger}_{k\sigma} \hat{C}_{k\sigma} \tag{4.3.6}$$

Substituting equations (4.3.2), (4.3.5) and (4.3.6) into equation (4.3.1), we get an effective Hamiltonian,

$$\hat{H} = \sum_{k\sigma} \varepsilon(k) \hat{C}^{\dagger}_{k\sigma} \hat{C}_{k\sigma} - \sum_{kk'} V_{kk'} \hat{C}^{\dagger}_{k\uparrow} \hat{C}^{\dagger}_{-k\downarrow} \hat{C}_{-k'\downarrow} \hat{C}_{k'\uparrow} + E_0 + \sum_{k} \omega_k \hat{b}^{\dagger}_k \hat{b}_k - \frac{1}{2} g\hbar \langle S^z \rangle \sum_{k\sigma} \hat{C}^{\dagger}_{k\sigma} \hat{C}_{k\sigma} \tag{4.3.7}$$

4.3.1 Equation of Motion

To get the equation of motion we use the double-time temperature dependent Greens function which is defined by:

$$\omega << A; B >>_{\omega} = < [A, B] >_{\omega} + << [A, \hat{H}]; B >>_{\omega} \tag{4.3.8}$$

$$\omega << \hat{C}_{k\uparrow}; \hat{C}^{\dagger}_{k\uparrow} >>_{\omega} = 1 + << [\hat{C}_{k\uparrow}, \hat{H}]; \hat{C}^{\dagger}_{k\uparrow} >>_{\omega} \tag{4.3.9}$$

Now to solve equation (4.3.9) let us evaluate the following commutating relation

$$\begin{aligned} [\hat{C}_{k\uparrow}, \hat{H}] &= [\hat{C}_{k\uparrow}, \hat{H}_{iti} + \hat{H}_{loc} + \hat{H}_{int}] \\ &= [\hat{C}_{k\uparrow}, \hat{H}_{iti}] + [\hat{C}_{k\uparrow}, \hat{H}_{loc}] + [\hat{C}_{k\uparrow}, \hat{H}_{int}] \end{aligned}$$

From which we obtain,

$$\begin{aligned} [\hat{C}_{k\uparrow}, \hat{H}_{iti}] &= [\hat{C}_{k\uparrow}, \sum_{k\sigma} \varepsilon(k) \hat{C}^{\dagger}_{k\sigma} \hat{C}_{k\sigma} - \sum_{kk'} V_{kk'} \hat{C}^{\dagger}_{k\uparrow} \hat{C}^{\dagger}_{-k\downarrow} \hat{C}_{-k'\downarrow} \hat{C}_{k'\uparrow}] \\ &= \sum_{k\sigma} \varepsilon(k) \hat{C}_{k\sigma} \{\hat{C}_{k\uparrow}, \hat{C}^{\dagger}_{k\sigma}\} - \sum_{kk'} V_{kk'} [\hat{C}_{k\uparrow}, \hat{C}^{\dagger}_{k\uparrow} \hat{C}^{\dagger}_{-k\downarrow}] \hat{C}_{-k'\downarrow} \hat{C}_{k'\uparrow} \\ &= \sum_{k\sigma} \varepsilon(k) \hat{C}_{k\sigma} \delta_{kk} \delta_{\uparrow\sigma} - \sum_{kk'} V_{kk'} \hat{C}_{-k'\downarrow} \hat{C}_{k'\uparrow} (\{\hat{C}_{k\uparrow}, \hat{C}^{\dagger}_{k\uparrow}\} \hat{C}^{\dagger}_{-k\downarrow} - \hat{C}^{\dagger}_{k\uparrow} \{\hat{C}_{k\uparrow}, \hat{C}^{\dagger}_{-k\downarrow}\}) \\ \therefore [\hat{C}_{k\uparrow}, \hat{H}_{iti}] &= \varepsilon_k \hat{C}_{k\uparrow} - \sum_{kk'} V_{kk'} \hat{C}^{\dagger}_{-k\downarrow} \hat{C}_{-k'\downarrow} \hat{C}_{k'\uparrow} \end{aligned} \tag{4.3.10}$$

we used similar procedure for $[\hat{C}_{k\uparrow}, \hat{H}_{loc}]$, that is,

$$[\hat{C}_{k\uparrow}, \hat{H}_{loc}] = [\hat{C}_{k\uparrow}, (E_0 + \sum_k \omega_k \hat{b}_k^\dagger \hat{b}_k)] = 0 \tag{4.3.11}$$

In a similar manner we applied for $[\hat{C}_{k\uparrow}, \hat{H}_{int}]$, and obtain,

$$\begin{aligned} [\hat{C}_{k\uparrow}, \hat{H}_{int}] &= [\hat{C}_{k\uparrow}, -\frac{1}{2} g\hbar \langle S^z \rangle \sum_{k\sigma} \hat{C}_{k\sigma}^\dagger \hat{C}_{k\sigma}] \\ \therefore [\hat{C}_{k\uparrow}, \hat{H}_{int}] &= -\frac{1}{2} g\hbar \langle S^z \rangle \hat{C}_{k\uparrow} \end{aligned} \tag{4.3.12}$$

Thus,

$$[\hat{C}_{k\uparrow}, \hat{H}] = (\varepsilon_k - \frac{1}{2} g\hbar \langle S^z \rangle) \hat{C}_{k\uparrow} - \sum_{kk'} V_{kk'} \hat{C}_{-k'\downarrow} \hat{C}_{k'\uparrow} \hat{C}_{-k\downarrow}^\dagger \tag{4.3.13}$$

Hence, equation (4.3.9) becomes,

$$\omega << \hat{C}_{k\uparrow}; \hat{C}_{k\uparrow}^\dagger >> = 1 + (\varepsilon_k - \frac{1}{2} g\hbar \langle S^z \rangle) << [\hat{C}_{k\uparrow}; \hat{C}_{k\uparrow}^\dagger >> - \sum_{kk'} V_{kk'} << \hat{C}_{-k'\downarrow} \hat{C}_{k'\uparrow} \hat{C}_{-k\downarrow}^\dagger; \hat{C}_{k\uparrow}^\dagger >> \tag{4.3.14}$$

In general, we have to write the higher order Greens function into lower order Greens function by using Wicks theorem or decoupling procedure. Thus,

$$<< \hat{C}_{-k'\downarrow} \hat{C}_{k'\uparrow} \hat{C}_{-k\downarrow}^\dagger; \hat{C}_{k\uparrow}^\dagger >> = < \hat{C}_{-k'\downarrow}, \hat{C}_{k'\uparrow} >< < \hat{C}_{-k\downarrow}^\dagger; \hat{C}_{k\uparrow}^\dagger >>$$

Now, substituting this expression into equation (4.3.14) we get,

$$\begin{aligned} (\omega - \varepsilon_k + \frac{1}{2} g\hbar \langle S^z \rangle) << \hat{C}_{k\uparrow}; \hat{C}_{k\uparrow}^\dagger >> &= 1 - \sum_{kk'} V_{kk'} < \hat{C}_{-k'\downarrow}, \hat{C}_{k'\uparrow} >< < \hat{C}_{-k\downarrow}^\dagger; \hat{C}_{k\uparrow}^\dagger >> \\ &= 1 - \Delta << \hat{C}_{-k\downarrow}^\dagger; \hat{C}_{k\uparrow}^\dagger >> \end{aligned} \tag{4.3.15}$$

from this we get,

$$\therefore << \hat{C}_{k\uparrow}; \hat{C}_{k\uparrow}^\dagger >> = \frac{1}{(\omega - \varepsilon_k + \frac{1}{2} g\hbar \langle S^z \rangle)} - \frac{\Delta}{(\omega - \varepsilon_k + \frac{1}{2} g\hbar \langle S^z \rangle)} << \hat{C}_{-k\downarrow}^\dagger; \hat{C}_{k\uparrow}^\dagger >> \tag{4.3.16}$$

where

$$\Delta = \sum_{kk'} V_{kk'} < \hat{C}_{-k'\downarrow}, \hat{C}_{k'\uparrow} >$$

One can also obtain the equation of motion for the expression $<< \hat{C}^{\dagger}_{-k\downarrow}; \hat{C}^{\dagger}_{k\uparrow} >>$ using,

$$\begin{aligned} \omega << \hat{C}^{\dagger}_{-k\downarrow}; \hat{C}^{\dagger}_{k\uparrow} >>_{\omega} &= [\hat{C}^{\dagger}_{-k\downarrow}, \hat{C}^{\dagger}_{k\uparrow}] + << [\hat{C}^{\dagger}_{-k\downarrow}, \hat{H}]; \hat{C}^{\dagger}_{k\uparrow} >>_{\omega} \\ &= 0 + << [\hat{C}^{\dagger}_{-k\downarrow}, \hat{H}_{iti} + \hat{H}_{loc} + \hat{H}_{int}]; \hat{C}^{\dagger}_{k'\uparrow} >>_{\omega} \end{aligned} \tag{4.3.17}$$

Applying the same technique as above, we obtain,

$$\begin{aligned} [\hat{C}^{\dagger}_{-k\downarrow}, \hat{H}_{iti} + \hat{H}_{loc} + \hat{H}_{int}] &= (\frac{1}{2} g\hbar \langle S^z \rangle - \varepsilon_{-k}) \hat{C}^{\dagger}_{-k\downarrow} - \sum_{kk'} V_{kk'} \hat{C}^{\dagger}_{k\uparrow} \hat{C}^{\dagger}_{-k\downarrow} \hat{C}_{k'\uparrow} \\ &= (\frac{1}{2} g\hbar \langle S^z \rangle - \varepsilon_{-k}) \hat{C}^{\dagger}_{-k\downarrow} - \sum_{kk'} V_{kk'} < \hat{C}^{\dagger}_{k\uparrow} \hat{C}^{\dagger}_{-k\downarrow} >< < \hat{C}_{k'\uparrow}, \hat{C}^{\dagger}_{k'\uparrow} >> \end{aligned} \tag{4.3.18}$$

Substituting equation (4.3.18) into equation (4.3.17) yields,

$$\begin{aligned} (\omega + \varepsilon_{-k} - \frac{1}{2} g\hbar \langle S^z \rangle) << \hat{C}^{\dagger}_{-k\downarrow}; \hat{C}^{\dagger}_{k\uparrow} >> &= -\sum_{kk'} V_{kk'} < \hat{C}^{\dagger}_{k\uparrow} \hat{C}^{\dagger}_{-k\downarrow} >< < \hat{C}_{k\uparrow}, \hat{C}^{\dagger}_{k\uparrow} >> \\ \therefore (\omega + \varepsilon_{-k} - \frac{1}{2} g\hbar \langle S^z \rangle) << \hat{C}^{\dagger}_{-k\downarrow}; \hat{C}^{\dagger}_{k\uparrow} >> &= -\Delta^* << \hat{C}_{k\uparrow}, \hat{C}^{\dagger}_{k\uparrow} >> \end{aligned} \tag{4.3.19}$$

from this we get,

$$<< \hat{C}^{\dagger}_{-k\downarrow}; \hat{C}^{\dagger}_{k\uparrow} >> = -\frac{\Delta^{\dagger}}{(\omega + \varepsilon_{-k} - \frac{1}{2} g\hbar \langle S^z \rangle)} << \hat{C}_{k\uparrow}, \hat{C}^{\dagger}_{k\uparrow} >> \tag{4.3.20}$$

where

$$\Delta^{\dagger} = \sum_{kk'} V_{kk'} < \hat{C}^{\dagger}_{k\uparrow} \hat{C}^{\dagger}_{-k\downarrow} >$$

For $\varepsilon_k = \varepsilon_{-k}$ (the kinetic energy of the conduction electrons) and $\Delta = \Delta^{\dagger}$ (taking the order parameter is real), and also by comparing equations (4.3.16) and (4.3.20), we obtain the following expression

$$<< \hat{C}^{\dagger}_{-k\downarrow}, \hat{C}^{\dagger}_{k'\uparrow} >> = \frac{-\Delta}{\omega^2 - \epsilon^2 - \Delta^2} \tag{4.3.21}$$

where $\epsilon = \varepsilon_k - \frac{1}{2}g\hbar\langle S^z\rangle$

The superconducting order parameter (Δ) is defined as,

$$\Delta = \sum_{kk'} \frac{V_{kk'}}{\beta} << \hat{C}^{\dagger}_{-k\downarrow}, \hat{C}^{\dagger}_{k'\uparrow} >>= \sum_{kk'} \frac{V_{kk'}}{\beta} \frac{-\Delta}{\omega^2 - \epsilon^2 - \Delta^2} \tag{4.3.22}$$

The summation may be changed to integration by introducing the density of state $N(\epsilon)$, and equation (4.3.22) becomes,

$$\begin{aligned} \Delta &= \frac{1}{\beta} \sum \int d\varepsilon_0 N(\varepsilon) V_{kk'} \frac{-\Delta}{\omega^2 - \epsilon^2 - \Delta^2} \\ 1 &= \frac{1}{\beta} \sum \int d\varepsilon_0 N(\varepsilon) V_{kk'} \frac{-1}{\omega^2 - \epsilon^2 - \Delta^2} \end{aligned} \tag{4.3.23}$$

where $\beta = \frac{1}{k_\beta T}$ and k_β is the Bolthmann constant.

Attractive interaction is effective for the region $-\hbar\omega_b < \varepsilon < \hbar\omega_b$, and assuming the density of states does not vary over this integral, the expression becomes,

$$\frac{1}{\lambda} = \int_0^{\hbar\omega_b} \frac{2}{\beta} \sum_0^{\infty} \frac{-1}{\omega^2 - \epsilon^2 - \Delta^2} \tag{4.3.24}$$

Applying Laplaces transform with replacement of ω by Matsubara frequency $\omega_n = (2n+1)\frac{\pi}{\beta}$, and using the approximation,

$$\frac{1}{\omega^2 - \epsilon^2 - \Delta^2} \simeq \frac{1}{\omega^2 + \epsilon^2} - \frac{\Delta^2}{(\omega^2 + \epsilon^2)^2}$$

Thus, equation (4.3.24) becomes,

$$\frac{1}{\lambda} = \int_0^{\hbar\omega_b} d\varepsilon \frac{\tanh(\beta/2)\varepsilon}{\varepsilon} - 4\Delta^2 \sum_0^{\infty} (\frac{\beta}{\pi(2n+1)^2})^3 \int_0^{\infty} \frac{1}{(1+x^2)^2} dx = I_1 + I_2 \tag{4.3.25}$$

where $x = \varepsilon/a$; $a = (2n+1)\pi/\beta$

The first integral in equation (4.3.25) becomes,

$$\begin{aligned} I_1 &= \int_0^{\frac{\beta}{2}\hbar\omega_b} \frac{\tanh y}{y} dy; y = \frac{\beta}{2}\varepsilon \\ &= \ln\tanh y|_0^{\frac{\beta}{2}\hbar\omega_b} - \int_0^{\frac{\beta}{2}\hbar\omega_b} \frac{\ln y}{\cosh^2 y} dy \end{aligned} \tag{4.3.26}$$

For low temperature, equation (4.3.26) becomes,

$$I_1 = \ln \frac{1.14}{k_\beta T}(\hbar\omega_b - \frac{1}{2}g\hbar\langle S^z\rangle) \tag{4.3.27}$$

and the second integral becomes,

$$I_2 = 1.05(\frac{\Delta}{\pi k_\beta T})^2 \tag{4.3.28}$$

Hence

$$\frac{1}{\lambda} = \ln \frac{1.14}{k_\beta T}(\hbar\omega_b - \frac{1}{2}g\hbar\langle S^z\rangle) - 1.05(\frac{\Delta}{\pi k_\beta T})^2 \tag{4.3.29}$$

From equation (4.3.29) we can get the superconducting order parameter as a function of temperature to be,

$$\Delta(T) = \frac{\pi k_\beta T}{\sqrt{1.05}}\sqrt{\ln \frac{1.14}{k_\beta T}(\hbar\omega_b - \frac{1}{2}g\hbar\langle S^z\rangle) - \frac{1}{\lambda}} \tag{4.3.30}$$

4.4 Result and Discussion

Using the model Hamiltonian and green function formalism we obtained the result expressed by Equation (4.3.30). We examined the effect of magnetism and temperature on superconducting order parameter.

Now, let us study equation (4.3.29) by considering different cases,

(i). At $T = T_c$, $\Delta = 0$, we get,

$$T_C = \frac{1.14}{k_\beta}(\hbar\omega_b - \frac{1}{2}g\hbar\langle S^z\rangle)e^{-\frac{1}{\lambda}} \tag{4.4.1}$$

II. In the absence of magnetic term ($\langle S^z\rangle = 0$), Equation (4.4.1) reduces to,

$$T_C = \frac{1.14}{k_\beta}\hbar\omega_b e^{-\frac{1}{\lambda}} \tag{4.4.2}$$

and this is the well known BCS expression.

Using the relation $ln(1-x) = -x - x^2/2 + ...$, we get,

$$ln(T/T_c) = ln(1-(1-T/T_c)) = -(1-T/T_c) - (1-T/T_c)^2/2 + ...$$
$$\approx -(1-T/T_c)$$

For $\omega_b = \omega_D$, Equation (4.3.25) can be simplified and obtain,

$$ln(T/T_c) = -\Delta^2(\frac{1}{\pi k_B T})^2 1.05 + ...$$

Therefore,

$$ln(T/T_c) \approx -(1-T/T_c) = -\Delta^2(\frac{1}{\pi k_B T})^2 1.05 + ...$$

Hence,

$$\Rightarrow \Delta(T) = 3.06 k_B T_c (1-\frac{T}{T_c})^{1/2} \tag{4.4.3}$$

This is the expression that shows how the superconducting order parameter, $\Delta(T)$, varies with temperature and it is similar to the BCS theory.

Now, using the Matsubara frequency, we change $\omega \rightarrow i\omega_n$ and using the relation,

$$\frac{1}{2x} tanh(\frac{x}{2}) = \sum_{n=-\infty}^{+\infty} \frac{1}{(2n+1)^2\pi^2 + x^2}$$

we can write equation (4.3.23) as follows,

$$\begin{aligned} \frac{1}{\lambda} &= \int_0^{\hbar\omega_b} \frac{d\varepsilon}{\sqrt{\epsilon^2+\Delta^2}} = \arcsin(\frac{\epsilon}{\Delta})|_0^{\hbar\omega_b} \\ &= \arcsin(\frac{\varepsilon_k - \frac{1}{2}g\hbar\langle S^z\rangle}{\Delta})|_0^{\hbar\omega_b} \\ &\approx \ln(\frac{\hbar\omega_b - \frac{1}{2}g\hbar\langle S^z\rangle}{\Delta} + \sqrt{(\frac{\hbar\omega_b - \frac{1}{2}g\hbar\langle S^z\rangle}{\Delta})^2 + 1}) \end{aligned} \tag{4.4.4}$$

for $(\frac{\hbar\omega_b - \frac{1}{2}g\hbar\langle S^z\rangle}{\Delta})^2 >> 1$ the above equation becomes:-

$$\frac{1}{\lambda} \approx \ln(\frac{2(\hbar\omega_b - \frac{1}{2}g\hbar\langle S^z\rangle)}{\Delta}) \tag{4.4.5}$$

This implies that,

$$\Delta(T \to 0) = 2(\hbar\omega_b - \frac{1}{2}g\hbar\langle S^z\rangle)e^{-\frac{1}{\lambda}} \tag{4.4.6}$$

which is similar to the BCS with an additional term of $\langle S^z\rangle$

4.5 Conclusion

In this chapter, we have proposed a minimal model and shown that it can provide a systematic and quantitative account for a series of anomalous magnetic and Superconducting properties observed in the iron pnictides. This is a Heisenberg model, composed of two independent and distinct components, i.e. the itinerant electrons and local moments, respectively. These two independent degrees of freedom are coupled together by the local Hunds rule interaction at each iron site.

Thus, equation (4.4.1) is clearly in agreement with the fact that as the net magnetization increases, superconductivity decreases. The result clearly indicate that localized magnetism can coexist with itinerant magnetism in iron based superconductor below the critical temperature. Our theoretical predictions are in broad agreement with experimental findings [21, 99, 100] and the result may help in explaining experimental observations.

Chapter 5

Mathematical Techniques

In this chapter, we derive the equation of motion using mathematical techniques that is used to determine the superconducting order parameter(Δ) and the superconducting transition temperature (T_s). There are different types of mathematical methods such as the Green function, the Hubbard model, Stoner model etc. In this work, we used the extended Hubbard model to obtain the expressions of superconducting order parameter(Δ)and superconducting transition temperature (T_c). The extended Hubbard model is useful because it is used for our further study in order to calculate the linearized gap equation of both single spin and triplet equal spin pairing state to investigate the interplay of localized and itinerant electrons of iron based materials.

After a brief survey of the development and uses of the Hubbard model, the hamiltonian is examined using Hartree-Fock approximation which would form the basis of this thesis from an extended Hubbard model.

5.1 The Hubbard Model

In 1963 Hubbard in a series of papers [101–106] developed a "model for electron correlations in narrow energy bands". Although Gutzwiller and Kanamori considered similar models at about the same time, this paradigm of condensed matter physics is universally known as the Hubbard model.

In his original paper [101], Hubbard postulated a Hamiltonian for the electrons in a band and then, by introducing the Wannier functions, derived his Hamiltonian. However, from the perspective of tight binding theory which is the perspective we predominantly take in this thesis, the correct thing to do is to postulate the Hubbard Hamiltonian and proceed from there. We will therefore take the later approach.

Within the tight binding approximation it is natural to consider a lattice of "sites". Each site represents a single orbital of a single atom which can accommodate, at most, two electrons (one of each spin).

The multi-band Hubbard Hamiltonian hopping with intra and inter Coulomb interaction can be written as [107];

$$\begin{aligned} \hat{H} &= \hat{H}_{iti} + \hat{H}_{loc} \\ &= \hat{H}_{Kin} + \hat{H}_{intra} + \hat{H}_{inter} \\ \therefore \hat{H} &= -\sum_{ij\sigma\alpha\alpha'} t_{ij\alpha\alpha'} \hat{C}^{+}_{i\sigma\alpha} \hat{C}_{j\sigma\alpha'} + U \sum_{i} \hat{n}_{i\uparrow} \hat{n}_{i\downarrow} + U' \sum_{ij\sigma\sigma'\alpha\alpha'} \hat{n}^{+}_{i\sigma\alpha} \hat{n}_{j\sigma'\alpha'} \end{aligned} \tag{5.1.1}$$

In eqn.(5.1.1), the first term (the kinetic term) therefore hops fermions from one lattice site i to another site j with a matrix element t_{ij} and α and α' indicates the electron and hole band respectively. The second term describes the local Coulomb interaction (the intra-orbital Coulomb interaction) of electrons at the same site i, and

it is a product of fermionic number operators of opposite spins, and hence this term is zero when there is zero or one fermion on a site and gives an energy penalty U for having two fermions on the same site [107]. The third term describes the inter-orbital Coulomb interaction, where U and U' are respectively the intra- and inter-orbital Hubbard interaction. U is the potential between an electron on site i and an electron with the opposite spin on the same site. U is therefore described as an "on-site" potential. For the interaction energy term, the on-site energy,U, is chosen to be either negative or positive depending on whether the interaction between electrons is attractive or repulsive. The particle number operator, $\hat{n}_{i\sigma\alpha\alpha'} = \hat{C}^{+}_{i\sigma\alpha}\hat{C}_{i\sigma\alpha'}$, is the number of electrons at site i with spin σ, and clearly takes only the values 0 or 1.
From eq. (5.1.1), $\hat{C}^{+}_{i}$ increases the number of particles, $\hat{n}_i$, in the state by one, $\hat{C}^{+}_{i}$ is therefore known as a creation operator. Similarly $\hat{C}_i$ decreases, $\hat{n}_i$, by one and is therefore known as an annihilation operator.

There are many ways in which the Hubbard model can be extended and in its various formulations many solutions have been found. With $U > 0$ paramagnetic-metallic [108], ferromagnetic-metallic [101] and Antiferromagnetic-insulating [109] solutions have been found. For $U < 0$ there are normal Fermi liquid [110], insulating charge density wave [111], insulating normal Bose liquid [112], Bose-Einstein type (bipolaron) superfluid [112] and superconducting [108] solutions.

When applying the Hubbard model to iron-based superconductors, we have to consider their multi-orbital nature. There are six electrons in five Fe 3d orbitals. First-principles calculations show that, the d_{xz} and d_{yz} orbitals play a key role in the

density of states near the Fermi level [49, 50], although we need to include orbitals d_{xy} , $d_{x^2-y^2}$ and $d_{3z^2-r^2}$ too in many cases. In iron-based superconductors, partial 3d electrons are itinerant (e.g., d_{xz} and d_{yz} electrons), the rest of them are mainly localized [97, 113]. Theoretically, various multi-orbital models have been proposed to describe the systems, like two, three, four and five-orbital Hubbard models [114].

Because of the complexity, it is hard to study the multi-orbital models. A lot of computing methods have been used to deal with them, such as mean-field approximation (MFA), random phase approximation (RPA), fluctuation exchange approximation (FLEX), functional renormalization group (FRG), Gutzwiller variational method, exact diagonalization (ED), dynamical mean-field theory (DMFT), and quantum Monte Carlo (QMC) method. However, each method has its own limitations. For instance, the exact diagonalization method can only deal with some small systems and the problem in QMC for Fermi systems is still difficult to be solved. The mean-field approximation is a useful method to deal with the multi-orbital Hubbard models.
To derive the Hartree - Fork approximation, we can write the intra Coulomb interaction term of Hubbard Hamiltonian (5.1.1) in terms of the mean values of number operators as [107];

$$\begin{aligned}
\hat{H}_{intra} &= U\sum_i \hat{n}_{i\uparrow}\hat{n}_{i\downarrow} \\
&= U\sum_i (\hat{C}^+_{i\uparrow}\hat{C}_{i\uparrow}\hat{C}^+_{i\downarrow}\hat{C}_{i\downarrow}) \\
\therefore \hat{H}_{intra} &= U\sum_i \{(\hat{C}^+_{i\uparrow}\hat{C}_{i\uparrow} - \langle\hat{C}^+_{i\uparrow}\hat{C}_{i\uparrow}\rangle + \langle\hat{C}^+_{i\uparrow}\hat{C}_{i\uparrow}\rangle)(\hat{C}^+_{i\downarrow}\hat{C}_{i\downarrow} - \langle\hat{C}^+_{i\downarrow}\hat{C}_{i\downarrow}\rangle + \langle\hat{C}^+_{i\downarrow}\hat{C}_{i\downarrow}\rangle)\}
\end{aligned} \tag{5.1.2}$$

clearly,$\langle \hat{C}^+_{i\sigma}\hat{C}_{i\sigma}\rangle$ is the mean of $\hat{n}_{i\sigma}$ and the fluctuations about the mean are given by $\hat{C}^+_{i\sigma}\hat{C}_{i\sigma} - \langle \hat{C}^+_{i\sigma}\hat{C}_{i\sigma}\rangle$. Thus we find that,

$$\begin{aligned}\hat{H}_{intra} = U\sum_i \{&(\hat{C}^+_{i\uparrow}\hat{C}_{i\uparrow} - \langle \hat{C}^+_{i\uparrow}\hat{C}_{i\uparrow}\rangle)(\hat{C}^+_{i\downarrow}\hat{C}_{i\downarrow} - \langle \hat{C}^+_{i\downarrow}\hat{C}_{i\downarrow}\rangle) + (\hat{C}^+_{i\uparrow}\hat{C}_{i\uparrow} - \langle \hat{C}^+_{i\uparrow}\hat{C}_{i\uparrow}\rangle)\langle \hat{C}^+_{i\downarrow}\hat{C}_{i\downarrow}\rangle \\ &+ \langle \hat{C}^+_{i\uparrow}\hat{C}_{i\uparrow}\rangle(\hat{C}^+_{i\downarrow}\hat{C}_{i\downarrow} - \langle \hat{C}^+_{i\downarrow}\hat{C}_{i\downarrow}\rangle) + \langle \hat{C}^+_{i\uparrow}\hat{C}_{i\uparrow}\rangle\langle \hat{C}^+_{i\downarrow}\hat{C}_{i\downarrow}\rangle\}\end{aligned} \tag{5.1.3}$$

The basic idea of the mean field approximation (MFA) is that the physical quantities show only minor fluctuations about their mean value. For instance, we will consider $\hat{C}^+_{i\sigma}\hat{C}_{i\sigma} - \langle \hat{C}^+_{i\sigma}\hat{C}_{i\sigma}\rangle$ an inherently small quantity. Accordingly, the term in the first line of equation (5.1.3), being the product of two small quantities, is much smaller than the other terms, and can be safely neglected. So, the first order in fluctuation, we have;

$$\begin{aligned}\hat{H}_{intra} &\approx U\sum_i \{(\hat{C}^+_{i\uparrow}\hat{C}_{i\uparrow} - \langle \hat{C}^+_{i\uparrow}\hat{C}_{i\uparrow}\rangle)\langle \hat{C}^+_{i\downarrow}\hat{C}_{i\downarrow}\rangle + \langle \hat{C}^+_{i\uparrow}\hat{C}_{i\uparrow}\rangle(\hat{C}^+_{i\downarrow}\hat{C}_{i\downarrow} - \langle \hat{C}^+_{i\downarrow}\hat{C}_{i\downarrow}\rangle) \\ &\quad + \langle \hat{C}^+_{i\uparrow}\hat{C}_{i\uparrow}\rangle\langle \hat{C}^+_{i\downarrow}\hat{C}_{i\downarrow}\rangle\} \\ \therefore \hat{H}_{intra} &= U\sum_i \{\langle \hat{C}^+_{i\downarrow}\hat{C}_{i\downarrow}\rangle\hat{C}^+_{i\uparrow}\hat{C}_{i\uparrow} + \langle \hat{C}^+_{i\uparrow}\hat{C}_{i\uparrow}\rangle\hat{C}^+_{i\downarrow}\hat{C}_{i\downarrow} - \langle \hat{C}^+_{i\uparrow}\hat{C}_{i\uparrow}\rangle\langle \hat{C}^+_{i\downarrow}\hat{C}_{i\downarrow}\rangle\}\end{aligned} \tag{5.1.4}$$

Ignoring the last term of the right side of equation (the constant term) (5.1.4), one can get the Hartree - Fork approximation;

$$\hat{H}_{intra} = U\sum_i \{\langle \hat{C}^+_{i\downarrow}\hat{C}_{i\downarrow}\rangle\hat{C}^+_{i\uparrow}\hat{C}_{i\uparrow} + \langle \hat{C}^+_{i\uparrow}\hat{C}_{i\uparrow}\rangle\hat{C}^+_{i\downarrow}\hat{C}_{i\downarrow}\} \tag{5.1.5}$$

Similarly, to derive the Hartree- Fork approximation for the inter coulomb interaction;

$$\begin{aligned}\hat{H}_{inter} &= U'\sum_{ij\sigma\sigma'\alpha\alpha'} \hat{n}^+_{i\sigma\alpha}\hat{n}_{j\sigma'\alpha'} \\ &= U'\sum_{ij\sigma\sigma'\alpha\alpha'} (\hat{C}^+_{i\sigma\alpha}\hat{C}_{i\sigma\alpha}\hat{C}^+_{j\sigma'\alpha'}\hat{C}_{j\sigma'\alpha'}) \\ \therefore \hat{H}_{inter} &= U'\sum_{ij\sigma\sigma'\alpha\alpha'} \{\langle \hat{C}^+_{j\sigma'\alpha'}\hat{C}_{j\sigma'\alpha'}\rangle\hat{C}^+_{i\sigma\alpha}\hat{C}_{i\sigma\alpha} + \langle \hat{C}^+_{i\sigma\alpha}\hat{C}_{i\sigma\alpha}\rangle\hat{C}^+_{j\sigma'\alpha'}\hat{C}_{j\sigma'\alpha'}\}\end{aligned} \tag{5.1.6}$$

Therefore, equation (5.1.1) is approximated to be,

$$\begin{aligned}\hat{H} = &- \sum_{ij\sigma\alpha\alpha'} t_{ij\alpha\alpha'} \hat{C}^{+}_{i\sigma} \hat{C}_{j\sigma} + U \sum_{i} \{\langle \hat{C}^{+}_{i\downarrow} \hat{C}_{i\downarrow} \rangle \hat{C}^{+}_{i\uparrow} \hat{C}_{i\uparrow} + \langle \hat{C}^{+}_{i\uparrow} \hat{C}_{i\uparrow} \rangle \hat{C}^{+}_{i\downarrow} \hat{C}_{i\downarrow} \} \\ &+ U' \sum_{ij\sigma\sigma'\alpha\alpha'} \{\langle \hat{C}^{+}_{j\sigma'\alpha'} \hat{C}_{j\sigma'\alpha'} \rangle \hat{C}^{+}_{i\sigma\alpha} \hat{C}_{i\sigma\alpha} + \langle \hat{C}^{+}_{i\sigma\alpha} \hat{C}_{i\sigma\alpha} \rangle \hat{C}^{+}_{j\sigma'\alpha'} \hat{C}_{j\sigma'\alpha} \}\end{aligned} \tag{5.1.7}$$

We now introduce the lattice Fourier transformations such that,

$$\hat{C}_{i\sigma} = \frac{1}{\sqrt{N}} \sum_{k} e^{ik.R_i} \hat{C}_{k\sigma} \tag{5.1.8}$$

and

$$\hat{C}^{+}_{i\sigma} = \frac{1}{\sqrt{N}} \sum_{k} e^{-ik.R_j} \hat{C}^{+}_{k\sigma} \tag{5.1.9}$$

and the hopping t_{ij}, must clearly be Fourier transformation of the state of energy, $\epsilon_{k\sigma}$.

Thus,

$$\epsilon_{k\sigma} = \sum_{ij} t_{ij} e^{ik.(R_i - R_j)} \tag{5.1.10}$$

where the Kronecker delta function is given by,

$$\delta(R_i - R_j) = \frac{1}{N} \sum_{k} e^{-ik.(R_i - R_j)} = \begin{cases} 1 & \text{if } i = j \\ 0 & \text{otherwise} \end{cases}$$

Thus, equation (5.1.7), can be written as:

$$\begin{aligned}\hat{H} = &- \sum_{kk'\sigma\alpha\alpha'} \epsilon_{k\sigma\alpha\alpha'} \hat{C}^{+}_{k\sigma} \hat{C}_{k'\sigma} + U \sum_{k} \{\langle \hat{C}^{+}_{k\downarrow} \hat{C}_{k\downarrow} \rangle \hat{C}^{+}_{k\uparrow} \hat{C}_{k\uparrow} + \langle \hat{C}^{+}_{k\uparrow} \hat{C}_{k\uparrow} \rangle \hat{C}^{+}_{k\downarrow} \hat{C}_{k\downarrow} \} \\ &+ U' \sum_{kk'\sigma\sigma'\alpha\alpha'} \{\langle \hat{C}^{+}_{k'\sigma'\alpha'} \hat{C}_{k'\sigma'\alpha'} \rangle \hat{C}^{+}_{k\sigma\alpha} \hat{C}_{k\sigma\alpha} + \langle \hat{C}^{+}_{k\sigma\alpha} \hat{C}_{k\sigma\alpha} \rangle \hat{C}^{+}_{k'\sigma'\alpha'} \hat{C}_{k'\sigma'\alpha'} \}\end{aligned} \tag{5.1.11}$$

But at the absence of Hund's coupling constant ($J_H = 0$), the intra and inter repulsive Coulomb interaction may be similar, i.e. $U \approx U'$. Thus, it is worthwhile to discuss the two limiting cases: $U = 0$, when we have just non-interacting band

electrons, and $t = 0$ when the system decomposes into a set of isolated atoms. The latter can be also understood as the limit of extremely strong interaction with $U/t = \infty$.

The atomic limit of the Hubbard model corresponds to the opposite case: $t = 0$ but $U \neq 0$. Thus, the Hamiltonian has the form,

$$\hat{H}_{t=0} = U \sum_{i} \{\hat{n}_{i\uparrow}\hat{n}_{i\downarrow} + \hat{n}_{i\sigma}\hat{n}_{j\sigma'}\} \tag{5.1.12}$$

while the band limit corresponds to the case U= 0 and the Hamiltonian has the form,

$$\hat{H}_{U=0} = -\sum_{k\sigma} \epsilon_k \hat{C}^{+}_{k\sigma}\hat{C}_{k\sigma} \tag{5.1.13}$$

where,

$$\epsilon_k = -\sum_{ij\sigma} t_{ij} exp(i\vec{k}.\vec{R}_i) \tag{5.1.14}$$

and $\vec{k}$ belongs to the Brillouin zone. In the case of a 2D square lattice with lattice step a, it can be shown that,

$$\epsilon_k = -2t(\cos k_x a + \cos k_y a) \tag{5.1.15}$$

The ground state is obtained by filling up the band to the Fermi level. As each single-particle state, labeled by the quasi-momentum vector k, is spin-doubly degenerate, the total number of states for a system of N sites is $2N$. If there are also N electrons, one for each site, the band is half-filled and the Fermi level is given by,

$$\cos k_x a + \cos k_y a = 0, i.e. |k_x| + |k_y| = \frac{\pi}{a} \tag{5.1.16}$$

According to single-band theory, such system is a good metal. However, the undoped cuprate superconductor materials are instead good insulators. This clearly shows the failure of standard band theory to describe such materials. It is therefore necessary to

add an interaction $U > t$ into the system. However, adding a small perturbation to a non-interacting electron Hamiltonian only renormalizes the free electron gas, affecting only the energy levels ϵ_k close to the Fermi energy. In order to radically change the physics of the system, we must consider an interaction U strong enough to break the free-electron energy band and produce a new kind of fermionic gas.

Chapter 6

Formulation Of The Problem

In this chapter we first use the extended Hubbard model to the iron based superconductor. From this Hamiltonian we derive a spin-generalised Bogoliubov -de Gennes(BdG) equations. The spin dependent order parameter is then separated in to triplet and singlet parts and the BdG equations are thus separated into equations for singlet (even-parity) and for triplet(odd-parity) superconductivity. These two cases are then studied independently. Analytical results for the spectrum of the elementary excitations and various thermodynamic quantities are derived for both cases. We reproduce several well know results for singlet superconductors in zero field and describe the effect of an exchange field on an s-wave superconductor. Finally, we further estimate the superconducting transition temperature of iron based superconductor and the equation of motion for both itinerant and localized electrons.

6.1 Gap equation for iron based superconductors

We will now use the Hubbard model to study superconductivity. Cooper showed that [116], in the presence of an arbitrarily weak, attractive interaction of two electrons near the Fermi level is always unstable with respect to the formation of a bound state (a Cooper pair). The BCS theory extends this simple model to deal with the full many body problem within mean field theory. Thus, as we want to study superconductivity, it is natural to consider effective attractive pairwise potentials i.e. negative U models.

It is easy to see that, on site potentials in eqn.(5.1.1), cannot give triplet superconductivity. As only one electron of each spin can occupy each site the equal spin pairing (ESP) states will clearly not arise from on site potentials. However, one can see that, no triplet states can arise from an on site potential as all triplet states must have odd parity and on site potentials cannot give a k dependent order parameter, which means that, the order parameter is, trivially, even.[1] Thus, we can take account of this by introducing inter-site interaction constants, $U'_{ij\sigma\sigma'}$, acting between electrons at crystal sites, i, j with spins $\sigma = \pm 1$, which will in general depend on the spin of the two electrons.

So, the complete Hamiltonian for Hubbard model is given by,

$$\hat{H} = \hat{H}_0 + \hat{H}_I + \hat{H}_Z \tag{6.1.1}$$

[1] This is not strictly true, Spalek and co-workers [117] have considered on site potentials in multiple orbital models and have found triplet solutions. However, for single orbital models the above discussion is correct.

where $\hat{H}_0$ is the Hamiltonian of free or non-interacting electrons and is given by;

$$\hat{H}_0 = -\sum_{ij\sigma\alpha\alpha'} t_{ij\alpha\alpha'}\hat{C}^{+}_{i\sigma\alpha}\hat{C}_{j\sigma\alpha'} = \sum_{k\sigma\alpha\alpha'} \varepsilon_{k\sigma\alpha\alpha'}\hat{C}^{+}_{k\sigma\alpha}\hat{C}_{k\sigma\alpha'} \tag{6.1.2}$$

where $\hat{C}^{+}_{i\sigma}$ and $\hat{C}_{j\sigma}$ are the usual creation and annihilation operators for electrons on sites i and j, respectively. t_{ij} is the hopping integral and $\varepsilon(k)$ is the band energy.

$$\hat{H}_I = \frac{1}{2}\sum_{ij\sigma\sigma'\alpha\alpha'} U'_{ij\sigma\sigma'\alpha\alpha'}\hat{n}_{i\sigma\alpha}\hat{n}_{j\sigma'\alpha'} \tag{6.1.3}$$

is the interaction term of Hubbard Hamiltonian, the number operators $\hat{n}_{i\sigma\alpha} = \hat{C}^{+}_{i\sigma\alpha}\hat{C}_{i\sigma\alpha'}$, $\hat{n}_{j\sigma'\alpha'} = \hat{C}^{+}_{j\sigma'\alpha}\hat{C}_{j\sigma'\alpha'}$ and the factor $1/2$ to take ease of a double counting.

and

$$\hat{H}_Z = \mu_B \sum_{i\sigma\sigma'\alpha\alpha'} \hat{C}^{+}_{i\sigma\alpha'}(\sigma_{\sigma\sigma'}.\mathbf{H})\hat{C}_{i\sigma\alpha} \tag{6.1.4}$$

is the Hamiltonian of Zeeman splitting with σ and denotes the component of the vector of Pauli matrices.

Substituting equations (6.1.2), (6.1.3) and (6.1.4) into (6.1.1), we get:

$$\hat{H} = -\sum_{ij\sigma\alpha\alpha'} t_{ij\alpha\alpha'}\hat{C}^{+}_{i\sigma\alpha}\hat{C}_{j\sigma\alpha'} + \frac{1}{2}\sum_{ij\sigma\sigma'\alpha\alpha'} U'_{ij\sigma\sigma'\alpha\alpha'}\hat{n}_{i\sigma\alpha}\hat{n}_{j\sigma'\alpha'} + \mu_B \sum_{i\sigma\sigma'} \hat{C}^{+}_{i\sigma}(\sigma_{\sigma\sigma'}.\mathbf{H})\hat{C}_{i\sigma} \tag{6.1.5}$$

we can modify this Hamiltonian using Hartree- Fork approximation similar to that of the previous chapter.

That is,

$$\begin{aligned}\hat{H} = &-\sum_{ij\sigma\alpha\alpha'} t_{ij\alpha\alpha'}\hat{C}^{+}_{i\sigma\alpha}\hat{C}_{j\sigma\alpha'} - \frac{1}{2}\sum_{ij\sigma\sigma'\alpha\alpha'} U'_{ij\sigma\sigma'\alpha\alpha'}\{\langle\hat{C}_{i\sigma\alpha}\hat{C}_{j\sigma'\alpha'}\rangle\hat{C}^{+}_{i\sigma\alpha}\hat{C}^{+}_{j\sigma'\alpha'} \\ &+ \langle\hat{C}^{+}_{i\sigma\alpha}\hat{C}^{+}_{j\sigma'\alpha'}\rangle\hat{C}_{i\sigma\alpha}\hat{C}_{j\sigma'\alpha'}\} + \mu_B \sum_{i\sigma\sigma'\alpha\alpha'} \hat{C}^{+}_{i\sigma\alpha'}(\sigma_{\sigma\sigma'}.\mathbf{H})\hat{C}_{i\sigma\alpha}\end{aligned} \tag{6.1.6}$$

Using Hartree-Fock-Gorkov approximation, the order parameter, $\Delta_{ij\sigma\sigma'}$ and its Hermitian conjugate, which are defined by,

$$\Delta_{ij\sigma\sigma'\alpha\alpha'} = -U'_{ij\sigma\sigma'\alpha\alpha'}\langle\hat{C}_{i\sigma\alpha}\hat{C}_{j\sigma'\alpha}\rangle \tag{6.1.7}$$

and

$$\Delta^{\dagger}_{ij\sigma\sigma'\alpha\alpha'} = -U'_{ij\sigma\sigma'\alpha\alpha'}\langle\hat{C}^{\dagger}_{j\sigma'\alpha'}\hat{C}^{\dagger}_{i\sigma\alpha}\rangle \tag{6.1.8}$$

We express equation (6.1.6) in the form of,

$$\begin{aligned}\hat{H} = &-\sum_{ij\sigma\alpha\alpha} t_{ij\alpha\alpha'}\hat{C}^{+}_{i\sigma\alpha}\hat{C}_{j\sigma\alpha'} - \frac{1}{2}\sum_{ij\sigma\sigma'\alpha\alpha'}\{-\Delta_{ij\sigma\sigma'\alpha\alpha'}\hat{C}^{+}_{i\sigma\alpha}\hat{C}^{+}_{j\sigma'\alpha'} + \Delta^{+}_{ij\sigma\sigma'\alpha\alpha'}\hat{C}_{i\sigma\alpha}\hat{C}_{j\sigma'\alpha'}\} \\ &+ \mu_B\sum_{i\sigma\sigma'\alpha\alpha'}\hat{C}^{+}_{i\sigma\alpha'}(\sigma_{\sigma\sigma'}.\mathbf{H})\hat{C}_{i\sigma\alpha} \\ \therefore \hat{H} = &-\sum_{ij\sigma\sigma'\alpha\alpha'}\{t_{ij\alpha\alpha'}\delta_{\sigma\sigma'\alpha\alpha'}\hat{C}^{+}_{i\sigma\alpha}\hat{C}_{j\sigma\alpha'} + \frac{1}{2}\Delta_{ij\sigma\sigma'\alpha\alpha'}\hat{C}^{+}_{i\sigma\alpha}\hat{C}^{+}_{j\sigma'\alpha'} + \frac{1}{2}\Delta^{+}_{ij\sigma\sigma'\alpha\alpha'}\hat{C}_{i\sigma\alpha}\hat{C}_{j\sigma'\alpha'} \\ &- \mu_B\hat{C}^{+}_{i\sigma}(\sigma_{\sigma\sigma'}.\mathbf{H})\hat{C}_{i\sigma}\}\end{aligned} \tag{6.1.9}$$

For further simplification, we use Bogoliubov-Valatin transformations [115], such that,

$$\hat{C}_{i\sigma\alpha} = \sum_{k\sigma\sigma'\alpha}\{u_{k\sigma\sigma'\alpha}(R_i)\hat{\gamma}_{k\sigma'} + v^{*}_{k\sigma\sigma'\alpha}(R_i)\hat{\gamma}^{+}_{k\sigma'}\} \tag{6.1.10}$$

and

$$\hat{C}_{j\sigma'\alpha'} = \sum_{k\sigma'\sigma''\alpha'}\{u_{k'\sigma'\sigma''\alpha'}(R_j)\hat{\gamma}_{k'\sigma''} + v^{*}_{k'\sigma'\sigma''\alpha'}(R_j)\hat{\gamma}^{+}_{k'\sigma''}\} \tag{6.1.11}$$

similarly for $\hat{C}_{i\uparrow}$ and $\hat{C}_{i\downarrow}$, we have,

$$\hat{C}_{i\uparrow} = \sum_{k}\{u_k(R_i)\hat{\gamma}_{k\uparrow} + v^{*}_{k}(R_i)\hat{\gamma}^{+}_{k\downarrow}\} \tag{6.1.12}$$

and

$$\hat{C}_{j\downarrow} = \sum_{k}\{u_k(R_j)\hat{\gamma}_{k\downarrow} + v^{*}_{k}(R_j)\hat{\gamma}^{+}_{k\uparrow}\} \tag{6.1.13}$$

where v and u are Bogoliubov coefficients to be determined, $\hat{\gamma}$ is fermions operator that satisfies,

$$\{\hat{C}^{+}_{i\sigma}, \hat{C}_{j\sigma'}\} = \delta_{ij}\delta_{\sigma\sigma'},$$

$$\{\hat{\gamma}^{+}_{k\sigma}, \hat{\gamma}_{k'\sigma'}\} = \delta(k-k')\delta_{\sigma\sigma'}$$

and

$$u_k(R_i)u^*_k(R_j) + v_k(R_i)v^*_k(R_j) = \delta_{ij}$$

Substituting equations (6.1.10) and (6.1.11) into equation (6.1.7) gives,

$$\begin{aligned}
\Delta_{ij\sigma\sigma'\alpha\alpha'} &= -U'_{ij\sigma\sigma'\alpha\alpha'}\langle\hat{C}_{i\sigma\alpha}\hat{C}_{j\sigma'\alpha'}\rangle \\
&= -U'_{ij\sigma\sigma'\alpha\alpha'}\langle\sum_{k\sigma'}\{u_{k\sigma\sigma'}(R_i)\hat{\gamma}_{k\sigma'} + v^*_{k\sigma\sigma'}(R_i)\hat{\gamma}^{+}_{k\sigma'}\}, \sum_{k\sigma'\sigma''}\{u_{k'\sigma'\sigma''}(R_j)\hat{\gamma}_{k'\sigma''} + v^*_{k'\sigma'\sigma''}(R_j)\hat{\gamma}^{+}_{k'\sigma} \\
&= -U'_{ij\sigma\sigma'\alpha\alpha'}\sum_{k'\sigma''}\{u_{k'\sigma\sigma''}(R_i)v^*_{k'\sigma'\sigma''}(R_j)\langle\hat{\gamma}_{k'\sigma''}, \hat{\gamma}^{+}_{k'\sigma''}\rangle + v^*_{k'\sigma\sigma''}(R_i)u_{k'\sigma'\sigma''}(R_j)\langle\hat{\gamma}^{+}_{k'\sigma''}, \hat{\gamma}_{k'\sigma''}\rangle \\
\therefore \Delta_{ij\sigma\sigma'} &= -U'_{ij\sigma\sigma'}\sum_{k'\sigma''}\{u_{k'\sigma\sigma''}(R_i)v^*_{k'\sigma'\sigma''}(R_j)(1-f(E_{k'\sigma''})) + v^*_{k'\sigma\sigma''}(R_i)u_{k'\sigma'\sigma''}(R_j)f(E_{k'\sigma})\}
\end{aligned} \tag{6.1.14}$$

Here, $\langle\hat{\gamma}_{k'\sigma''}, \hat{\gamma}^{+}_{k'\sigma''}\rangle = 1 - f(E_{k'\sigma})$ and $\langle\hat{\gamma}^{+}_{k'\sigma''}, \hat{\gamma}_{k'\sigma''}\rangle = f(E_{k'\sigma})$is a fermi function which is expressed by,

$$f(E_{k'\sigma}) = \frac{1}{exp(\beta E_{k'\sigma}) + 1}$$

and, the order parameter $\Delta_{ij\sigma\sigma'}$ is antisymmetric under the exchange of spin and coordinate label. That is,

$$\begin{aligned}
\Delta_{ij\sigma\sigma'\alpha\alpha'} &= -\Delta_{ij\sigma'\sigma\alpha\alpha'} \\
&= -U'_{ij\sigma\sigma'\alpha\alpha'}\sum_{k'\sigma''}\{u_{k'\sigma'\sigma''}(R_j)v^*_{k'\sigma\sigma''}(R_i)(1-f(E_{k'\sigma''})) + (v^*_{k'\sigma'\sigma''}(R_j)u_{k'\sigma\sigma''}f(E_{k'\sigma''}))\}
\end{aligned} \tag{6.1.15}$$

Subtracting equation (6.1.15) from equation (6.1.14), we obtain,

$$\Delta_{ij\sigma\sigma'\alpha\alpha'} = -\frac{1}{2}U'_{ij\sigma\sigma'\alpha\alpha'}\sum_{k'\sigma''}\{u_{k'\sigma\sigma''}(R_i)v^*_{k'\sigma\sigma''}(R_j) - v^*_{k'\sigma\sigma''}(R_i)u_{k'\sigma'\sigma''}(R_j)\}(1-2f(E_{k'\sigma''})) \tag{6.1.16}$$

We find that the order parameter $\Delta_{\sigma\sigma'\alpha\alpha'}(k)$ shall be determined using Fourier transformation as,

$$\Delta_{\sigma\sigma'\alpha\alpha'}(k) = -\frac{1}{2}\sum_{k'\sigma''\alpha\alpha'} U_{\sigma\sigma'\alpha\alpha'}(k-k')\{(u_{\sigma\sigma''}(-k')v^*_{\sigma'\sigma''}(-k') - v^*_{\sigma\sigma''}(k')u_{\sigma'\sigma''}(k'))(1-2f(E_{k'\sigma''}))\} \tag{6.1.17}$$

and, we can write the self consistency equation of (6.1.17) as,

$$\Delta_{\sigma\sigma'\alpha\alpha'}(k) = \sum_{k'\sigma\alpha\alpha'} U'_{\sigma\sigma\alpha\alpha'}(k-k')u_{\sigma\sigma}(k')v^*_{\sigma\sigma}(k')(1-2f(E_{k'\sigma})) \tag{6.1.18}$$

where $U'_{\sigma\sigma\alpha\alpha'}(k-k')$ is the lattice Fourier transformation of $U'_{ij\sigma\sigma'\alpha\alpha'}$.

To determine the variables $u_{\sigma\sigma'}(k')$ and $v_{\sigma\sigma}(k')$, we use the following methods. We now choose our Bogoliubov-Valatin transformation to diagonalize the Hamiltonian or equivalently,

$$\hat{H}' = \sum_{k\sigma} E_{k\sigma}\hat{\gamma}^+_{k\sigma}\hat{\gamma}_{k\sigma} \tag{6.1.19}$$

where $E_{k\sigma}$ is a single particle unperturbed energy or it is a quasi particle spectrum. Now from equations (6.1.9) and (6.1.10), we have,

$$\begin{aligned}
[\hat{H}, \hat{C}_{i\sigma}] &= [-\sum_{ij\sigma\sigma'\alpha\alpha'} \{t_{ij\alpha\alpha'}\delta_{\sigma\sigma'}\hat{C}^{+}_{i\sigma}\hat{C}_{j\sigma} + \frac{1}{2}\Delta_{ij\sigma\sigma'}\hat{C}^{+}_{i\sigma}\hat{C}^{+}_{j\sigma'} - \frac{1}{2}\Delta^{+}_{ij\sigma\sigma'}\hat{C}_{i\sigma}\hat{C}_{j\sigma'} \\
&\quad - \delta_{ij}\mu_B\hat{C}^{+}_{i\sigma}\hat{C}_{i\sigma}(\sigma_{\sigma\sigma'}.\mathbf{H})\}, \hat{C}_{i\sigma}] \\
&= -\sum_{ij\sigma\sigma'} t_{ij}\delta_{\sigma\sigma'}\{\hat{C}^{+}_{i\sigma}\hat{C}_{j\sigma}, \hat{C}_{i\sigma}\} + \frac{1}{2}\Delta_{ij\sigma\sigma'}\{\hat{C}^{+}_{i\sigma}\hat{C}^{+}_{j\sigma'}, \hat{C}_{i\sigma}\} - \frac{1}{2}\Delta^{+}_{ij\sigma\sigma'}\{\hat{C}_{i\sigma}\hat{C}_{j\sigma'}, \hat{C}_{i\sigma}\} \\
&\quad - \delta_{ij}\mu_B(\sigma_{\sigma\sigma'}.\mathbf{H})\{\hat{C}^{+}_{i\sigma}\hat{C}_{i\sigma}, \hat{C}_{i\sigma}\} \\
&= \sum_{ij\sigma\sigma'} (t_{ij}\delta_{\sigma\sigma'}\hat{C}_{j\sigma} + \frac{1}{2}\Delta_{ij\sigma\sigma'}\hat{C}^{+}_{j\sigma'} - \hat{C}_{i\sigma}\delta_{ij}\mu_B(\sigma_{\sigma\sigma'}.\mathbf{H})) \\
&= \sum_{ij\sigma\sigma'} t_{ij}\delta_{\sigma\sigma'}(\sum_{k\sigma'\sigma''} u_{k'\sigma'\sigma''}(R_j)\hat{\gamma}_{k'\sigma''} + v^{*}_{k'\sigma'\sigma''}(R_j)\hat{\gamma}^{+}_{k'\sigma''}) + \frac{1}{2}\Delta_{ij\sigma\sigma'}(\sum_{k\sigma'\sigma''} u^{*}_{k'\sigma'\sigma''}(R_j)\hat{\gamma}^{+}_{k'\sigma''} \\
&\quad + v_{k'\sigma'\sigma''}(R_j)\hat{\gamma}_{k'\sigma''}) - \delta_{ij}\mu_B(\sigma_{\sigma\sigma'}.\mathbf{H})(\sum_{k\sigma\sigma'} u_{k\sigma\sigma'}(R_i)\hat{\gamma}_{k\sigma'} + v^{*}_{k\sigma\sigma'}(R_i)\hat{\gamma}^{+}_{k\sigma'}) \\
\therefore [\hat{H}, \hat{C}_{i\sigma}] &= \sum_{ij\sigma'\sigma''\alpha\alpha'} \{(t_{ij\alpha\alpha'}\delta_{\sigma\sigma'} - \mu_B(\sigma_{\sigma\sigma'}.\mathbf{H}))(u_{k'\sigma'\sigma''}(R_j)\hat{\gamma}_{k'\sigma''} + v^{*}_{k'\sigma'\sigma''}(R_j)\hat{\gamma}^{+}_{k'\sigma''}) \\
&\quad - \Delta_{ij\sigma\sigma'\alpha\alpha'}(\sum_{k\sigma'\sigma''} u^{*}_{k'\sigma'\sigma''}(R_j)\hat{\gamma}^{+}_{k'\sigma''} + v_{k'\sigma'\sigma''}(R_j)\hat{\gamma}_{k'\sigma''})\}
\end{aligned} \tag{6.1.20}$$

Similarly, from equations (6.1.19) and (6.1.10), we have,

$$\begin{aligned}
[\hat{H}', \hat{C}_{i\sigma}] &= [\hat{H}', \sum_{k\sigma''} u_{k\sigma\sigma''}(R_i)\hat{\gamma}_{k\sigma''} + v^{*}_{k\sigma\sigma''}(R_i)\hat{\gamma}^{+}_{k\sigma''}] \\
&= \sum_{k\sigma''} E_{k\sigma''}u_{k\sigma\sigma''}(R_i)\{\hat{\gamma}^{+}_{k\sigma''}\hat{\gamma}_{k\sigma''}, \hat{\gamma}_{k\sigma''}\} \\
&\quad + \sum_{k\sigma''} E_{k\sigma''}v^{*}_{k\sigma\sigma''}(R_i)\{\hat{\gamma}^{+}_{k\sigma''}\hat{\gamma}_{k\sigma''}, \hat{\gamma}^{+}_{k\sigma''}\} \\
\therefore [\hat{H}', \hat{C}_{i\sigma}] &= \sum_{k\sigma''}(-E_{k\sigma''}u_{k\sigma\sigma''}(R_i)\hat{\gamma}_{k\sigma''} + E_{k\sigma''}v^{*}_{k\sigma\sigma''}(R_i)\hat{\gamma}^{+}_{k\sigma''})
\end{aligned} \tag{6.1.21}$$

Equating coefficients of $\hat{\gamma}_{k'\sigma''}$ to equations (6.1.20) and (6.1.21), we get,

$$\sum_{j\sigma''}\{(t_{ij}\delta_{\sigma'\sigma''} + \mu_B(\sigma_{\sigma'\sigma''}.\mathbf{H}))u_{k\sigma''\sigma}(R_j) + \Delta_{ij\sigma'\sigma''}v_{k\sigma''\sigma}(R_j)\} = E_{k\sigma}u_{k\sigma'\sigma}(R_i) \tag{6.1.22}$$

Similarly equating coefficients of $\hat{\gamma}^{+}_{k'\sigma''}$ gives,

$$\sum_{j\sigma''\alpha\alpha'} (-t_{ij\alpha\alpha'}\delta_{\sigma'\sigma''} - \mu_B(\sigma^*_{\sigma\sigma''}.\mathbf{H}))v_{k\sigma''\sigma}(R_j) - \Delta^*_{ij\sigma'\sigma''}u_{k\sigma''\sigma}(R_j) = E_{k\sigma}v_{k\sigma'\sigma}(R_i) \tag{6.1.23}$$

Here, equations (6.1.22) and (6.1.23) are the spin generalized Bogoliubov- de Gennes (BdG) equations in real space. In principle we could solve these but the sum over (infinitely many) lattice sites (in thermodynamic limit) makes this impossible in practice. Fortunately we can avoid this problem by Fourier transforming the BdG equations, which give,

$$\sum_{\sigma''}(\varepsilon_k\delta_{\sigma'\sigma''} + \mu_B(\sigma_{\sigma'\sigma''}.\mathbf{H}))u_{k\sigma''\sigma} + \Delta_{\sigma'\sigma''}(k)v_{k\sigma''\sigma} = E_{k\sigma}u_{k\sigma'\sigma} \tag{6.1.24}$$

and

$$\sum_{\sigma''}(-\varepsilon_k\delta_{\sigma'\sigma''} - \mu_B(\sigma^*_{\sigma'\sigma''}.\mathbf{H}))v_{k\sigma''\sigma} - \Delta^*_{\sigma'\sigma''}(k)u_{k\sigma''\sigma} = E_{k\sigma}v_{k\sigma'\sigma} \tag{6.1.25}$$

We shall now consider Pseudo-Spinor notations using $\mathbf{H} = H_1 + H_2 + H_3$ as,

$$\begin{pmatrix} \xi(k) & \Delta_k \\ -\Delta^*_{-k} & -\xi(k) \end{pmatrix} \begin{pmatrix} u_\sigma(k) \\ v_\sigma(k) \end{pmatrix} = E_\sigma(k) \begin{pmatrix} u_\sigma(k) \\ v_\sigma(k) \end{pmatrix}$$

where,

$$\xi(k) = \begin{pmatrix} \varepsilon_k + \mu_B H_3 & \mu_B(H_1 - iH_2) \\ \mu_B(H_1 + iH_2) & \varepsilon_k - \mu_B H_3 \end{pmatrix}$$

$$\Delta_k = \begin{pmatrix} \Delta_{\uparrow\uparrow}(k) & \Delta_{\uparrow\downarrow}(k) \\ \Delta_{\downarrow\uparrow}(k) & \Delta_{\downarrow\downarrow}(k) \end{pmatrix}$$

$$u_\sigma(k) = \begin{pmatrix} u_{\uparrow\sigma}(k) \\ u_{\downarrow\sigma}(k) \end{pmatrix}$$

$$v_\sigma(k) = \begin{pmatrix} v_{\uparrow\sigma}(k) \\ v_{\downarrow\sigma}(k) \end{pmatrix}$$

$$-\xi(k) = \begin{pmatrix} -\varepsilon_{-k} - \mu_B H_3 & \mu_B(-H_1 - iH_2) \\ \mu_B(-H_1 + iH_2) & -\varepsilon_{-k} + \mu_B H_3 \end{pmatrix}$$

and

$$-\Delta^*_{-k} = \begin{pmatrix} -\Delta^*_{\uparrow\uparrow}(-k) & -\Delta^*_{\uparrow\downarrow}(k) \\ -\Delta^*_{\downarrow\uparrow}(-k) & -\Delta^*_{\downarrow\downarrow}(-k) \end{pmatrix}$$

Using this notation, we can write equations (6.1.24) and (6.1.25) in their more familiar matrix form (which is called Bogoliubov-de Genness (BdG) equation) as:

$$\begin{pmatrix} \varepsilon_k + \mu_B H_3 & \mu_B(H_1 - iH_2) & \Delta_{\uparrow\uparrow}(k) & \Delta_{\uparrow\downarrow}(k) \\ \mu_B(H_1 + iH_2) & \varepsilon_k - \mu_B H_3 & \Delta_{\downarrow\uparrow}(k) & \Delta_{\downarrow\downarrow}(k) \\ -\Delta^*_{\uparrow\uparrow}(-k) & -\Delta^*_{\uparrow\downarrow}(k) & -\varepsilon_{-k} - \mu_B H_3 & \mu_B(-H_1 - iH_2) \\ -\Delta^*_{\downarrow\uparrow}(-k) & -\Delta^*_{\downarrow\downarrow}(-k) & \mu_B(-H_1 + iH_2) & -\varepsilon_{-k} + \mu_B H_3 \end{pmatrix} \begin{pmatrix} u_{\uparrow\sigma}(k) \\ u_{\downarrow\sigma}(k) \\ v_{\uparrow\sigma}(k) \\ v_{\downarrow\sigma}(k) \end{pmatrix}$$
$$= E_\sigma(k) \begin{pmatrix} u_{\uparrow\sigma}(k) \\ u_{\downarrow\sigma}(k) \\ v_{\uparrow\sigma}(k) \\ v_{\downarrow\sigma}(k) \end{pmatrix} \tag{6.1.26}$$

6.1.1 Separation of Singlet and triplet Superconductors

It is natural to separate the spin-generalised BdG equation into triplet and singlet parts. In the Balian and Werthamer (BW) notation [119];

$$\Delta_k = \begin{pmatrix} \Delta_{\uparrow\uparrow}(k) & \Delta_{\uparrow\downarrow}(k) \\ \Delta_{\downarrow\uparrow}(k) & \Delta_{\downarrow\downarrow}(k) \end{pmatrix} = (d_o(k) + \sigma.d(k))i\sigma_2{}^2$$

[2]In the Balian and Werthamer (BW) notation, we rewrite the matrix order parameter as

$$\Delta_k = \sum_{\mu=0}^{3} d_\mu(k)\sigma_\mu i\sigma_2$$

where the σ_μ are the Pauli matrices(including the 2×2 identity matrix,σ_0.) We will now prove that $d_0(k)$ transforms as a scalar under rotation, and therefore is the order parameter for singlet

where $d_o(k)$ is the (scalar) singlet order parameter and $d(k)$ is the (vector) triplet order parameter.[3] The singlet order parameter is symmetric under spatial inversion while the triplet order parameter in anti-symmetric under spatial inversion. Hence, the BdG equation can be rewritten as:

$$\begin{pmatrix} \varepsilon_k + \mu_B H_3 & \mu_B(H_1 - iH_2) & -d_1(k) + id_2(k) & d_o(k) + d_3(k) \\ \mu_B(H_1 + iH_2) & \varepsilon_k - \mu_B H_3 & -d_o(k) + d_3(k) & d_1(k) + id_2(k) \\ -d_1^*(k) - id_2^*(k) & -d_o^*(k) + d_3^*(k) & -\varepsilon_k - \mu_B H_3 & \mu_B(-H_1 - iH_2) \\ d_o^*(k) + d_3^*(k) & d_1^*(k) - id_2^*(k) & \mu_B(-H_1 + iH_2) & -\varepsilon_k + \mu_B H_3 \end{pmatrix} \begin{pmatrix} u_{\uparrow\sigma}(k) \\ u_{\downarrow\sigma}(k) \\ v_{\uparrow\sigma}(k) \\ v_{\downarrow\sigma}(k) \end{pmatrix}$$
$$= E_\sigma(k) \begin{pmatrix} u_{\uparrow\sigma}(k) \\ u_{\downarrow\sigma}(k) \\ v_{\uparrow\sigma}(k) \\ v_{\downarrow\sigma}(k) \end{pmatrix} \tag{6.1.27}$$

---

superconductivity. Furthermore we will show that,

$$d(k) = (d_1(k), d_2(k), d_3(k))$$

transforms as a vector under rotation, and is therefore the order parameter for triplet superconductivity.

[3]We note that we have separated the singlet and triplet parts using the quaternion group [120]

$$\{\sigma_o i\sigma_2, \sigma_1 i\sigma_2, \sigma_2 i\sigma_2, \sigma_3 i\sigma_2\}$$

Quaternions were first introduced by Hamilton [121] as a generalisation to complex numbers, and interestingly enough, are where the letters i, j and k as commonly used for the unit vectors in Cartesian space originate.

6.1.2 Energy spectrum and Gap equation for singlet superconductors

If there is no superconductivity in the triplet channel[4] the BdG equations are:

$$\begin{pmatrix} \varepsilon_k + \mu_B H_3 & \mu_B(H_1 - iH_2) & 0 & d_o(k) \\ \mu_B(H_1 + iH_2) & \varepsilon_k - \mu_B H_3 & -d_o(k) & 0 \\ 0 & -d_o^*(k) & -\varepsilon_k - \mu_B H_3 & \mu_B(-H_1 - iH_2) \\ d_o^*(k) & 0 & \mu_B(-H_1 + iH_2) & -\varepsilon_k + \mu_B H_3 \end{pmatrix} \begin{pmatrix} u_{\uparrow\sigma}(k) \\ u_{\downarrow\sigma}(k) \\ v_{\uparrow\sigma}(k) \\ v_{\downarrow\sigma}(k) \end{pmatrix}$$
$$= E_\sigma(k) \begin{pmatrix} u_{\uparrow\sigma}(k) \\ u_{\downarrow\sigma}(k) \\ v_{\uparrow\sigma}(k) \\ v_{\downarrow\sigma}(k) \end{pmatrix} \tag{6.1.28}$$

[4] if we considering rotation about the $\hat{z}$-axis, so we have the relation between the two particle singlet state and triplet state with singlet and triplet superconductivity respectively as;

$$d_0(k) = \frac{1}{2}(\Delta_{\uparrow\downarrow}(k) - \Delta_{\downarrow\uparrow}(k))$$

$$d_1(k) = \frac{1}{2}(\Delta_{\downarrow\downarrow}(k) - \Delta_{\uparrow\uparrow}(k))$$

$$d_2(k) = \frac{-i}{2}(\Delta_{\downarrow\downarrow}(k) + \Delta_{\uparrow\uparrow}(k))$$

$$d_3(k) = \frac{1}{2}(\Delta_{\uparrow\downarrow}(k) + \Delta_{\downarrow\uparrow}(k))$$

Since $d_0(k)$ transforms as a scalar under rotation. This means that we can always rotate the system so that $\mathbf{H}$ is parallel to $\hat{z}$. The BdG equations then become,

$$\begin{pmatrix} \varepsilon_k + \mu_B\mathbf{H} & 0 & 0 & d_o(k) \\ 0 & \varepsilon_k - \mu_B\mathbf{H} & -d_o(k) & 0 \\ 0 & -d_o^*(k) & -\varepsilon_k - \mu_B\mathbf{H} & 0 \\ d_o^*(k) & 0 & 0 & -\varepsilon_k + \mu_B\mathbf{H} \end{pmatrix} \begin{pmatrix} u_{\uparrow\sigma}(k) \\ u_{\downarrow\sigma}(k) \\ v_{\uparrow\sigma}(k) \\ v_{\downarrow\sigma}(k) \end{pmatrix} = E_\sigma(k) \begin{pmatrix} u_{\uparrow\sigma}(k) \\ u_{\downarrow\sigma}(k) \\ v_{\uparrow\sigma}(k) \\ v_{\downarrow\sigma}(k) \end{pmatrix} \tag{6.1.29}$$

we can now easily separate (6.1.29) into sets of BdG equations, so we have,

$$\begin{pmatrix} \varepsilon_k + \mu_B\mathbf{H} & d_o(k) \\ d_o^*(k) & -\varepsilon_k + \mu_B\mathbf{H} \end{pmatrix} \begin{pmatrix} u_{\uparrow\uparrow}(k) \\ v_{\downarrow\uparrow}(k) \end{pmatrix} = E_\uparrow(k) \begin{pmatrix} u_{\uparrow\uparrow}(k) \\ v_{\downarrow\uparrow}(k) \end{pmatrix} \tag{6.1.30}$$

and

$$\begin{pmatrix} \varepsilon_k - \mu_B\mathbf{H} & -d_o(k) \\ -d_o^*(k) & -\varepsilon_k - \mu_B\mathbf{H} \end{pmatrix} \begin{pmatrix} u_{\downarrow\downarrow}(k) \\ v_{\uparrow\downarrow}(k) \end{pmatrix} = E_\downarrow(k) \begin{pmatrix} u_{\downarrow\downarrow}(k) \\ v_{\uparrow\downarrow}(k) \end{pmatrix} \tag{6.1.31}$$

It is now a simple matter to regain the standard result for the spectrum of a singlet superconductor in a spin only magnetic field,

$$E_\sigma(k) = \sqrt{\varepsilon_k^2 + |d_0(k)|^2} + \sigma\mu_B|\mathbf{H}| \tag{6.1.32}$$

with $\sigma = \uparrow \equiv 1$ and $\sigma = \downarrow \equiv -1$. Equation (6.1.32) clearly reduces to the standard BCS expression for the spectrum of a singlet superconductor in zero field as $\mathbf{H} \to 0$.

Substituting our expressions for the eigenvectors of the BdG into the self-consistency condition (6.1.18) we find that the gap equation is given by,

$$d_0(k) = -\frac{1}{4}\sum_{k'} \frac{U_{\sigma\sigma'}(k)d_0(k)}{E_0(k)} \tanh\left(\frac{E_0(k) + \sigma\mu_B\mathbf{H}}{2k_BT_{sc}}\right) \tag{6.1.33}$$

At T=0 and H=0, it is clear from equation (6.1.29) that,

$$u_{\sigma-\sigma}(k) = v_{\sigma\sigma}(k) = 0$$

While it is trivial to show that,

$$u_{\sigma\sigma}(k) = \frac{d_0(k)}{(\sqrt{E_0(k) - \varepsilon_k)^2 + |d_3(k)|^2}}$$

and

$$v_{\sigma\sigma'}(k) = \frac{E_0(k) - \varepsilon_k}{(\sqrt{E_0(k) - \varepsilon_k)^2 + |d_3(k)|^2}}$$

where

$$E_0(k) = \sqrt{\varepsilon_k + |d_0(k)|^2}$$

$E_0(k)$ is, of course, of the same mathematical form as the spectrum of a singlet superconductor in zero field.

And the gap equation becomes,

$$d_0(k) = -\frac{1}{4}\sum_{k'} \frac{U_{\sigma\sigma'}(k) d_0(k)}{E_0(k)} \tag{6.1.34}$$

which is independent of **H**.

6.1.3 Thermodynamic properties of a singlet superconductor

One of the great successes of BCS theory was that it correctly predicted the behaviour of wide variety of measurable quantities. Some of the simplest quantities (either to calculate or to measure) are the thermodynamic properties of a superconductor. We will now describe such calculations for our model.

Specific heat

Recall from thermodynamics that the specific heat is given by,

$$C_V = \frac{\partial F}{\partial T} = T\frac{\partial S}{\partial T} \tag{6.1.35}$$

and for a Fermionic system

$$S = -k_B \sum_{k\sigma} [f_{k\sigma} \ln f_{k\sigma} + (1 - f_{k\sigma}) \ln(1 - f_{k\sigma})] \tag{6.1.36}$$

Hence we have

$$C_V = -k_B T \sum_{k\sigma} \frac{\partial}{\partial f_{k\sigma}} [f_{k\sigma} \ln f_{k\sigma} + (1 - f_{k\sigma}) \ln(1 - f_{k\sigma})] \frac{\partial f_{k\sigma}}{\partial T} \tag{6.1.37}$$

It is straight forward to show that,

$$\frac{\partial}{\partial f_{k\sigma}} [f_{k\sigma} \ln f_{k\sigma} + (1 - f_{k\sigma}) \ln(1 - f_{k\sigma})] = -\frac{E_{k\sigma}}{k_B T} \tag{6.1.38}$$

And

$$\frac{\partial f_{k\sigma}}{\partial T} = f_{k\sigma}(1 - f_{k\sigma})(\frac{E_{k\sigma}}{k_B T^2} - \frac{1}{k_B T}\frac{\partial E_{k\sigma}}{\partial T}) \tag{6.1.39}$$

From(6.1.32) we have,

$$\frac{\partial E_{k\sigma}}{\partial T} = \frac{1}{\sqrt{\varepsilon_k^2 + |\Delta(k)|^2}} \frac{\partial |\Delta(k)|^2}{\partial T} \tag{6.1.40}$$

So we have

$$C_V = \sum_{k\sigma} \frac{1}{k_B T^2} f_{k\sigma}(1 - f_{k\sigma})(E_{k\sigma}^2 - \frac{1}{E_{k\sigma} - \sigma\mu_B H} \frac{\partial |\Delta(k)|^2}{\partial T}) \tag{6.1.41}$$

Magnetization

The magnetization, M, of a singlet superconductor must come solely from the elementary excitations, as the Cooper pairs are spin zero and therefore do not contribute to

the magnetization. Thus, the magnetization is given by,

$$M = \mu_B \sum_k (f_{k\uparrow} - f_{k\downarrow}) \tag{6.1.42}$$

For small $H(= |\mathbf{H}|)$

$$\frac{\partial f_{k0}}{\partial E} \simeq \frac{f_{k\uparrow} - f_{k\downarrow}}{2\mu_B} \tag{6.1.43}$$

where f_{k0} is the Fermi function of the zero field spectrum,

$$E_{k0} = \sqrt{\varepsilon_k^2 + |\Delta(k)|^2}$$

Hence we have,

$$\begin{aligned} M &\simeq -2\mu_B^2 H \sum_k \frac{\partial f_{k0}}{\partial E} \\ &\simeq -2\mu_B^2 H (\frac{V}{2\pi^3}) \int \frac{d\Omega}{4\pi} \int dk \frac{\partial f_{k0}}{\partial E} \\ &\simeq -2\mu_B^2 H (\frac{V}{2\pi^3}) \int \frac{d\Omega}{4\pi} \int d\varepsilon D(\varepsilon_F) \frac{\partial f_{k0}}{\partial E} \\ \therefore M &= 2\mu_B H D(\varepsilon_F) \int \frac{d\Omega}{4\pi} \int d\varepsilon \frac{\beta}{4} sech^2(\beta E_{k0}/2) \end{aligned} \tag{6.1.44}$$

where $\beta = \frac{1}{k_B T}$

Magnetic susceptibility

The magnetic susceptibility, χ, is given by:

$$\chi = \frac{\partial M}{\partial H} \tag{6.1.45}$$

So for small H,

$$\chi_{singlet} = 2\mu_B D(\varepsilon_F) \int \frac{d\Omega}{4\pi} \int d\varepsilon \frac{\beta}{4} sech^2(\beta E_{k0}/2) \tag{6.1.46}$$

But using Yosida function, the normal state energy in a magnetic field is given by,

$$\varepsilon_{k\sigma} = \varepsilon_k - \mu_\beta \sigma \mathbf{H} \tag{6.1.47}$$

Hence,

$$\begin{aligned} M = \frac{\partial \Omega}{\partial \mathbf{H}} &= -\frac{1}{\beta} \sum_{k\sigma} \frac{\partial}{\partial \mathbf{H}} \ln(1 + e^{-\beta(\varepsilon_{k\sigma} - \mu)}) \\ &= -\frac{\mu_\beta V}{(2\pi)^3} \sum_{\sigma} \sigma \int d^3k \frac{1}{1 + e^{\beta(\varepsilon_{k\sigma} - \mu)}} \end{aligned} \tag{6.1.48}$$

At low temperatures, we therefore have,

$$\begin{aligned} M &= -\frac{\mu_\beta V}{2\pi^3} \sum_{\sigma} \sigma \int_0^{k_{k\sigma}} dk k^2 \\ &= -\frac{\mu_\beta V}{2\pi^3} \sum_{\sigma} \sigma \frac{k_{k\sigma}^3}{3} \end{aligned} \tag{6.1.49}$$

But

$$\begin{aligned} N_\sigma &= \sum_k n_{k\sigma} = \frac{v}{(2\pi)^3} \int d^3k \theta(|k| - k_F) \\ \therefore N_\sigma &= \frac{v}{\pi^2} \frac{k_F^2}{6} \end{aligned}$$

So,

$$\begin{aligned} M &= -\mu_\beta \sum_{\sigma} \sigma N_\sigma \\ &= -\frac{1}{2} \mu_\beta \left(\int_0^{\varepsilon_{F\uparrow}} D(\epsilon) d\epsilon - \int_0^{\varepsilon_{F\downarrow}} D(\epsilon) d\epsilon \right) \\ &\simeq -\frac{1}{2} \mu_\beta D(\epsilon_F) \int_{\varepsilon_{F\downarrow}}^{\varepsilon_{F\uparrow}} d\epsilon \\ \therefore M &\approx \mu_\beta^2 \mathbf{H} D(\epsilon_F) \end{aligned} \tag{6.1.50}$$

From which get,

$$\chi = \frac{\partial M}{\partial \mathbf{H}} \simeq \mu_\beta^2 D(\epsilon_F) \tag{6.1.51}$$

6.1.4 Energy spectrum and Gap Equation of a triplet superconductor in a magnetic field

By setting the singlet order parameter, $d_0(k)$, to zero we can write down the BdG equations for a triplet superconductor in magnetic field,

$$\begin{pmatrix} \varepsilon_k + \mu_B H_3 & \mu_B(H_1 - iH_2) & -d_1(k) + id_2(k) & d_3(k) \\ \mu_B(H_1 + iH_2) & \varepsilon_k - \mu_B H_3 & d_3(k) & d_1(k) + id_2(k) \\ -d_1^*(k) - id_2^*(k) & d_3^*(k) & -\varepsilon_k - \mu_B H_3 & \mu_B(-H_1 - iH_2) \\ d_3^*(k) & d_1^*(k) - id_2^*(k) & \mu_B(-H_1 + iH_2) & -\varepsilon_k + \mu_B H_3 \end{pmatrix} \begin{pmatrix} u_{\uparrow\sigma}(k) \\ u_{\downarrow\sigma}(k) \\ v_{\uparrow\sigma}(k) \\ v_{\downarrow\sigma}(k) \end{pmatrix}$$
$$= E_\sigma(k) \begin{pmatrix} u_{\uparrow\sigma}(k) \\ u_{\downarrow\sigma}(k) \\ v_{\uparrow\sigma}(k) \\ v_{\downarrow\sigma}(k) \end{pmatrix} \tag{6.1.52}$$

Then by considering the eigenvalues of the BdG equations and on noting that $|d(k)|^4 - |d(k).d^*(k)|^2 = |d(k) \times d^*(k)|^2$ we find that,

$$E_\sigma(k) = \sqrt{\varepsilon_k^2 + \mu_B^2 |\mathbf{H}|^2 + |d(k)|^2 + \sigma\sqrt{\Lambda(k)}} \tag{6.1.53}$$

where

$$\Lambda(k) = |d(k) \times d^*(k)|^2 + 4\varepsilon_k^2 \mu_B^2 |\mathbf{H}|^2 + 4\mu_B^2 |\mathbf{H}.d(k)|^2 + 4i\varepsilon_k \mu_B \mathbf{H}.d(k) \times d^*(k)$$

It should be noted that this doesnot assume a unitary order parameter [5]. Also in zero field we clearly have the usual result for a triplet superconductor that,

$$E_\sigma(k) = \sqrt{\varepsilon_k^2 + |d(k)|^2 + \sigma |d(k) \times d^*(k)|^2} \tag{6.1.54}$$

[5] A unitary state is any state for which $d(k) \times d^*(k) = 0$.

cases

Case I. d(k) parallel to H

For a triplet superconductor with **H** parallel to **d(k)** and **z**, from the BdG equations we find that, the eigenvalues are

$$E_\sigma(k) = E_0(k) + \sigma\mu_\beta \mathbf{H}$$

where

$$E_0(k) = \sqrt{\varepsilon_k + |d_3(k)|^2}$$

Which has the same form as the spectrum in zero field. The eigenvectors are,

$$u_{\sigma\sigma}(k) = \frac{d_3(k)}{(\sqrt{E_0(k) - \varepsilon_k)^2 + |d_3(k)|^2}}$$

and

$$v_{\sigma\sigma'}(k) = \frac{E_0(k) - \varepsilon_k}{(\sqrt{E_0(k) - \varepsilon_k)^2 + |d_3(k)|^2}}$$

Substituting these into the self-consistency condition of equation (6.1.18) we find that the gap equation to be,

$$d_3(k) = -\frac{1}{4}\sum_{k\sigma} U_{\sigma\sigma'}(k)\frac{d_3(k)}{E_0(k)} tanh(\frac{E_0(k) + \sigma\mu_B \mathbf{H}}{2k_B T}) \tag{6.1.55}$$

when T=0 the gap equation becomes,

$$d_3(k) = -\frac{1}{4}\sum_{k\sigma} U_{\sigma\sigma'}(k)\frac{d_3(k)}{E_0(k)} \tag{6.1.56}$$

which is independent of **H**.

Hence we find that, for this symmetry the zero temperature gap is independent of the magnetic field strength.We also note that the gap equation has the same form as

the singlet gap equation (equation 6.1.33).[6]

Case II. d(k) parallel to $\hat{x}$; H parallel to $\hat{z}$

At this condition, we find that both the eigenvectors and eigenvalues have an explicit field dependence, this means that the gap has a field dependence at all temperatures.

case III. d(k) parallel to $\hat{z}$; H parallel to $\hat{x}$

Once again we find that the eigenvectors and hence the order parameter are field dependent at all temperatures. We therefore expect this type solution to strongly coupled to the magnetic field and that this type of solution($S_z = \pm 1$) will behave markedly differently from the $S_z = 0$ solution in a magnetic field.

6.1.5 Thermodynamic properties of a triplet superconductor in a magnetic field

As for the singlet case one can calculate thermodynamic properties for a triplet superconductor. Below we examine the same case which we considered for the singlet case.

[6]In particular we may expect to see a Clogston-Chandrasekhar limit. This makes qualitative sense as we are considering the $\hat{S}_z = 0$ projection, $\frac{1}{\sqrt{2}}(|\uparrow\downarrow\rangle + |\downarrow\uparrow\rangle)$. We now see that in a spin only magnetic field the important difference between pairing states, so far as many probes are concerned is not the difference between singlet and triplet pairing, but the difference between opposite spin pairing (OSP) states and equal spin pairing (ESP) states. An OSP state (e.g. a singlet state or the triplet state considered in this section) is destroyed by the magnetic field as it separates the $(|k\uparrow\rangle, |-k\downarrow\rangle$ states which are available for pairing in zero field. On the other hand ESP states are not destroyed as the relevant states here $(|k\sigma\rangle, |-k\sigma\rangle$ are not torn apart by the magnetic field.

Specific heat

The specific heat is given by,

$$\begin{aligned} C_V &= T\frac{\partial S}{\partial T} \\ &= -k_B T\frac{\partial}{\partial T}\sum_{k\sigma}[f_{k\sigma}\ln f_{k\sigma} + (1-f_{k\sigma})\ln(1-f_{k\sigma})] \\ \therefore C_V &= \sum_{k\sigma} f_{k\sigma}(1-f_{k\sigma})(\frac{E_\sigma^2(k)}{k_B T^2} + \frac{E_\sigma(k)}{k_B T}\frac{\partial}{\partial T}E_\sigma(k)) \end{aligned} \tag{6.1.57}$$

From(6.1.53)we have,

$$\begin{aligned} E_\sigma(k)\frac{\partial}{\partial T}E_\sigma(k) &= E_\sigma(k)[\frac{\partial d(k)}{\partial T}\frac{\partial}{\partial d(k)} + \frac{\partial d^*(k)}{\partial T}\frac{\partial}{\partial d^*(k)} + \frac{\partial \Lambda(k)}{\partial T}\frac{\partial}{\partial \Lambda(k)}]E_\sigma(k) \\ &= \sum_\sigma[\frac{d^*(k)}{2}\frac{\partial d^*(k)}{\partial T} + \frac{d(k)}{2}\frac{\partial d^*(k)}{\partial T} + \sigma\frac{\partial \Lambda(k)}{\partial T}] \\ \therefore E_\sigma(k)\frac{\partial}{\partial T}E_\sigma(k) &= \frac{1}{2}\frac{\partial}{\partial T}|d(k)|^2 \end{aligned} \tag{6.1.58}$$

Hence we get,

$$C_V = \sum_{k\sigma} f_{k\sigma}\frac{1-f_{k\sigma}}{K_B T^2}[E_\sigma^2(k) + \frac{T}{2}\frac{d}{dT}|d(k)|^2] \tag{6.1.59}$$

Magnetization

The fact that the magnetic field only appears in the third term of the Hamiltonian greatly simplifies the calculation of the magnetization. That is,

$$\mathbf{M} = \frac{\partial F}{\partial \mathbf{H}} \tag{6.1.60}$$

where F is the free energy which is given by,

$$F = \hat{H} + TS = \hat{H}_0 + \hat{H}_{int} + \hat{H}_Z + TS$$

with

$$\hat{H}_0 = \sum_{ij\sigma} t_{ij}\hat{C}_{i\sigma}^+\hat{C}_{j\sigma}$$

$$\hat{H}_{int} = \frac{1}{2}\sum_{ij\sigma\sigma'} U_{ij\sigma\sigma'}\hat{n}_{i\sigma}\hat{n}_{j\sigma'}$$

and

$$\hat{H}_Z = \mu_B \sum_{i\sigma\sigma'} \hat{C}^+_{i\sigma}(\sigma_{\sigma\sigma'}.\mathbf{H})\hat{C}_{i\sigma}$$

Thus we obtain,

$$\begin{aligned}\mathbf{M} &= \frac{\partial\langle\hat{H}_0\rangle}{\partial\mathbf{H}} + \frac{\partial\langle\hat{H}_{int}\rangle}{\partial\mathbf{H}} + \frac{\partial\langle\hat{H}_Z\rangle}{\partial\mathbf{H}} + T\frac{\partial S}{\partial\mathbf{H}} \\ &= \frac{\partial\langle\hat{H}_Z\rangle}{\partial\mathbf{H}} + T\frac{\partial S}{\partial\mathbf{H}}\end{aligned} \tag{6.1.61}$$

Assuming $\frac{\partial S}{\partial\mathbf{H}}$ is small we have

$$\begin{aligned}\mathbf{M} &\simeq \mu_B \sum_{k\alpha\beta}\langle\hat{C}^+_{k\alpha}\sigma_{\alpha\beta}\hat{C}_{k\beta}\rangle \\ &= \sum_k \{u^*_{\uparrow\sigma}(k)u_{\downarrow\sigma}(k)f_{k\sigma} + v_{\uparrow\sigma}(k)v^*_{\downarrow\sigma}(k)(1-f_{k\sigma}) \\ &+ u^*_{\downarrow\sigma}(k)u_{\uparrow\sigma}(k)f_{k\sigma} + v_{\downarrow\sigma}(k)v^*_{\uparrow\sigma}(k)(1-f_{k\sigma}) \\ &- iu^*_{\uparrow\sigma}(k)u_{\downarrow\sigma}(k)f_{k\sigma} - iv_{\uparrow\sigma}(k)v^*_{\downarrow\sigma}(k)(1-f_{k\sigma}) \\ &+ iu^*_{\downarrow\sigma}(k)u_{\uparrow\sigma}(k)f_{k\sigma} + iv_{\downarrow\sigma}(k)v^*_{\uparrow\sigma}(k)(1-f_{k\sigma}) \\ &+ u^*_{\uparrow\sigma}(k)u_{\uparrow\sigma}(k)f_{k\sigma} + v_{\downarrow\sigma}(k)v^*_{\downarrow\sigma}(k)(1-f_{k\sigma}) \\ &- u^*_{\downarrow\sigma}(k)u_{\uparrow\sigma}(k)f_{k\sigma}v_{\downarrow\sigma}(k)v^*_{\uparrow\sigma}(k)(1-f_{k\sigma})\}\end{aligned} \tag{6.1.62}$$

Note that here we have calculated the magnetization vector because in many triplet systems the direction of the applied field will often affect the magnetisation, where as in the more isotropic singlet system we calculated $M = |\mathbf{M}|$.

Magnetic susceptibility (χ_m)

It is not clear how to calculate the susceptibility in the general case, so to take the derivatives of the magnetisation equation (6.1.62), one must know how the self-consistent solution of the BdG equations evolves with **H**. This means that, in numerical calculations the best strategy is to evaluate the susceptibility tensor (defined by $M_\alpha = \chi_{\alpha\beta}H_\beta$) by taking numerical derivatives of the magnetization. Therefore, equation (6.1.50) also holds for a triplet superconductor.

Generally, for both singlet and triplet superconductors, we can conclude that, the gap equations are given by,

$$\Delta_{\sigma\sigma}(k) = -\sum_{k'} \frac{U_{\sigma\sigma}(k-k')\Delta_{\sigma\sigma}(k')}{2E_\sigma(k')}(1 - 2f(E_\sigma(k'))) \tag{6.1.63}$$

To proceed further, we replace $f(E_\sigma(k'))$ by $\frac{1}{exp(\beta E_\sigma(k'))+1}$. Thus, equation (6.1.63) becomes,

$$\begin{aligned}
\Delta_{\sigma\sigma}(k) &= -\sum_{k'} \frac{U_{\sigma\sigma}(k-k')\Delta_{\sigma\sigma}(k')}{4E_0(k)}(1 - \frac{2}{exp(\beta E_\sigma(k'))+1}) \\
&= -\sum_{k'} \frac{U_{\sigma\sigma}(k-k')\Delta_{\sigma\sigma}(k')}{4E_0(k)}(\frac{exp(\beta E_\sigma(k'))}{exp(\beta E_\sigma(k'))+1} - \frac{1}{exp(\beta E_\sigma(k'))+1}) \\
\therefore \Delta_{\sigma\sigma}(k) &= -\frac{1}{4}\sum_{k'} \frac{U_{\sigma\sigma}(k-k')\Delta_{\sigma\sigma}(k')}{E_0(k)} tanh(\frac{\beta E_\sigma(k')}{2})
\end{aligned} \tag{6.1.64}$$

As $T \to T_c$ from below, $|\Delta_{\sigma\sigma}(k)| \to 0$ and hence $E_\sigma(k) \to \varepsilon(k) - \sigma\mu_B\mathbf{H}$, and we obtain the linearized gap equation to be,

$$\Delta_{\sigma\sigma}(k) = -\frac{1}{4}\sum_{k'} \frac{U_{\sigma\sigma}(k-k')\Delta_{\sigma\sigma}(k')}{E_0(k)} tanh(\frac{\varepsilon(k') - \sigma\mu_B\mathbf{H}}{2k_\beta T_{sc}}) \tag{6.1.65}$$

where

$$E(k) = \sqrt{\varepsilon_k^2 + |\Delta(k)|^2} \tag{6.1.66}$$

6.2 The Superconducting Transition Temperature ($\mathbf{T}_{sc}$)

Based on the linearized gap equation (6.1.65), some simplifying assumptions are made to solve the equation. In this sub section, we shall be interested to derive and to calculate the equations of T_{sc} in two cases: $\mathbf{H} = 0$ and $\mathbf{H} \neq 0$.

First, for zero field (i.e. $\mathbf{H} = 0$), the mathematical form of equation (6.1.65) becomes,

$$\Delta_{\sigma\sigma}(k) = \sum_{k'} \frac{U_{\sigma\sigma}(k-k')\Delta_{\sigma\sigma}(k')}{2\varepsilon(k')} \tanh(\frac{\varepsilon(k)}{2k_B T_c}) \tag{6.2.1}$$

For further simplification, it is often assume that, the potential $U(k-k')$ is constant, i.e. $U(k-k') = U$, which results in a constant gap $\Delta(k) = \Delta(k') = \Delta$. This considerably simplifies the problem since a factor Δ can be removed from both sides in equation(6.2.1). With this assumption equation (6.2.1) becomes,

$$1 = U \sum_{k'} \frac{1}{2\varepsilon_{k'}} \tanh(\frac{\varepsilon_{k'}}{2k_B T_c}) \tag{6.2.2}$$

Further, we assume the spherical Fermi surface, we replace the summation over k in equation (6.2.2) with an integration in the form,

$$\begin{aligned} 1 &= U \int_0^{\hbar\omega_c} \frac{d^3k}{(2\pi)^3 \varepsilon_{k'}} \tanh(\frac{\varepsilon_{k'}}{2k_B T_{sc}}) \\ &= U \int_0^{\hbar\omega_c} \frac{m}{2\pi^2\hbar^2} \frac{d\varepsilon_{k'}}{\varepsilon_{k'}} \tanh(\frac{\varepsilon_{k'}}{2k_B T_{sc}}) \\ \therefore 1 &= UD(E_f) \int_0^{\hbar\omega_c} \frac{d\varepsilon_{k'}}{\varepsilon_{k'}} \tanh(\frac{\varepsilon_{k'}}{2k_B T_{sc}}) \end{aligned} \tag{6.2.3}$$

From which we get,

$$\begin{aligned} \frac{1}{\lambda'} &= \int_0^{\frac{\hbar\omega_c}{2k_BT_{sc}}} \frac{\tanh(x)}{x}dx \\ \therefore \frac{1}{\lambda'} &= (\ln(x)\tanh x)|_0^{\frac{\hbar\omega_c}{2k_BT_{sc}}} - \int_0^{\frac{\hbar\omega_c}{2k_BT_{sc}}} \frac{\ln(x)}{\cosh^2(x)}dx \end{aligned} \tag{6.2.4}$$

where $\lambda' = UD(E_f)$ and $x = \frac{\varepsilon_{k'}}{2k_BT_c}$

Now, let us study eq.(6.2.4) by considering different cases:

Case I. For low temperature, as T $\to 0$, $\beta = \frac{1}{k_BT_{sc}} = \infty$

$\Rightarrow \tanh(\frac{\hbar\omega_c}{2k_BT_c}) \to 1$

and extend the upper limit of the integral to infinity to obtain,

$$\begin{aligned} \frac{1}{\lambda'} &= \ln(\frac{\hbar\omega_c}{2k_BT_{sc}}) - \int_0^{\infty} \frac{\ln(x)}{\cosh^2(x)}dx \\ &= \ln(\frac{\hbar\omega_c}{2k_BT_{sc}}) - \ln(\frac{\pi}{4\gamma}) \\ \therefore \frac{1}{\lambda'} &= \ln(\frac{2\gamma}{\pi}\frac{\hbar\omega_c}{k_BT_{sc}}) \end{aligned} \tag{6.2.5}$$

From which we get,

$$T_{sc} = \frac{2\gamma}{\pi}\frac{\hbar\omega_c}{k_B}e^{-\frac{1}{UD(E_f)}} \tag{6.2.6}$$

where γ denotes the Euler's constant, $\gamma = 1.78$, ω_c is the cut of frequency and λ (the dimensionless parameter) is interaction coupling constant.

Thus, equation (6.2.6) becomes,

$$T_{sc} = 1.14\frac{\hbar\omega_c}{k_B}e^{-\frac{1}{\lambda'}} \tag{6.2.7}$$

This is in the form of the well known BCS theory of superconductivity .

Case II. Now let us consider the case of **H** $\neq 0$. We can write equation (6.2.3) as follows,

$$1 = U\int_0^{\hbar\omega_c} D_\sigma(\varepsilon_{k'} + \sigma V_c)\frac{d\varepsilon_{k'}}{\varepsilon_{k'} - \sigma V_c}\tanh(\frac{\varepsilon_{k'} - \sigma V_c}{2k_BT_{sc}^\sigma}) \tag{6.2.8}$$

Here, the density of state, D, is dependent on exchange splitting (V_c) i.e. $V_c = \frac{1}{2}\mu_\beta \sigma H$. Expanding $D_\sigma(\varepsilon_{k'} + \sigma V_c)$ in Taylor Series [126] for small values of magnetic field H, about the Fermi energy and neglecting higher derivative terms, we obtain,

$$D(\varepsilon_{k'} + \sigma V_c) = D(\varepsilon_{k'})|_{E_f} + \sigma V_c \frac{dD(\varepsilon_{k'})}{d\varepsilon_{k'}}|_{E_f} \tag{6.2.9}$$

By substituting equation (6.2.9) into equation (6.2.8), we obtain,

$$1 = U[D(\varepsilon_{k'})|_{E_f} + \sigma V_c \frac{dD(\varepsilon_{k'})}{d\varepsilon_{k'}}|_{E_f}] \int_0^{\hbar\omega_c} \frac{d\varepsilon_{k'}}{\varepsilon_{k'} - \sigma V_c} \tanh(\frac{\varepsilon_{k'} - \sigma V_c}{2k_B T_c^\sigma}) \tag{6.2.10}$$

This can be reduced to,

$$\frac{1}{\lambda^{\uparrow,\downarrow}} = \int_{\frac{-\sigma V_c}{2k_B T_c}}^{\frac{\hbar\omega_c - \sigma V_c}{2k_B T_c}} \frac{\tanh x}{x} dx \tag{6.2.11}$$

where $x = \frac{\varepsilon_{k'} - \sigma V_c}{2k_B T_c^\sigma}$ and $\lambda^{\uparrow,\downarrow} = U[D(\varepsilon_{k'})|_{E_f} \pm V_c \frac{dD(\varepsilon_{k'})}{d\varepsilon_{k'}}|_{E_f}]$. But, for small magnetic field, we take the lower limit of integration as zero. So, equation (6.2.11) becomes,

$$\frac{1}{\lambda^{\uparrow,\downarrow}} = \int_0^{\frac{\hbar\omega_c - \sigma V_c}{2k_B T_c}} \frac{\tanh x}{x} dx \tag{6.2.12}$$

Next, following the same procedure as we have done for the case $V_c = 0$, we get the following expression,

$$\frac{1}{\lambda^{\uparrow,\downarrow}} = \ln\{\frac{2\gamma}{\pi}(\frac{\hbar\omega_c - \sigma V_c}{k_B T_c^\sigma})\} \tag{6.2.13}$$

This can be rewritten as,

$$-\frac{1}{\lambda^{\uparrow,\downarrow}} = \ln\{\frac{\pi}{2\gamma}(\frac{k_B T_c^\sigma}{\hbar\omega_c - \sigma V_c})\}$$

from which we get,

$$T_c^\sigma = \frac{2\gamma}{\pi}(\frac{\hbar\omega_c - \sigma V_c}{k_B}) e^{-\frac{1}{\lambda^{\uparrow,\downarrow}}} \tag{6.2.14}$$

We assume that, for small magnetic field H, $\sigma V_c \approx 0$, so equation (6.2.14) becomes,

$$T_{sc}^{\uparrow,\downarrow} = \frac{2\gamma}{\pi}(\frac{\hbar\omega_c}{k_B}) e^{-\frac{1}{U[D(\varepsilon_{k'})|_{E_f} \pm V_c \frac{dD(\varepsilon_{k'})}{d\varepsilon_{k'}}|_{E_f}]}} \tag{6.2.15}$$

Now, using the final results of equations (6.2.7) and (6.2.15), by considering the constant values from experiment, we can estimate T_{sc} numerically for both $|\uparrow\uparrow\rangle$ and $|\downarrow\downarrow\rangle$ states.

6.3 Equation of Motion of parallel and anti parallel Spin pairing

To obtain equation of motion for the spin pairing lets start from the Green's functions of the form of,

$$\omega << A; B >>_{\omega} =< [A, B] >_{\omega} + << [A, \hat{H}]; B >>_{\omega}$$

Thus,

$$\omega << \hat{C}_{k\uparrow}; \hat{C}^{+}_{k\uparrow} >>_{\omega} = 1 + << [\hat{C}_{k\uparrow}, \hat{H}]; \hat{C}^{+}_{k\uparrow} >>_{\omega} \tag{6.3.1}$$

Now, we shall make use of eqn.(5.1.1) in the next subsection to compute the equation of motions.

6.3.1 For itinerant Electrons

Now, by applying the double time temperature dependent Greens function we can find the equation of motion using creation and destruction operators as eqn. (6.3.1).

Now let us compute the commutation $[\hat{C}_{k\uparrow}, \hat{H}]$.where $\hat{H}$ is given by

$$\hat{H} = \hat{H}_1 + \hat{H}_2 + \hat{H}_3 \tag{6.3.2}$$

and are the Hamiltonian of itinerant electrons (kinetic term), localized electrons and the interaction term between itinerant electrons and localized electrons due to inter

coulomb interaction mechanism respectively.

where

$$\hat{H}_1 = -\sum_{ij\sigma\alpha\alpha'} t_{ij\alpha\alpha'} \hat{C}^+_{i\sigma\alpha} \hat{C}_{j\sigma\alpha'} \tag{6.3.3}$$

$$\hat{H}_2 = -U \sum_i (< \hat{C}^+_{i\uparrow} \hat{C}^+_{i\downarrow} > \hat{C}_{i\uparrow} \hat{C}_{i\downarrow} + < \hat{C}_{i\uparrow} \hat{C}_{i\downarrow} > \hat{C}^+_{i\uparrow} \hat{C}^+_{i\downarrow}) \tag{6.3.4}$$

$$\hat{H}_3 = -U' \sum_{ij\sigma\sigma'\alpha\alpha'} (< \hat{C}^+_{i\sigma\alpha} \hat{C}^+_{j\sigma'\alpha'} > \hat{C}_{i\sigma\alpha} \hat{C}_{j\sigma'\alpha'} + < \hat{C}_{i\sigma\alpha} \hat{C}_{j\sigma'\alpha'} > \hat{C}^+_{i\sigma\alpha} \hat{C}^+_{j\sigma'\alpha'}) \tag{6.3.5}$$

Let

$$\Delta_{i\uparrow\downarrow} = U \sum_i (< \hat{C}_{i\uparrow} \hat{C}_{i\downarrow} >)$$

$$\Delta^*_{i\uparrow\downarrow} = U \sum_i (< \hat{C}^+_{i\uparrow} \hat{C}^+_{i\downarrow} >)$$

$$\eta_{ij\sigma\sigma'\alpha\alpha'} = U' \sum_{ij\sigma\sigma'\alpha\alpha'} (< \hat{C}_{i\sigma\alpha} \hat{C}_{j\sigma'\alpha'} >)$$

and

$$\eta^*_{ij\sigma\sigma'\alpha\alpha'} = U' \sum_{ij\sigma\sigma'\alpha\alpha'} (< \hat{C}^+_{i\sigma\alpha} \hat{C}^+_{j\sigma'\alpha'} >)$$

For the superconducting and magnetic order parameters become real, $\Delta_{i\uparrow\downarrow} = \Delta^*_{i\uparrow\downarrow} = \Delta$ and $\eta = \eta^* = \eta$

Hence, the full effective Hamiltonian can be expressed as,

$$\hat{H} = -\sum_{ij\sigma} t_{ij} \hat{C}^+_{i\sigma} \hat{C}_{j\sigma} - \Delta \sum_i (\hat{C}_{i\uparrow} \hat{C}_{i\downarrow} + \hat{C}^+_{i\uparrow} \hat{C}^+_{i\downarrow}) - \eta \sum_{ij\sigma\sigma'} (\hat{C}_{i\sigma} \hat{C}_{j\sigma'} + \hat{C}^+_{i\sigma} \hat{C}^+_{j\sigma'}) \tag{6.3.6}$$

In this section we will use the relation for three operators A, B, and C.

$$[A, BC] = \{A, B\}C - B\{A, C\}$$

And also for fermions, the anti commutation relations are;

$$\{\hat{C}_i, \hat{C}^+_j\} = \hat{C}_i \hat{C}^+_j + \hat{C}^+_j \hat{C}_i = \delta_{ij} \tag{6.3.7}$$

$$\{\hat{C}_i^+, \hat{C}_j^+\} = \hat{C}_i^+\hat{C}_j^+ + \hat{C}_j^+\hat{C}_i^+ = 0 \tag{6.3.8}$$

$$\{\hat{C}_i, \hat{C}_j\} = \hat{C}_i\hat{C}_j + \hat{C}_j\hat{C}_i = 0 \tag{6.3.9}$$

$$\{\hat{C}_{k\sigma}, \hat{C}_{k'\sigma'}^+\} = \delta_{kk'}\delta_{\sigma\sigma'} \tag{6.3.10}$$

where $\delta_{kk'} = 1$, if $k = k'$ and $\delta_{\sigma\sigma'} = 1$ if $\sigma = \sigma'$ otherwise zero.

The commutation with the first term of $\hat{H}$ (Kinetic Hamiltonian term) using anti-commutation relation for fermions becomes,

$$\begin{aligned} [\hat{C}_{k\uparrow}, \hat{H}_1] &= [\hat{C}_{k\uparrow}, -\sum_{ij} t_{ij}\hat{C}_{i\sigma}^+\hat{C}_{j\sigma}] = -\sum_{ij} t_{ij}[\hat{C}_{k\uparrow}, \hat{C}_{i\sigma}^+\hat{C}_{j\sigma}] \\ \therefore [\hat{C}_{k\uparrow}, \hat{H}_1] &= -\sum_{ij} t_{ij}[\hat{C}_{k\uparrow}, \hat{C}_{i\sigma}^+]\hat{C}_{j\sigma} \end{aligned} \tag{6.3.11}$$

where

$$\hat{C}_{i\sigma} = \frac{1}{\sqrt{N}}\sum_k e^{ik.R_i}\hat{C}_{k\sigma}$$

$$\hat{C}_{i\sigma}^+ = \frac{1}{\sqrt{N}}\sum_k e^{-ik.R_j}\hat{C}_{k\sigma}^+$$

Thus,

$$\begin{aligned} [\hat{C}_{k\uparrow}, \hat{H}_1] &= -\frac{1}{\sqrt{N}}\sum_{ij} t_{ij}\sum_k e^{-ik.(R_i-R_j)}[\hat{C}_{k\uparrow}, \hat{C}_{k\sigma}^+]\hat{C}_{k\sigma} \\ &= -\frac{1}{N}\sum_{ij} t_{ij}\sum_k e^{-ik.(R_i-R_j)}\delta_{kk}\delta_{\uparrow\sigma}\hat{C}_{k\sigma} \\ &= -\sum_{ij} t_{ij}\delta(R_i - R_j)\hat{C}_{k\uparrow} \\ \therefore [\hat{C}_{k\uparrow}, \hat{H}_1] &= -\sum_{ij} t_{ij}\hat{C}_{k\uparrow} \end{aligned} \tag{6.3.12}$$

where the Kronecker delta function is given by,

$$\delta(R_i - R_j) = \frac{1}{N}\sum_k e^{-ik.(R_i-R_j)} = \begin{cases} 1 & \text{if } i = j \\ 0 & \text{otherwise} \end{cases}$$

and for $\|\epsilon_k\| = -\sum_{ij} t_{ij} e^{ik.(R_i - R_j)}$ equation (6.3.12) becomes,

$$[\hat{C}_{k\uparrow}, \hat{H}_1] = \epsilon_k \hat{C}_{k\uparrow} \tag{6.3.13}$$

we used similar procedure for $[\hat{C}_{k\uparrow}, \hat{H}_2]$, that is,

$$\begin{aligned}
[\hat{C}_{k\uparrow}, \hat{H}_2] &= [\hat{C}_{k\uparrow}, -\Delta \sum_i (\hat{C}_{i\uparrow}\hat{C}_{i\downarrow} + \hat{C}^+_{i\uparrow}\hat{C}^+_{i\downarrow})] \\
&= -\Delta \sum_i ([\hat{C}_{k\uparrow}, \hat{C}_{i\uparrow}\hat{C}_{i\downarrow}] + [\hat{C}_{k\uparrow}, \hat{C}^+_{i\uparrow}\hat{C}^+_{i\downarrow}]) \\
&= -\Delta \sum_i ([\hat{C}_{k\uparrow}, \hat{C}^+_{i\uparrow}\hat{C}^+_{i\downarrow}]) \\
&= -\Delta \sum_i \frac{1}{N} \sum_k e^{-ik.(R_i - R_j)} ([\hat{C}_{k\uparrow}, \hat{C}^+_{k\uparrow}\hat{C}^+_{k\downarrow}]) \\
&= -\Delta \sum_i (\{\hat{C}_{k\uparrow}, \hat{C}^+_{k\uparrow}\}\hat{C}^+_{k\downarrow} - \hat{C}^+_{k\uparrow}\{\hat{C}_{k\uparrow}, \hat{C}^+_{k\downarrow}\}) \\
&= -\Delta \sum_i (\delta_{kk}\delta_{\uparrow\uparrow}\hat{C}^+_{k\downarrow} - \delta_{kk}\delta_{\uparrow\downarrow}\hat{C}^+_{k\uparrow}) \\
\therefore [\hat{C}_{k\uparrow}, \hat{H}_2] &= -\Delta \hat{C}^+_{k\downarrow}
\end{aligned} \tag{6.3.14}$$

In a similar manner we applied for $[\hat{C}_{k\uparrow}, \hat{H}_3]$, and obtain,

$$\begin{aligned}
[\hat{C}_{k\uparrow}, \hat{H}_3] &= [\hat{C}_{k\uparrow}, -\eta \sum_{ij\sigma\sigma'} (\hat{C}_{i\sigma}\hat{C}_{j\sigma'} + \hat{C}^+_{i\sigma}\hat{C}^+_{j\sigma'})] \\
&= -\eta \sum_{ij\sigma\sigma'} ([\hat{C}_{k\uparrow}, \hat{C}_{i\sigma}\hat{C}_{j\sigma'}] + [\hat{C}_{k\uparrow}, \hat{C}^+_{i\sigma}\hat{C}^+_{j\sigma'}]) \\
&= -\eta \sum_{ij\sigma\sigma'} ([\hat{C}_{k\uparrow}, \hat{C}^+_{i\sigma}\hat{C}^+_{j\sigma'}]) \\
&= -\eta \sum_{ij\sigma\sigma'} \frac{1}{N} \sum_{k'} e^{-ik'.(R_i - R_j)} ([\hat{C}_{k\uparrow}, \hat{C}^+_{k'\sigma}\hat{C}^+_{k'\sigma'}]) \\
&= -\eta \sum_{ij\sigma\sigma'} (\{\hat{C}_{k\uparrow}, \hat{C}^+_{k'\sigma}\}\hat{C}^+_{k'\sigma'} - \hat{C}^+_{k'\sigma}\{\hat{C}_{k\uparrow}, \hat{C}^+_{k'\sigma'}\}) \\
&= -\eta \sum_{ij\sigma\sigma'} (\delta_{kk'}\delta_{\uparrow\sigma}\hat{C}^+_{k'\sigma'} - \delta_{kk'}\delta_{\uparrow\sigma'}\hat{C}^+_{k'\sigma}) \\
\therefore [\hat{C}_{k\uparrow}, \hat{H}_3] &= -\eta \hat{C}^+_{k\downarrow}
\end{aligned} \tag{6.3.15}$$

Thus,

$$\Rightarrow [\hat{C}_{k\uparrow}, \hat{H}] = \epsilon_k \hat{C}_{k\uparrow} - \Delta \hat{C}^+_{k\downarrow} - \eta \hat{C}^+_{k\downarrow} = \epsilon_k \hat{C}_{k\uparrow} - \hat{C}^+_{k\downarrow}(\Delta + \eta) \tag{6.3.16}$$

Substituting equation (6.3.16) into equation (6.3.1) gives,

$$\begin{aligned} \omega << \hat{C}_{k\uparrow}, \hat{C}^+_{k\uparrow} >>_\omega &= 1 + << \epsilon_k \hat{C}_{k\uparrow} - \hat{C}^+_{k\downarrow}(\Delta + \eta), \hat{C}^+_{k\uparrow} >>_\omega \\ \therefore \omega << \hat{C}_{k\uparrow}, \hat{C}^+_{k\uparrow} >>_\omega &= 1 + \epsilon_k << \hat{C}_{k\uparrow}, \hat{C}^+_{k\uparrow} >> -(\Delta + \eta) << \hat{C}^+_{k\downarrow}, \hat{C}^+_{k\uparrow} >> \end{aligned} \tag{6.3.17}$$

From equation (6.3.17), we obtain,

$$\Rightarrow << \hat{C}_{k\uparrow}, \hat{C}^+_{k\uparrow} >> = \frac{1}{\omega - \epsilon_k} - \frac{(\Delta + \eta)}{\omega - \epsilon_k} << \hat{C}^+_{k\downarrow}, \hat{C}^+_{k\uparrow} >> \tag{6.3.18}$$

Now let us solve the last term of equation (6.3.18) i.e. $<< \hat{C}^+_{k\downarrow}, \hat{C}^+_{k\uparrow} >>$ using similar techniques of Green's function techniques,

$$\begin{aligned} \omega << \hat{C}^+_{k\downarrow}, \hat{C}^+_{k\uparrow} >> &= \delta_{\uparrow\downarrow} + << [\hat{C}^+_{k\downarrow}, \hat{H}], \hat{C}^+_{k\uparrow} >> \\ \therefore \omega << \hat{C}^+_{k\downarrow}, \hat{C}^+_{k\uparrow} >> &= << [\hat{C}^+_{k\downarrow}, \hat{H}], \hat{C}^+_{k\uparrow} >> \end{aligned} \tag{6.3.19}$$

let us compute the commutation of $[\hat{C}^+_{k\downarrow}, \hat{H}]$

$$\begin{aligned} [\hat{C}^+_{k\downarrow}, \hat{H}_1] &= [\hat{C}^+_{k\downarrow}, -\sum_{ij} t_{ij} \hat{C}^+_{i\sigma} \hat{C}_{j\sigma}] \\ &= -\sum_{ij} t_{ij} [\hat{C}^+_{k\downarrow}, \hat{C}^+_{i\sigma} \hat{C}_{j\sigma}] \\ &= -\sum_{ij} t_{ij} [\{\hat{C}^+_{k\downarrow}, \hat{C}^+_{i\sigma}\} \hat{C}_{j\sigma} - \hat{C}^+_{i\sigma} \{\hat{C}^+_{k\downarrow}, \hat{C}_{j\sigma}\}] \\ &= -\frac{1}{N} \sum_{ij} t_{ij} \sum_k e^{-ik.(R_i - R_j)} [\{\hat{C}^+_{k\downarrow}, \hat{C}^+_{k\sigma}\} \hat{C}_{k\sigma} - \hat{C}^+_{k\sigma} \{\hat{C}^+_{k\downarrow}, \hat{C}_{k\sigma}\}] \\ &= -\frac{1}{N} \sum_{ij} t_{ij} \sum_k e^{-ik.(R_i - R_j)} [-\delta_{kk} \delta_{\downarrow\sigma} \hat{C}^+_{k\sigma}] \\ &= -\sum_{ij} \epsilon_k \delta(R_i - R_j) \hat{C}^+_{k\downarrow} \\ \therefore [\hat{C}^+_{k\downarrow}, \hat{H}_1] &= -\epsilon_k \hat{C}^+_{k\downarrow} \end{aligned} \tag{6.3.20}$$

and

$$\begin{aligned}
[\hat{C}^{+}_{k\downarrow}, \hat{H}_2] &= [\hat{C}^{+}_{k\downarrow}, -\Delta \sum_i (\hat{C}_{i\uparrow}\hat{C}_{i\downarrow} + \hat{C}^{+}_{i\uparrow}\hat{C}^{+}_{i\downarrow})] \\
&= -\Delta \sum_i ([\hat{C}^{+}_{k\downarrow}, \hat{C}_{i\uparrow}\hat{C}_{i\downarrow}] + [\hat{C}^{+}_{k\downarrow}, \hat{C}^{+}_{i\uparrow}\hat{C}^{+}_{i\downarrow}]) \\
&= -\Delta \sum_i ([\{\hat{C}^{+}_{k\downarrow}, \hat{C}_{i\uparrow}\}\hat{C}_{i\downarrow} - \hat{C}_{i\uparrow}\{\hat{C}^{+}_{k\downarrow}, \hat{C}_{i\downarrow}\}] \qquad (6.3.21) \\
&= -\Delta \frac{1}{N} \sum_i \sum_k e^{-ik.(R_i - R_j)} [\{\hat{C}^{+}_{k\downarrow}, \hat{C}_{k\uparrow}\}\hat{C}_{k\downarrow} - \hat{C}_{k\uparrow}\{\hat{C}^{+}_{k\downarrow}, \hat{C}_{k\downarrow}\}] \\
\therefore [\hat{C}^{+}_{k\downarrow}, \hat{H}_2] &= \Delta \hat{C}_{k\uparrow}
\end{aligned}$$

and also

$$\begin{aligned}
[\hat{C}^{+}_{k\downarrow}, \hat{H}_3] &= [\hat{C}^{+}_{k\downarrow}, -\eta \sum_{ij\sigma\sigma'} (\hat{C}_{i\sigma}\hat{C}_{j\sigma'} + \hat{C}^{+}_{i\sigma}\hat{C}^{+}_{j\sigma'})] \\
&= -\eta \sum_{ij\sigma\sigma'} ([\hat{C}^{+}_{k\downarrow}, \hat{C}_{i\sigma}\hat{C}_{j\sigma'}] + [\hat{C}^{+}_{k\downarrow}, \hat{C}^{+}_{i\sigma}\hat{C}^{+}_{j\sigma'}]) \\
&= -\eta \sum_{ij\sigma\sigma'} ([\{\hat{C}^{+}_{k\downarrow}, \hat{C}_{i\sigma}\}\hat{C}_{j\sigma'} - \hat{C}_{i\sigma}\{\hat{C}^{+}_{k\downarrow}, \hat{C}_{j\sigma'}\}] \qquad (6.3.22) \\
&= -\eta \frac{1}{N} \sum_i \sum_k e^{-ik.(R_i - R_j)} [\{\hat{C}^{+}_{k\downarrow}, \hat{C}_{k\sigma}\}\hat{C}_{k\sigma'} - \hat{C}_{k\sigma}\{\hat{C}^{+}_{k\downarrow}, \hat{C}_{k\sigma'}\}] \\
\therefore [\hat{C}^{+}_{k\downarrow}, \hat{H}_3] &= \eta \hat{C}_{k\uparrow}
\end{aligned}$$

Therefore,

$$[\hat{C}^{+}_{k\downarrow}, \hat{H}] = \epsilon_k \hat{C}^{+}_{k\downarrow} - \hat{C}_{k\uparrow}(\Delta + \eta) \qquad (6.3.23)$$

Now, by substituting equation (6.3.23) into equation (6.3.19), we obtained,

$$\omega << \hat{C}^{+}_{k\downarrow}, \hat{C}^{+}_{k\uparrow} >> = - << \epsilon_k \hat{C}^{+}_{k\downarrow} + (\Delta + \eta)\hat{C}_{k\uparrow}, \hat{C}^{+}_{k\uparrow} >> \qquad (6.3.24)$$

Now, using equations (6.3.18) and (6.3.24), we obtain the following expression,

$$\begin{aligned} << \hat{C}^{+}_{k\downarrow}, \hat{C}^{+}_{k\uparrow} >> &= \frac{(\Delta+\eta)}{(\omega+\epsilon_k)} << \hat{C}_{k\uparrow}, \hat{C}^{+}_{k\uparrow} >> \\ &= \frac{(\Delta+\eta)}{(\omega+\epsilon_k)}(\frac{1}{\omega-\epsilon_k} - \frac{(\Delta+\eta)}{\omega-\epsilon_k} << \hat{C}^{+}_{k\downarrow}, \hat{C}^{+}_{k\uparrow} >>) \\ &= \frac{(\Delta+\eta)}{(\omega^2-\epsilon_k^2)} - \frac{(\Delta+\eta)^2}{\omega^2-\epsilon_k^2} << \hat{C}^{+}_{k\downarrow}, \hat{C}^{+}_{k\uparrow} >> \\ \therefore << \hat{C}^{+}_{k\downarrow}, \hat{C}^{+}_{k\uparrow} >> &= \frac{(\Delta+\eta)}{(\omega^2-\epsilon_k^2)+(\Delta+\eta)^2} \end{aligned} \tag{6.3.25}$$

and

$$<< \hat{C}_{k\uparrow}, \hat{C}^{+}_{k\uparrow} >> = \frac{\omega+\epsilon_k}{\omega^2-\epsilon_k^2+(\Delta+\eta)^2} \tag{6.3.26}$$

The superconducting order parameters (Δ)for itinerant electrons can be related with Green's function as,

$$\begin{aligned} \Delta &= \frac{U}{\beta}\sum_k << \hat{C}^{+}_{k\downarrow}, \hat{C}^{+}_{k\uparrow} >> \\ \therefore \Delta &= \frac{U}{\beta}\sum_k \frac{\Delta+\eta}{(\omega^2-\epsilon_k^2)+(\Delta+\eta)^2} \end{aligned} \tag{6.3.27}$$

The sum may be changed into an integral by introducing the density of states at the fermi level (N(0)) i.e.

$$\frac{1}{U}\sum_k \rightarrow \frac{1}{(2\pi)^3}\int d^3k = \int_{-\epsilon_f}^{\infty} N(0)d\epsilon$$

The summation with respect to k and n extends over all allowed pair states. Therefore, we get,

$$\Delta = \frac{1}{\beta}\sum_k \int_{-\epsilon_f}^{\infty} N(0)U(\frac{\Delta+\eta}{(\omega^2-\epsilon_k^2)+(\Delta+\eta)^2})d\epsilon \tag{6.3.28}$$

But, $\omega \rightarrow i\omega_n$, using the Matsubara frequency [127],

$$\omega_n = \frac{2n+1}{\beta}\pi \tag{6.3.29}$$

Now, using equation (6.3.29) in equation (6.3.28), we get,

$$\Delta = -2N(0)U\beta \sum_k \int_0^{\hbar\omega_b} (\frac{\Delta+\eta}{(2n+1)^2\pi^2+\beta^2\epsilon^2})d\epsilon \tag{6.3.30}$$

where $E^2 = \epsilon_k^2 + (\Delta+\eta)^2$.

Using the relation,

$$\frac{1}{2x}tanh(\frac{x}{2}) = \sum_{n=-\infty}^{+\infty} \frac{1}{(2n+1)^2\pi^2+x^2}$$

we can write equation (6.3.30) as,

$$\Delta = -2N(0)U\beta \int_0^{\hbar\omega_b} \frac{\Delta+\eta}{2\beta\epsilon} tanh(\beta E/2)d\epsilon \tag{6.3.31}$$

let $\lambda'' = N(0)U$, then

$$\frac{\Delta}{\lambda''} = -\int_0^{\hbar\omega_b} \frac{\Delta+\eta}{\sqrt{\epsilon_k^2+(\Delta+\eta)^2}} tanh(\frac{\beta\sqrt{\epsilon_k^2+(\Delta+\eta)^2}}{2})d\epsilon \tag{6.3.32}$$

Now, let us study equation (6.3.32) by considering different cases,

Case (I)

As $T \to 0$, $\beta = \infty$, so one can take $tanh(\beta E/2) \to 1$

$$\frac{\Delta}{\lambda''} = -\int_0^{\hbar\omega_b} \frac{\Delta+\eta}{\sqrt{\epsilon_k^2+(\Delta+\eta)^2}} d\epsilon \tag{6.3.33}$$

Using the integral $\int \frac{a}{a^2+x^2}dx = a\sinh^{-1}(x/2)$ where $a = \Delta+\eta$, equation (6.3.33) becomes,

$$\frac{1}{\lambda''} = (1+\frac{\eta}{\Delta})\sinh^{-1}(\frac{\hbar\omega_b}{\Delta+\eta}) \tag{6.3.34}$$

$$\frac{1}{\lambda''} = (1+\frac{\eta}{\Delta})\ln\{\frac{\hbar\omega_b}{\Delta+\eta} + \sqrt{\{\frac{\hbar\omega_b}{\Delta+\eta}\}^2+1}\} \tag{6.3.35}$$

for $\{\frac{\hbar\omega_b}{\Delta+\eta}\}^2 \gg 1$, the above equation becomes,

$$\frac{1}{\lambda''} \approx (1+\frac{\eta}{\Delta})\ln\{\frac{2\hbar\omega_b}{\Delta+\eta}\} \tag{6.3.36}$$

This implies that,

$$\Delta + \eta = 2\hbar\omega_b exp\{-\frac{1}{\lambda''(1+\eta/\Delta)}\} \tag{6.3.37}$$

which is similar to the BCS with an additional term of η and $(1+\eta/\Delta)$ and reduces to the BCS model for $\eta = 0$

Case II At $T = T_c$, $\Delta = 0$, the expression for η (using eq.(6.3.37)) becomes,

$$\eta = -1.75k_\beta T_c + 2\hbar\omega_b exp\{-\frac{1}{\lambda''(1+\eta/1.75k_\beta T_c)}\} \tag{6.3.38}$$

when the magnetic order parameter is zero ($\eta = 0$), eqn.(6.3.39) reduces to:

$$T_c = \frac{1.14}{k_\beta} exp\{\frac{-1}{\lambda''}\} \tag{6.3.39}$$

Case III when $T \to 0$ and $\eta \to 0$, so $tanh(\beta E/2) \to 1$

To obtain temperature dependent of energy gap of equation (6.3.32), we used the same techniques to solve the integral

$$\begin{aligned} \frac{1}{\lambda''} &= \int_0^{\hbar\omega_b} \frac{1}{\sqrt{\epsilon_k^2+\Delta^2}} tanh(\beta \frac{\sqrt{\epsilon_k^2+\Delta^2}}{2} d\epsilon \\ &= \ln 1.14\frac{\hbar\omega_b}{k_B T} - \Delta^2(\frac{1}{\pi k_B T})^2 1.05 + ... \end{aligned} \tag{6.3.40}$$

But equation (6.3.39) can be reduced in to the BCS expression given by,

$$\frac{1}{\lambda''} = ln 1.14\frac{\hbar\omega_b}{k_B T_c} \tag{6.3.41}$$

Equating equations (6.3.40) and (6.3.67) we get,

$$ln 1.14\frac{\hbar\omega_b}{k_B T_c} = \ln 1.14\frac{\hbar\omega_b}{k_B T} - \Delta^2(\frac{1}{\pi k_B T})^2 1.05 + ... \tag{6.3.42}$$

$$\Rightarrow ln(T/T_c) = -\Delta^2(\frac{1}{\pi k_B T})^2 1.05 + ...$$

Using the relation $ln(1-x) = -x - x^2/2 + ...$, we get,

$$ln(T/T_c) = ln(1-(1-T/T_c)) = -(1-T/T_c) - (1-T/T_c)^2/2 + ...$$
$$\approx -(1-T/T_c)$$

Therefore,

$$ln(T/T_c) \approx -(1-T/T_c) = -\Delta^2(\frac{1}{\pi k_B T})^2 1.05 + ...$$

Hence,

$$\Rightarrow \Delta(T) = 3.06 k_B T_c (1-\frac{T}{T_c})^{1/2} \tag{6.3.43}$$

This is the expression that shows how the superconducting order parameter, $\Delta(T)$, varies with temperature and it is similar to the BCS theory.

From the BCS theory $\Delta(0) \approx 1.76 k_B T_c$, then,

$$\Delta(T) = 1.74\Delta(0)(1-\frac{T}{T_c})^{1/2} \tag{6.3.44}$$

$$\Rightarrow \frac{\Delta(T)}{\Delta(0)} = 1.53(1-\frac{T}{T_c})^{1/2} \tag{6.3.45}$$

Magnetization of the itinerant electrons

For the itinerant electrons, the magnetism as a function of temperature (T) is given by,

$$m(T) = g\mu_\beta \sum (< \hat{n}_{k\uparrow} > - < \hat{n}_{k\downarrow} >) \tag{6.3.46}$$

where

$$< \hat{n}_{k\uparrow} > = << \hat{C}^+_{k\uparrow}, \hat{C}_{k\uparrow} >>$$

and

$$< \hat{n}_{k\downarrow} > = << \hat{C}^+_{k\downarrow}, \hat{C}_{k\downarrow} >>$$

If the spins are symmetry, it implies that,

$$<< \hat{C}^{+}_{k\uparrow}, \hat{C}_{k\uparrow} >> = << \hat{C}^{+}_{k\downarrow}, \hat{C}_{k\downarrow} >>$$

But if we allow them to be different we have the possibility of obtaining a ferromagnetic solution by allowing for the expectation values to depend on the direction of the spin. the mean field parameters are,

$$<< \hat{C}^{+}_{k\uparrow}, \hat{C}_{k'\uparrow} >> = \delta_{kk'}\bar{n}_{k\uparrow} \tag{6.3.47}$$

and

$$<< \hat{C}^{+}_{k\downarrow}, \hat{C}_{k'\downarrow} >> = \delta_{kk'}\bar{n}_{k\downarrow} \tag{6.3.48}$$

The average number of fermions in a single-particle state k can relate with Fermi function ($F(E_F)$) like,

$$\bar{n}_{k\uparrow} = \sum_k F(E_F) = \sum_k \frac{1}{e^{\frac{\hbar\omega_c}{k_\beta T}} + 1} \tag{6.3.49}$$

and

$$\bar{n}_{k\downarrow} = \sum_k (1 - F(E_F)) = \sum_k \frac{e^{\frac{\hbar\omega_c}{k_\beta T}}}{e^{\frac{\hbar\omega_c}{k_\beta T}} + 1} \tag{6.3.50}$$

Thus, equation (6.3.46) becomes,

$$m(T) = g\mu_\beta \sum_k (\frac{1 - e^{\frac{\hbar\omega_c}{k_\beta T}}}{e^{\frac{\hbar\omega_c}{k_\beta T}} + 1}) = -g\mu_\beta \sum_k (\frac{e^{\frac{\hbar\omega_c}{k_\beta T}} - 1}{e^{\frac{\hbar\omega_c}{k_\beta T}} + 1}) \tag{6.3.51}$$

Using the relation $\tanh(x) = \frac{e^{2x}-1}{e^{2x}+1}$ and let $x = \frac{\hbar\omega_c}{2k_\beta T}$ we can write the above equation as follows:

$$m(T) = -g\mu_\beta \sum_k \tanh(\frac{\hbar\omega_c}{2k_\beta T}) \tag{6.3.52}$$

By expanding the above equation, we obtain the finite temperature dependence of Magnetization:

$$m(T) \approx m(0)(1 - (\frac{T}{T_c})^2)^{\frac{1}{2}} \tag{6.3.53}$$

6.3.2 For Localized Electrons

Using Greens function formalism, the equation of motion for the localized electrons, has been obtained to be,

$$\omega << \hat{C}_{k\uparrow}; \hat{C}^{+}_{i\uparrow} >>_{\omega} = 1 + << [\hat{C}_{i\uparrow}, \hat{H}]; \hat{C}^{+}_{i\uparrow} >>_{\omega} \tag{6.3.54}$$

Now using similar techniques as above and by assuming that,for $U \gg t$ electrons localize: Mott insulator, we finally get,

$$<< \hat{C}^{+}_{k\downarrow}, \hat{C}^{+}_{k'\uparrow} >> = \frac{\Delta_{loc}}{(\omega^2 - \epsilon_k^2) + \Delta_{loc}^2} \tag{6.3.55}$$

and

$$<< \hat{C}_{k\uparrow}, \hat{C}^{+}_{k\uparrow} >> = \frac{\omega + \epsilon_k}{\omega^2 - \epsilon_k^2 + \Delta_{loc}^2} \tag{6.3.56}$$

where

$$\Delta_{loc} = U \sum_{i\sigma\sigma'} (< \hat{C}_{i\sigma} \hat{C}_{i\sigma'} >)$$

The equation of motion that shows the correlation between the itinerant and localized electrons can be expressed as follows. Using similar definition as for Δ we can write the parameter η as,

$$\begin{aligned} \eta &= \frac{U'}{\beta} \sum_{kk'} << \hat{C}^{+}_{k\downarrow}, \hat{C}^{+}_{k'\uparrow} >> \\ \therefore \eta &= \frac{U'}{\beta} \sum_{k} \frac{\Delta_{loc}}{(\omega^2 - \epsilon_k^2) + \Delta_{loc}^2} \end{aligned} \tag{6.3.57}$$

The sum may be changed into an integral by introducing the density of states at the fermi level (N(0)). Thus,

$$\eta = \frac{1}{\beta} \sum_{n} \int_{-\epsilon_f}^{\infty} d\epsilon N(0) U' \frac{\Delta_{loc}}{\omega^2 - \epsilon_k^2 + \Delta_{loc}^2} \tag{6.3.58}$$

For effective attractive interaction region and assuming the density of states to be constant, equation (6.3.58) becomes,

$$\eta = \frac{2N(0)U'}{\beta}\sum_{n}\int_{0}^{\hbar\omega_b} d\epsilon[\frac{\Delta_{loc}}{\omega^2 - \epsilon_k^2 + \Delta_{loc}^2}] \tag{6.3.59}$$

Now, using the Matsubara frequency, we change $\omega \rightarrow i\omega_n$ and using the relation,

$$\frac{1}{2x}tanh(\frac{x}{2}) = \sum_{n=-\infty}^{+\infty}\frac{1}{(2n+1)^2\pi^2 + x^2}$$

we can write equation (6.3.59) as follows,

$$\eta = \lambda_l\Delta_l\int_{0}^{\hbar\omega_b} d\epsilon\frac{1}{\epsilon_k^2 + \Delta_{loc}^2}\tanh(\beta\sqrt{\epsilon_k^2 + \Delta_{loc}^2}/2) \tag{6.3.60}$$

Let us first solve for,

$$I_1 = \frac{\tanh(\beta\sqrt{\epsilon_k^2 + \Delta_{loc}^2}/2)}{\epsilon_k^2 + \Delta_{loc}^2}d\epsilon \tag{6.3.61}$$

and can be transformed by using the technique of Laplace transform and expressed as,

$$\begin{aligned} I_1 = &\int_{0}^{\hbar\omega_b}\frac{2}{\beta}\sum_{n=-\infty}^{n=\infty}\frac{1}{\omega_n^2 - \epsilon^2} \\ &- \int_{0}^{\hbar\omega_b}\Delta_{loc}^2\frac{2}{\beta}\sum_{n=-\infty}^{n=\infty}\frac{1}{(\omega_n^2 - \epsilon^2)^2} + ... \end{aligned} \tag{6.3.62}$$

Thus,

$$\begin{aligned} \int_{0}^{\hbar\omega_b}\frac{tanh(\frac{\beta\sqrt{\epsilon_k^2+\Delta_{loc}^2}}{2})}{\sqrt{\epsilon_k^2 + \Delta_{loc}^2}}d\epsilon = &\int_{0}^{\hbar\omega_b}\frac{tanh(\frac{\beta\sqrt{\epsilon_k^2+\Delta_{loc}^2}}{2})}{\sqrt{\epsilon_k^2 + \Delta_{loc}^2}}d\epsilon \\ &- \int_{0}^{\hbar\omega_b}\Delta_{loc}^2\frac{2}{\beta}d\epsilon\sum_{n=-\infty}^{n=\infty}\frac{1}{(\omega_n^2 + \epsilon^2)^2} + ... \end{aligned} \tag{6.3.63}$$

substituting the value for the Matsubara frequency

$$\omega_n = \frac{\pi(2n+1)}{\beta}$$

equation (6.3.63) can be rewritten as,

$$\int_0^{\hbar\omega_b} \frac{tanh(\frac{\beta\sqrt{\epsilon_k^2+\Delta_{loc}^2}}{2})}{\sqrt{\epsilon_k^2+\Delta_{loc}^2}}d\epsilon = \int_0^{\hbar\omega_b} \frac{tanh(\frac{\beta\sqrt{\epsilon_k^2+\Delta_{loc}^2}}{2})}{\sqrt{\epsilon_k^2+\Delta_{loc}^2}}d\epsilon - \int_0^{\hbar\omega_b} \Delta_{loc}^2 d\epsilon \frac{2}{\beta}\sum_{n=-\infty}^{n=\infty} \frac{1}{((\frac{\pi(2n+1)}{\beta})^2+\epsilon^2)^2} + ... \tag{6.3.64}$$

Rearranging this equation, we get,

$$\int_0^{\hbar\omega_b} \frac{tanh(\frac{\beta\sqrt{\epsilon_k^2+\Delta_{loc}^2}}{2})}{\sqrt{\epsilon_k^2+\Delta_{loc}^2}}d\epsilon = \int_0^{\hbar\omega_b} \frac{tanh(\frac{\beta\sqrt{\epsilon_k^2+\Delta_{loc}^2}}{2})}{\sqrt{\epsilon_k^2+\Delta_{loc}^2}}d\epsilon - 2\beta^3\Delta_{inter}^2 \int_0^{\hbar\omega_b} d\epsilon \sum_{n=-\infty}^{n=\infty} \frac{1}{(\pi(2n+1))^4\{1+(\frac{\beta\epsilon}{\pi(2n+1)})^2\}^2} + ...$$

$$\therefore \int_0^{\hbar\omega_b} \frac{tanh(\frac{\beta\sqrt{\epsilon_k^2+\Delta_{loc}^2}}{2})}{\sqrt{\epsilon_k^2+\Delta_{loc}^2}}d\epsilon = I_1' + I_1'' \tag{6.3.65}$$

The first integral of equation (6.3.65) can be integrated by using integration by parts. Now, let,

$$x = \frac{\beta\epsilon}{2}, dx = \frac{\beta d\epsilon}{2}$$

$$I_1' = \int_0^{\hbar\omega_b} \frac{tanh(\frac{\beta\epsilon}{2})}{\epsilon}d\epsilon = \int_0^{\frac{\beta\hbar\omega_b}{2}} \frac{tanh(x)}{x}dx \tag{6.3.66}$$

$$tanhx = \frac{e^x - e^{-x}}{e^x + e^{-x}}$$

As $x \to \infty$ then $tanhx \to 1$, using this assumption equation (6.3.66) becomes

$$I_1' = [ln\frac{\beta\hbar\omega_b}{2} - ln\frac{\pi}{4}(e^{-b}) = \ln(1.14\beta\hbar\omega_b) \tag{6.3.67}$$

where b is the Euler's constant and its value is $b = 0.577$.

similarly, let,

$$I_1'' = -2\beta^3\Delta_{loc}^2 \int_0^{\hbar\omega_b} d\epsilon \sum_{n=-\infty}^{n=\infty} \frac{1}{(\pi(2n+1))^4\{1+(\frac{\beta\epsilon}{\pi(2n+1)})^2\}^2} + ... \tag{6.3.68}$$

Using substitution method we can integrate it as,

Let

$$y = \frac{\beta\epsilon}{\pi(2n+1)}, dy = \frac{\beta d\epsilon}{\pi(2n+1)}$$

Then, equation (6.3.68) can be rearranged as,

$$I_1'' = \frac{-4\beta^2\Delta_{loc}^2}{\pi^3}\sum_{n=0}^{n=\infty}\frac{1}{(2n+1)^3}\int_0^\infty \frac{1}{(1+y^2)^2}dy \tag{6.3.69}$$

Define,

$$\sum_{n=0}^{n=\infty}\frac{1}{(2n+1)^r} = (1-2^{-r})\zeta(r)$$

Thus, we have,

$$\sum_{n=0}^{n=\infty}\frac{1}{(2n+1)^3} = (1-2^{-3})\zeta(3) = \frac{7}{8}\zeta(3)$$

$$\oint_0 f(z)dz = 2\pi i\sum Residue \tag{6.3.70}$$

These are from the definitions of Riemann zeta functions and from the integration of functions having the singular points. We know the method of integration using Residue theorem. If f(z) has a pole of order m at $z = a$,then,

$$Res\{f(x), a\} = \frac{1}{(m-1)!}\lim_{z\to 0}\frac{d^{m-1}}{dz^{m-1}}[(z-a)^m f(z)]$$

using this definition,

$$\int_0^\infty \frac{1}{(1+y^2)^2}dy = \frac{\pi}{4}$$

Then equation (6.3.69) becomes,

$$I_1'' = \frac{-4\beta^2\Delta_{loc}^2}{\pi^3}\sum_{n=0}^{n=\infty}\frac{1}{(2n+1)^3}\int_0^\infty \frac{1}{(1+y^2)^2}dy = \frac{-7\beta^2\Delta_{loc}^2}{8\pi^2}\zeta(3) \tag{6.3.71}$$

where, r= 3, $\zeta(r) = 1.202$, ζ being the Zeta function.

Now adding equations (6.3.67) and (6.3.71), we get,

$$I_1 = -(I_1' + I_1'') \approx -\ln(1.14\beta\hbar\omega_b) + \Delta_{loc}^2(\frac{1}{\pi k_B T_m})^2\frac{8.414}{8} \tag{6.3.72}$$

Then, when we substitute equation (6.3.72) into equation (6.3.60), we get,

$$\begin{aligned} \eta &= \lambda_l \Delta_{loc}(-\ln(1.14\beta\hbar\omega_b) + \Delta_{loc}^2(\frac{1}{\pi k_B T_m})^2 \frac{8.414}{8}) \\ \therefore \eta &= -\lambda_l \Delta_{loc} \ln(1.14\beta\hbar\omega_b) + \lambda_l \Delta_{loc}^3(\frac{1}{\pi k_B T_m})^2 \frac{8.414}{8}) \end{aligned} \tag{6.3.73}$$

Since Δ_{loc} is very small, Δ_{loc}^3 can be neglected and eq.(6.3.73 becomes,

$$\eta = -\lambda_l \Delta_{loc} \ln(1.14\hbar\omega_b/(k_\beta T_m)) \tag{6.3.74}$$

from which we get,

$$T_m = \frac{1.14}{k_\beta}\hbar\omega_b) e^{\frac{\eta}{\lambda_l \Delta_{loc}}} \tag{6.3.75}$$

Magnetization of localized electrons

Based on Holstein-Primakoff theory, The magnetic moment of the localized electrons can be calculated from the equation,

$$M_S = g\mu_B \langle (NS - \sum_q b_q^+ b_q) \rangle \tag{6.3.76}$$

The deviation of the magnetization from its saturation value can be expressed as

$$\Delta M = M(0) - M(T) = g\mu_B \sum_q \langle \hat{n}_q \rangle \tag{6.3.77}$$

where $\langle \hat{n}_q \rangle$ is given by the well-known Bose-Einstein relation,

$$\langle \hat{n}_q \rangle = [exp(\frac{\hbar\omega_q}{k_B T}) - 1]^{-1} \tag{6.3.78}$$

Thus, equation (6.3.77) becomes,

$$\Delta M = M(0) - M(T) = \frac{g\mu_B}{(2\pi)^3} \int_0^{q_m} [exp(\frac{Dq^2}{k_B T}) - 1]^{-1} d^3q \tag{6.3.79}$$

where the lattice stiffnes denotes as $D = 2SJa^2$ and $x = Dq^2/k_BT$. At low temperatures ($Dq^2 \gg k_BT/J$) we obtain,

$$\begin{aligned}\Delta M &= \frac{g\mu_B}{2\pi^2}(\frac{k_BT}{JD})^{3/2}\int_0^\infty \frac{x^{1/2}}{exp(x)-1}dx \\ &= \frac{g\mu_B}{2\pi^2}(\frac{k_BT}{JD})^{3/2}\Gamma(\frac{5}{2})\zeta(\frac{3}{2},1)\end{aligned} \tag{6.3.80}$$

Here Γ and ζ denote the Gamma- and Riemann zeta-functions, respectively and their numerical values of relevant arguments are known to be $\Gamma(\frac{5}{2}) = \frac{3\sqrt{\pi}}{4}$ and $\zeta(\frac{3}{2},1) = 1.341$. Thus, we finally obtain,

$$\Delta M = 0.117 g\mu_B(\frac{k_BT}{D})^{3/2} \tag{6.3.81}$$

The finite-temperature magnetization can be then expressed as,

$$M(T) = M(0)[1-(\frac{T}{T_c})^{\frac{3}{2}}] \tag{6.3.82}$$

where the critical temperature T_c is given by

$$T_c = (\frac{M(0)}{0.117 g\mu_B})^{\frac{2}{3}}(\frac{D}{k_B}) \tag{6.3.83}$$

6.4 Results and Discussion

Figure (6.1) shows the calculated heat capacity, as a function of temperature. This shows the expected $\sim e^{-\frac{|\Delta(0)|}{k_BT}}$ temperature dependence at low temperatures. Where $\frac{|\Delta(0)|}{k_BT_c} = 1.76$ and $\frac{C_V^{SC}-C_V^N}{C_V^N} = 1.43$ are standard BCS results.

Using equation (6.2.7) the transition temperature (T_{sc}) versus electron coupling constant (λ_{el}) for selected sample of Iron-based superconductor $Ba_{1-x}K_xFe_2As_2$ can be demonstrated in figure (6.2).

As can be seen from figure (6.2), when the electron coupling constant (λ_{el}) increases

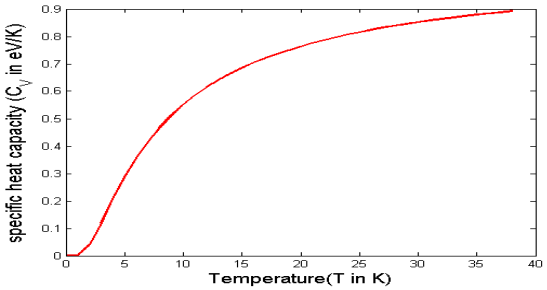

Figure 6.1: Low temperature heat capacity of a s-wave superconductor in zero field as a function of temperature for superconductor $Ba_{1-x}K_xFe_2As_2$. The line shown in the plot is $C_V = 1.06e^{-\Delta(0)/T}$.

the superconducting transition temperature T_c also increases and enhance its maximum value.

Using equation (6.3.43) the superconducting energy gap (Δ) is expressed as a function of the transition temperature (T_c) and be carried out graphically for selected sample of iron-based superconductor $Ba_{1-x}K_xFe_2As_2$ as depicted in figure (6.3).

As can be seen from figure (6.3), when the temperature increases the superconducting order parameter decreases and vanish at the transition temperature of each sample.

From equations (6.3.53) and (6.3.82) the temperature dependence of spontaneous magnetization at low temperatures for Iron-based superconductor $Ba_{1-x}K_xFe_2As_2$ can be demonstrated in figure (6.4).

As can be seen from figure (6.4), the spontaneous magnetization shows that, with $T^{3/2}$ decrease for localized moment ferromagnets at low temperatures, resulting from thermal spin-wave excitations. On the contrary, for weak itinerant ferromagnets, with T^2 decreases are rather well observed, seeming to be in agreement with the spin wave

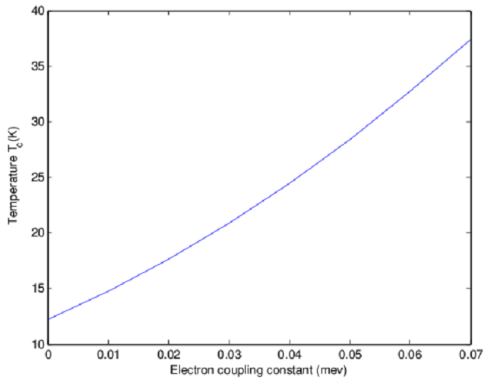

Figure 6.2: Electron coupling constant λ_{el}(mev) Vs Superconducting temperature T_c(K) for $Ba_{1-x}K_xFe_2As_2$ superconductor.

(SW) theory. By combining (a) and (b) in figure (6.4) we obtained a region where both localized and itinerant magnetism coexists in ferropnictide $Ba_{1-x}K_xFe_2As_2$.

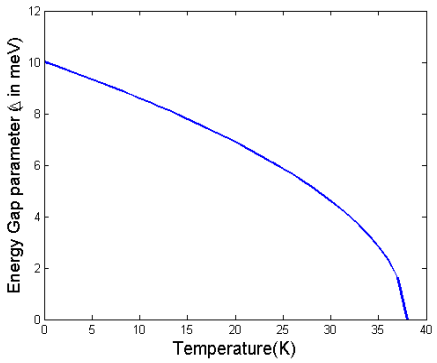

Figure 6.3: Temperature T(K) Vs superconducting order parameter Δ(T)(mev) for $Ba_{1-x}K_xFe_2As_2$ superconductor.

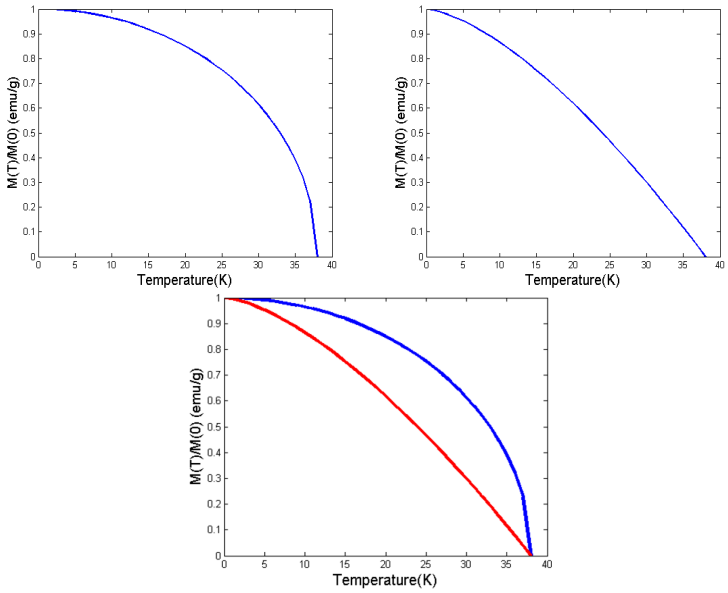

Figure 6.4: Magnetization, M (emu/g), Vs Temperature T(K) (a)for itinerant electrons in $Ba_{1-x}K_xFe_2As_2$ superconductor (b) for localized electrons in $Ba_{1-x}K_xFe_2As_2$ superconductor (c) Coexistence of itinerant magnetism and localized magnetism in $Ba_{1-x}K_xFe_2As_2$ superconductor

Chapter 7

Summary and Conclusion

Despite the fact that the Iron-based superconductors (IBScs) were discovered nearly ten years ago, the community is still devoting a tremendous effort towards elucidating their microscopic pairing mechanism(s) and interactions. The surprising discovery of high-Tc superconductivity in iron-based compounds has prompted an intensive investigation on the role of interaction and magnetism in these materials. It is from this point of view that, we have studied the interplay of local and itinerant electrons in Iron Based superconducting materials using Hubbard Model Hopping with intra and inter Coulomb interaction theoretically. In the first and second chapters of this work, we discussed the general introduction about Iron Based Superconductors. In chapter three, we presented the basic properties and experimental details of the sample of iron based superconductor $Ba_{1-x}K_xFe_2As_2$ compound, a general theoretical description of the interplay between itinerant SDW and SC orders in two-band superconductors and discussed the possible phase diagrams with focus on the coexistence between SC and SDW. It was shown that both orders are suppressed due to the competition between SDW and SC. The coexistence of superconductivity and spin density wave

has been discussed using the Model Hamiltonian which can be expressed using operators(annihilation and creation). We have used the Green's function formalism to find the equation of motion that help us to determine the superconducting and spin density wave order parameters. The magnetic ordering, concentration dependent phase diagram for $Ba_{1-x}K_xFe_2As_2$ which shows the coexistence of superconductivity and spin density wave is possible in $Ba_{1-x}K_xFe_2As_2$ which is in a good agreement with experimental observation.

In chapter four we dealt with the theoretical study of the interplay of itinerant and localized electrons in iron based superconductors. In chapter four,we have also proposed a minimal model composed of two independent and distinct components, i.e. the itinerant electrons and local moments, respectively. These two independent degrees of freedom are coupled together by the local Hunds rule interaction at each iron site.

In chapter five, we have used mathematical methods using Hubbard model and the equation simplified using Hartree-Fork approximation, which are tools to solve our main problem. In chapter six, we developed the Model Hamiltonian for the system and from this Hamiltonian we derived a spin-generalised Bogoliubov-de Gennes (BdG) equations. The spin dependent order parameter is then separated in to triplet and singlet parts and the BdG equations are thus separated in to equations for singlet(even-parity) and for triplet(odd-parity) superconductivity. These two cases were studied independently. Various thermodynamic quantities were derived for both singlet and triplet cases. We reproduced the well known superconducting order parameter results

for both singlet and triplet superconductors in zero field and described the effect of an exchange field on the superconductor. In developing the Model Hamiltonian, we considered the equation of motion of parallel and antiparallel spin pairing mechanisms and obtained expressions for superconducting order parameter (Δ) and superconducting transition temperature (Tc) by employing the Greens function formalism for Hubbard model and carry out various correlation functions by using suitable decoupling procedures. These gap equations have several remarkable qualities. Firstly, the exchange splitting plays only the role of a chemical potential. An alternative interpretation of this fact is that the exchange splitting only directly effects the normal state properties. Secondly, the exchange splitting completely separates the spin degrees of freedom in the absence of spin flip processes (which are not accounted for in this theory). This means that linearized gap equations can be used, not only to predict the global superconducting critical temperature, but uniquely, to calculate the temperature at which a transition from one superconducting phase to another occurs. Also in the same chapter we devoted on the calculation of temperature dependent of magnetization for both itinerant and localized electrons. We plotted figures using the equations developed and by using appropriate experimental values and considering suitable approximations, figures are plotted by using MATLAB scripts. In the last chapter of this paper, we discussed the summary obtained in the previous chapters.

Finally, the overall phase diagram of the iron-based compound may be qualitatively understood in the hybrid/two-fluid picture. Here in both the SDW and SC phases, the coexistence of the itinerant electrons and the local moments are crucial to the underlying mechanisms. In the SDW phase, the itinerant electrons and the local

moments mutually interact to facilitate a joint ordering, while in the SC phase, the itinerant charge carriers are paired via the gluon provided by the local moment fluctuations. In localized magnetism, the magnetic moments are there below and above the critical temperature while in itinerant magnetism there might be no magnetic moments above the critical temperature. The result clearly indicate that localized magnetism can coexist with itinerant magnetism in iron based superconductor below the critical temperature. Thus, we can conclude that, iron-based superconductors show both itinerant and localized properties depending on temperatures. Our theoretical predictions are in broad agreement with experimental findings [128, 129] and the result may help in explaining experimental observations.

Bibliography

[1] H. Kamerlingh Onnes, Leiden Comm. **120b**, **122b**, **124c** (1911).

[2] W. Meissner and R. Ochsenfeld,Short initial announcements, Naturwissenschaften **21**, 787 (1933).

[3] J.G. Bednorz and K. A. Muller, Zeitschrift fr Physik B **64**, 189(1986).

[4] J. Bardeen, L. N. Cooper, and J. R. Schrieffer, Physical Review **108**, 1175(1957).

[5] Y. Kamihara, T. Watanabe, M. Hirano, and H. Hosono, J. Am. Chem. Soc.**130**, 3296 (2008).

[6] Z.-A. Ren, W. Lu, J. Yang, W. Yi, X.-L. Shen, Z.-C. Li, G.-C. Che, X.-L. Dong, L.-L. Sun, F. Zhou, et al., Chinese Physics Letters **25**, 2215 (2008).

[7] H. Kito, H. Eisaki, and A. Iyo, Journal of the Physical Society of Japan **77**, 063707 (2008). http://jpsj.ipap.jp/link?JPSJ/77/063707/.

[8] M. Rotter, M. Tegel, and D. Johrendt,*Superconductivity at 38 K in the Iron Arsenide* $(Ba_{1-x}K_x)Fe_2As_2$, Phys. Rev. Lett. **101**, 107006 (2008).

[9] J. H. Tapp, Z. Tang, B. Lv, K. Sasmal, B. Lorenz, P. C. W. Chu, and A. M. Guloy, Physical Review B **78**, 060505 (2008). http://link.aps.org/doi/10.1103/PhysRevB.78.060505.

[10] X. C. Wang, Q. Q. Liu, Y. X. Lv, W. B. Gao, L. X. Yang, R. C. Yu, F. Y. Li, and C. Q. Jin, Solid State Communications **148**, 538 (2008).

[11] F. C. Hsu, J.-Y. Luo, K.-W. Yeh, T.-K. Chen, T.-W. Huang, P. M. Wu, Y.-C. Lee, Y.-L. Huang, Y.-Y. Chu, D.-C. Yan, and M.-K. Wu, Proceedings of the National Academy of Sciences **105**, 14262 (2008).

[12] D. Johrendt,*Structure property relationships of iron arsenide superconductors*, J. Mater. Chem.**21**, 13726 (2011).

[13] P. M. Shirage, K. Kihou, C.-H. Lee, H. Kito, H. Eisaki, and A. Iyo, *Emergence of Superconductivity in "32522" Structure of* $(Ca_3Al_2O_{5-y})(Fe_2Pn_2)$ *(Pn = As and P)*, J. Am. Chem. Soc. **133**, 9630 (2011).

[14] Hiroaki Ikeda, Ryotaro Arita, and Jan Kunes, *Phase diagram and gap anisotropy in iron-pnictide superconductors*,Phys. Rev. B **81**,054502(2010).

[15] Li Zheng-Cai, Lu Wei, Dong Xiao-Li, Zhou Fang, and Zhao Zhong-Xian, *Single crystal growth and characterizations of iron arsenide superconductor* $BaFe2 - xNi_xAs_2$ *(*$0.0 \leq x \leq 0.12$*)*, Chin. Phys. B **19**, 026103(2010).

[16] Walid Malaeb, *Iron-Pnictide and Cuprate High-temperature Superconductors Investigated by Photoemission Spectroscopy*, Doctor Thesis, (2009)

[17] X. G. Luo, X. F. Wang, J. J. Ying, Y. J. Yan, Z. Y. Li, M. Zhang, A. F. Wang, P.Cheng, Z. J. Xiang, G. J. Ye, R. H. Liu and X. H. Chen, *Crystal structure,physical properties and superconductivity in* $A_xFe_2Se_2$*single crystals*, cond-mat.supr-con **1**, 1101(2011)

[18] Q. Huang, Y. Qiu, W. Bao, M. A. Green, J.W. Lynn, Y. C. Gasparovic, T. Wu, G. Wu, and X. H.Chen, *Neutron-Diffraction Measurements of Magnetic Order and a Structural Transition in the Parent* $BaFe_2As_2$ *Compound of FeAs-Based High-Temperature Superconductors*, Phys. Rev. Lett. **101**, 257003 (2008).

[19] Mrianne Rotter, Marcus Tegel and Dir Jorendt, *Superconductivity at 38K in the iron arsenide* $(Ba_{1-x}K_x)Fe_2As_2$, cond-mat.supr.con **2**, 4630(2008)

[20] Athena S. Sefat, David J. Singh, Rongying Jin, Michael A. McGuire, Brian C.Sales, Filip Ronning, David Mandrus, BaT_2As_2 *single crystals* $(T = Fe; Co; Ni)$*and superconductivity upon Co-doping*, Phys. C **469**, 350-354(2009).

[21] S. Nandi, M. G. Kim, A. Kreyssig, R. M. Fernandes, D. K. Pratt, A. Thaler, N. Ni, S. L. Budko, P. C. Canfield, J. Schmalian, R. J. McQueeney, and A. I. Goldman, Physical Review Letters **104**, 057006(2010).

[22] B. I. Zimmer, W. Jeitschko,J. H. Albering, R. Glaum, and M. Reehuis, *The rare earth transition metal phosphide oxides LnFePO, LnRuPO and LnCoPO with ZrCuSiAs type structure*, J. Alloys Compd. **229**, 238 (1995).

[23] G. Wu, Y. L. Xie, H. Chen, M. Zhong, R. H. Liu, B. C. Shi, Q. J. Li, X. F. Wang, T. Wu, Y. J. Yan, J. J. Ying, and X. H. Chen, *Superconductivity at 56 K in samarium-doped SrFeAsF*, Condens. Matter **21**, 142203 (2009).

[24] X. Wang, Q. Liu, Y. Lv, W. Gao, L. Yang, R. Yu, F. Li, and C. Jin, *The superconductivity at 18 K in LiFeAs system*, Solid State Commun. **148**, 538 (2008).

[25] W. Si, Z.-W. Lin, Q. Jie, W.-G. Yin, J.Zhou, G. Gu, P. D. Johnson, and Q. Li, *Enhanced superconducting transition temperature in* $FeSe_{0.5}Te_{0.5}$ *thin films*, Appl. Phys. Lett.**95**, 052504 (2009).

[26] C.-C. Lee, W.-G. Yin, and W. Ku, Physical Review Letters **103**, 267001 (2009).

[27] M. Wang, H. Luo, J. Zhao, C. Zhang, M. Wang, K. Marty, S. Chi, J. W. Lynn, A. Schneidewind, S. Li, and P. Dai, Physical Review B **81**, 174524 (2010).

[28] S. Takeshita and R. Kadono, New Journal of Physics **11**, 035006(2009).

[29] T. Nakano, S. Tsutsumi, N. Fujiwara, S. Matsuishi, and H. Hosono, Physical Review B **83**, 180508(2011).

[30] T. J. Liu, J. Hu, B. Qian, D. Fobes, Z. Q. Mao, W. Bao, M. Reehuis, S. A. J. Kimber, K. Prokes, S. Matas, et al., Nature Materials **9**, 718 (2010). http://dx.doi.org/10.1038/nmat2800.

[31] Luetkens et al., Nature Materials **8**, 305-309(2009).

[32] Jun Zhao, Q. Huang, Clarina de la Cruz, Shiliang Li, Nature Materials **7**, 953-959(2008).

[33] A. J. Drew, C. Niedermayer, P. J. Baker, F. L. Pratt, S. J. Blundell, T. Lancaster, R. H. Liu, G. Wu, X. H. Chen, I. Watanabe, V. K. Malik, A. Dubroka, M. Rossle, K. W. Kim, C. Baines, and C. Bernhard, Nature Materials **8(4)**, 310-314 (2009).

[34] Chu et al., Physical Review B, **79**, 014506 (2009).

[35] A. N. Yaresko, G.-Q. Liu, V. N. Antonov, and O. K. Andersen, Phys. Rev. **79**, 144421 (2009).

[36] I.I. Mazine, J. Schkalian, PhysicaC **469**, 614-627(2009).

[37] D. J. Singh and M.-H. Du, D, Phys.Rev. Lett. **100**, 237003 (2008).

[38] http://superconductors.org/UBNews.htm

[39] K. Machida, Appl.*Coexistence Problem of Magnetism and Superconductivity*, Phys. A **35**, 193-217(1984)

[40] V.L.Ginzburg, Sov.Phys.JETP **4**,153(1957).

[41] Alexander B. Shick, Phys. Rev. B.**65**.180509(2002)

[42] Ruebenbauer, K. , Zukrowski , J. , Bukowski, Z. , Matusiak, M. and Karpinski , J. *Interplay between Spin Density Wave and Superconductivity in 122 Iron P nictides: 57Fe Mssbauer Study.* Acta Physica Polonica A , **121** , 726 -729(2012)

[43] Vorontsov, A.B. , Vavilov, M. G. and Chubukov, A. V. *Interplay between Magnetism and Superconductivity in Fe-Pnictides.* Physical Review B , **79**, 060508(2009).

[44] Rotter, M., et al. *Competition of Magnetism and Superconductivity in under Doped* $(Ba_{1-x}K_x)Fe_2As_2$. New Journal of Physics, **11**, 025014(2009).

[45] Blachowski , A. , et al. *Coexistence of Superconductivity and Magnetism Theoretical Predictions and Experimental Result.* Physical Review B, **84**, 174503(2011).

[46] Haule K, Shim J H and Kotliar G, Phys. Rev. Lett.**100**, 226402(2008).

[47] Borisenko S V, Zabolotnyy V B, Evtushinsky D V, Kim T K, Morozov I V, Yaresko A N, Kordyuk A A, Behr G, Vasiliev A, Follath R and Buchner B, Phys. Rev. Lett.**105**, 067002(2010).

[48] A. S. Sefat, R. Jin, M. A. McGuire, B. C. Sales, D. J. Singh, and D. Mandrus, *Superconductivity at 22 K in Co-Doped* $BaFe_2As_2$ *Crystals*, Phys. Rev. Lett. **101**, 117004 (2008).

[49] I. I. Mazin, D. J. Singh, M. D. Johannes, and M. H. Du, Physical Review Letters **101**, 057003(2008).

[50] Vildosola V, Pourovskii L, Arita R, Biermann S and Georges A, Phys. Rev. B.**78**,064518(2008).

[51] J. Zhao, D. T. Adroja, D.-X. Yao, R. Bewley, S. Li, X. F. Wang, G. Wu, X. H. Chen, J. Hu, and P. Dai, *Spin waves and magnetic exchange interactions in* $CaFe_2As_2$, Nat. Phys. **5**, 555 (2009).

[52] M. M. Qazilbash, J. J. Hamlin, R. E. Baumbach, L. Zhang, D. J. Singh, M. B. Maple, and D. N. Basov, *Electronic correlations in the iron pnictides*, Nat. Phys. **5**, 647 (2009).

[53] Dai J H, Si Q M, Zhu J X and Abrahams E, Proc. Natl. Acad. Sci. USA. **11**,4118(2009).

[54] Yao D X. Front. Phys. China. **6**,344(2011).

[55] Guidry M, Sun Y and Wu C L. Front. Phys. China. **4**,433(2009)

[56] Dai P, Hu J and Dagotto E. Nat. Phys.**8**,709(2012).

[57] Hirsch JE, *Electrodynamics of spin currents in superconductors*. Ann. Phys. (Berlin) **17**, 380-409(2008).

[58] G. M. Eliashberg, *Interactions between electrons and lattice vibrations in a superconductor*, Sov. Phys. JETP Lett, **11**,696(1960).

[59] C. R. Leavens and E. Talbot, *Effect of thermal phonons on the superconducting transition temperature*, Phys. Rev. B. **28**, 1304(1983).

[60] D. J. Scalapino (1969), *The Electron-phonon interaction and strong coupling superconductors*, in Superconductivity, R. D. Parks, Ed., p. 449(Marcel Dekker, New York).

[61] J. P. Carbotte, *Properties of boson-exchange superconductors*, Rev. Mod. Phys, **62**, 1027(1990).

[62] P. B. Allen and B. Mitrovich(1982), *Theory of superconducting Tc* , in Solid State Physics, H. Ehrenreich, F. Seitz, and D. Turnbull,Eds,37, (Academic Press, New York)

[63] Eremin, I. and Chubukov, A. V. *Magnetic degeneracy and hidden metallicity of the spin-density- wave state in ferropnictides.* Phys. Rev. B **81**, 024511(2010).

[64] Anupam, P. L . Paulose, H. S. Jeevan, C. Geibel, and Z . Hossain. *Interplay between superconductivity and magnetism in K-doped* $EuFe_2As_2$. Prog . Theor. Phys., **121**, 915(2009).

[65] F . Ronning , T. Klimczuk, E. D . Bauer, H. Volz, and J. D . Thompson. *Systhesis and properties of* caf_2As_2 *single crystals.* J. Phys . Condens . Matter, **20**, 322201(2008).

[66] M. Rotter , M. Tegel, D . Johrendt , I. Schellenberg , W. Hermes, and R . Pottgen. *Spin- density- wave anomaly at 140K internary iron arsenide* $BaFe_2As_2$. Phys . Rev . B, **78**, 020503(2008).

[67] Y. Y. Sun, I. Rusakova , R. L. Meng, Y. Cao , P. Gautier - Picard, and C. W. Chu. *The 23K superconducting phase* YPd_2B_2C. Physica C, **230**, 435-442(1994).

[68] M. Rotter , M. Tegel, and D. Johrendt. *Superconductivity at* $38K$ *in the Iron Arsenide* $(Ba_{1-x}K_x)Fe_2As_2$. Phys . Rev. Lett., **101**, 107006(2008).

[69] G . Wu, R. H. Liu, H. Chen, Y. J. Yan, Y. L. Xie, J. J. Ying , X. F. Wang, D. F. Fang, and X. H. Chen. *Transport properties and superconductivity in* $Ba_{1-x}M_xFe_2As_2$ *(M= La and K) with double FeAs layers.* Europhys . Lett., **84**, 27010(2008).

[70] N. Ni, S. L . Bud'ko , A. Kreyssig , S. Nandi, G. E. Rustan, A. I. Goldman, S. Gupta, J. D. Corbett, A. Kracher, and P. C. Canfield. *Anisotropic thermodynamic and transport properties of single crystalline* $(Ba_{1-x}K_x)Fe_2As_2$ *(x=0 and 0.45).* Phys. Rev. B, **78**, 014507(2008).

[71] D. Johrendt and R. Pottgen. *Superconductivity, magnetism and crystal chemistry of* $Ba_{1-x}K_xFe_2As_2$. arXiv:cond-mat/0902.1085, 2009.

[72] M. Rotter, M. Pangerl, M. Tegel, and D. Johrendt. *Superconductivity and Crystal Structures of (Ba1-xKx)Fe2As2(x=0-1).* Angew. Chem. Int. Ed., **47(41)**,7949-7952(2008).

[73] K. Sasmal, B. Lv, B. Lorenz, A. M. Guloy, F. Chen, Y. Y. Xue, and C. W. Chu. *Superconductivity up to* $37K$ *in* $(A_{1-x}Sr_x)Fe_2As_2$ *with* $A = K$ *and Cs.* Phys. Rev. Lett., **101**, 107007(2008).

[74] S. Avci, O. Chmaissem, E. A. Goremychkin, S. Rosenkranz, J.-P. Castellan, D. Y. Chung, I. S. Todorov, J. A. Schlueter, H. Claus, M. G. Kanatzidis, A. Daoud-Aladine, D. Khalyavin, and R. Osborn, *Magnetoelastic coupling in the phase diagram of* $Ba_{1-x}K_xFe_2As_2$ *as seen via neutron diffraction*, Phys. Rev. B **83**, 172503 (2011).

[75] J. Dong, H. J. Zhang, G. Xu, Z. Li, G. Li, W. Z. Hu, D. Wu, G. F. Chen, X. Dai, J. L. Luo, Z. Fang, and N. L. Wang. *Competing Orders and Spin-Density-Wave Instability in* $La(O_{1-x}F_x)FeAs$. Europhys. Lett., **83**, 27006(2008).

[76] Y. Su, P. Link, A. Schneidewind, T. Wolf, P. Adelmann, Y. Xiao, M. Meven, R. Mattal, M. Rotter, D. Johrendt, T. Brueckel, and M. Loewenhaupt. *Neutron Diffraction on antiferromagnetic ordering in single-crystal* $BaFe_2As_2$. Phys. Rev. B, **79**, 064504(2009).

[77] S. Jiang, C. Wang, Z. Ren, Y. Luo, G. Cao, and Z. Xu. *Superconductivity in* $BaFe_2(As_{1-x}P_x)_2$. arXiv:cond-mat/0901.3227v1, (2009).

[78] P. L. Alireza, Y. T. C. Ko, J. Gillett, C. M. Petrone, J. M. Cole, S. E. Sebastian, and G. G. Lonzarich. *Superconductivity up to* $29K$ *in* $SrFe_2As_2$ *and* $BaFe_2As_2$ *at high pressure.* J. Phys.:Condens. Matter, **21(1)**, 012208(2008).

[79] [] H. Fukazawa, N. Takeshita, T. Yamazaki, K. Kondo, K. Hirayama, Y. Kohori, K. Miyazawa, H. Kito, H. Eisaki, and A. Iyo. *Suppression of magnetic order by pressure in $BaFe_2As_2$.* J. Phys. Soc. Jpn., **77**, 105004(2008).

[80] L. J. Liu, Q. B. Wang, Y. K. Luo, H. Chen, Q. Tao, Y. K. Li, X. Lin, M. He, Z. W. Zhu, G. H. Cao, and Z. A. Xu. *Superconductivity induced by Ni doping in $BaFe_2As_2$.* New J. Phys., **11**, 025008(2009).

[81] M. A. Tanatar, N. Ni, C. Martin, R. T. Gordon, H. Kim, V. G. Kogan, G. D. Samolyuk, S. L. Budko, P. C. Canfield, and R. Prozorov. *Anisotropic of the Optimally-Doped Iron Pnictide Superconductor $Ba(Fe_{0.926}Co_{0.074})_2As_2$.* Phys. Rev. B, **79**, 094507(2009).

[82] S. Paulraj, S. Sharma, A. Bharathi, A. T. Satya, S. Chandra, Y. Hariharan, and C. S. Sundar. *Superconductivity in Ru substituted $BaFe_{2-x}Ru_xAs_2$.* arXiv:condmat/ 0902.2728, (2009).

[83] H. Takahashi, K. Igawa, K. Arii, Y. Kamihara, M. Hirano, and H. Hosono. *Superconductivity at 43 K in a iron-based layered compound $LaO_{1-x}F_xFeAs$.* Nature, **453**, 376-378(2008).

[84] M.S. Torikachvili, S. L. Budko, N. Ni, and P. C. Canfield. *Hydrostatic pressure study of the structural phase transitions and superconductivity in single crystals of $(Ba_{1-x}K_x)Fe_2As_2$ (x = 0 and 0.45) and $CaFe_2As_2$.* arXiv:cond-mat/0810.0241, (2008).

[85] M. S. Torikachvili, S. L. Budko, N. Ni, and P. C. Canfield. *Effect of pressure on the structural phase transition and superconductivity in $(Ba_{1-x}K_x)Fe_2As_2$ ($x = 0$ and 0.45) and SrFe2As2 single crystals.* Phys. Rev. B, **78**, 104527(2008).

[86] J. Bardeen, L. N. Cooper, and J. R. Schrieffer, Physical Review **106**, 162(1957). http://link.aps.org/doi/10.1103/PhysRev.106.162

[87] P. W. Anderson, Science **235**, 1196 (1987).

[88] P. W. Anderson, P. A. Lee, M. Randeria, T. M. Rice, N. Trivedi, and F. C. Zhang, Journal of Physics Condensed Matter **16**, 755(2004). arXiv:cond-mat/0311467.

[89] J. Bardeen and D. Pines, Physical Review **99**, 1140 (1955). http://link.aps.org/doi/10.1103/ PhysRev.99.1140.

[90] W. Kohn and J. M. Luttinger, Physical Review Letters **15**, 524 (1965). http://link.aps.org/doi/10. 1103/PhysRevLett.15.524.

[91] N. F. Berk and J. R. Schrieffer, Physical Review Letters **17**, 433 (1966), http://link.aps.org/doi/10.1103/PhysRevLett.17.433.

[92] D. Johnston, Advances in Physics **59**, 803 (2010).

[93] G. A. Ummarino, M. Tortello, D. Daghero, and R. S. Gonnelli, Physical Review B **80**, 172503(2009) http://link.aps.org/doi/10.1103/PhysRevB.80. 172503.

[94] Q. Si and E. Abrahams, Physical Review Letters **101**, 076401(2008).

[95] R. Flint and P. Coleman, Physical Review B **86**, 184508(2012). http://link.aps.org/doi/10. 1103/PhysRevB.86.184508.

[96] L. P. Gor'kov and G. B. Teitel'baum, Physical Review B **87**, 024504(2013). http://link.aps.org/doi/10. 1103/PhysRevB.87.024504.

[97] Su-Peng Kou, Tao Li, and Zheng-Yu Weng, *Coexistence of Itinerant Electrons and Local Moments in Iron-Based Superconductors.* Europhysics Letter, **88**,(2009).

[98] William, D. B. *Fundamentals of Many-Body Physics Principles and Methods.* Springer-Verlag, Berlin Heidelberg (2009).

[99] Han, F. , Zhu, X. Y. , Cheng, P. , et al . *Superconductivity and Phase Diagrams of the 4d -and 5d -Metal-Doped Iron Arsenides $SrFe_{2-x}M_xAs_2$ (M=Rh, Ir ,Pd).* Physical Review B, **80** , 024506(2009).

[100] Chen, H. , et al. *Coexistence of the Spin -Density Wave and Superconductivity in $Ba_{1-x}K_xFe_2As_2$.* Europhysics Letters , **85**, 17006(2009).

[101] J. Hubbard, Proceedings of the Royal Society of London. Series A. Mathematical and Physical Sciences **276**, 238 (1963).

[102] J.Hubbard, *Electron Correlations in Narrow Energy Bands. II. The Degenerate Band Case.* Proc.R.Soc.London A **277**, 237(1964).

[103] J.Hubbard, *Electron Correlations in Narrow Energy Bands. III.* Proc.R.Soc.London A **281**, 401(1964).

[104] J.Hubbard, *Electron Correlations in Narrow Energy Bands. IV.* Proc.R.Soc.London A **285**, 1403(1965).

[105] J.Hubbard, *Electron Correlations in Narrow Energy Bands. V.* Proc.R.Soc.London A **296**, 82(1967).

[106] J.Hubbard, *Electron Correlations in Narrow Energy Bands. VI.* Proc.R.Soc.London A **296**, 100(1967).

[107] B. J. Powell, *on the interplay of superconductivity and magnetism.* PhD thesis university of Bristol, UK, Functional Anal. Appl.(2002)

[108] M.C.Gutzwiller, Phys.Rev. Lett.**10**, 159(1963).

[109] E.H.Lieb and F.Y. Wu,Phys.Rev. Lett.**20**, 1445(1968).

[110] D.Vollhardt, Rev. Mod.Phys.**56**, 99(1984).

[111] E.B.Kolomeisky and J.P. Straley, Rev. Mod.Phys.**68**, 175(1996).

[112] R.Micnas,J.Ranninger, and S.Robaszkiewicz, Rev. Mod.Phys.**62**, 113(1990).

[113] W.-G. Yin, C.-C. Lee, and W. Ku, Physical Review Letters **105**, 107004(2010). http://link.aps.org/doi/10.1103/PhysRevLett.105.107004.

[114] S.-L. Yu, J. Kang, and J.-X. Li, Physical Review B **79**, 064517(2009). http://link.aps.org/doi/10. 1103/PhysRevB.79.064517.

[115] P.G. de Gennes, Superconductivity of Metals and Alloys, W.A. Benjamin, NewYork, 1966.

[116] L.N.Cooper, Phys.Rev. **104**, 1189(1956).

[117] J.Spalek, Phys.Rev. B **63**, 104513(2001).

[118] P. Miller and B. Z. Gyoffy, J phys. Cond. Mat., **7**, 5579(1995)

[119] R.Balian and N.R.Werthamer, Phys.Rev. **131**, 1553(1963).

[120] E.Cartan, *The Theory of Spinors*, M.I.T. Press,Cambridge,Massachusetts,1966.

[121] W.R. Hamilton, Transactions of the Royal Irish Academy **21**, 199(1848).

[122] J.B. Ketterson and S.N.Song, *Superconductivity*, Cambridge University Press, Cambridge, 1999.

[123] B.L.Gyorffy, J.B.Staunton, and G.M.Stocks, Phys.Rev. B **44**, 5190(1991).

[124] A.M. Clogston, Phys. Rev. Lett.**9**, 266(1962).

[125] P. Fulde and R.A. Ferrell, Phys.Rev. **135**, A550(1964).

[126] G. Arfken, *Mathematical methods for Physics*, Acadamic Press,Orlanda, (1985)

[127] D.Zubarev N. *Double -Time Green Functions in Statistical Physics*. Soviet Physics Uspekhi **3**, 320(1960).

[128] D. Arcon, P. Jegli c, A. Zorko, A. Potocnik, A. Y. Ganin, Y. Takabayashi, M. J. Rosseinsky and K. Prassides. *Coexistence of localized and itinerant electronic states in the multiband iron-based superconductor* $FeSe_{0.42}Te_{0.58}$.Phsical Review B **82**, 140508(R)(2010).

[129] Carlos A. Lpez, Martn E. Saleta, Jos C. Pedregosa, Rodolfo D. Snchez, Jos A. Alonso, and Mara T. Fernndez-Daz. *Coexistence of Localized and Itinerant Electrons in the Double-Perovskite* $Ba_2Fe_{2/3}Mo_{4/3}O_6$. Eur. J. Inorg. Chem. **2014**, 3555-3563(2014).

PUBLICATION

1. **Tadesse Desta**, Pooran Singh and Gebregziabher Kahsay. *Coexistence of Superconductivity and Spin Density Wave (SDW) in Ferropnictide* $Ba_{1-x}K_xFe_2As_2$. Journal of Superconductivity and Novel Magnetism (Springer), **29**, 1433-1438(2016).

2. **Tadesse Desta**, Pooran Singh and Gebregziabher Kahsay. *Study of Upper Critical Magnetic Field of Superconducting* $HoMo_6Se_8$. World Journal of Condensed Matter Physics, **5**, 105-117(2015).

3. **Tadesse Desta**, Pooran Singh and Gebregziabher Kahsay. *Coexistence of superconductivity and ferromagnetism in superconducting* $HoMo_6S_8$. World Journal of Condensed Matter Physics, **5**, 27-36(2015).

4. **Tadesse Desta**, Pooran Singh and Gebregziabher Kahsay. *Theoretical Analysis of Superconductivity in Iron Based Superconductor* $Ba_{1-x}K_xFe_2As_2$ *(Accepted by MEJS: on the way)*

Declaration

I hereby declare that this PhD dissertation is my original work, has not been presented for a degree in any other University and that all the sources of material used for the dissertation have been dully acknowledged.

Name: *Tadesse Desta*

Signature:_____

This PhD dissertation has been submitted for examination with my approval as University advisor.

Name: *prof. P. Singh*
Signature:_____

Place and date of submission:
Addis Ababa University
Department of Physics
May 2017